Attribute control charts for effective statistical process control

Salah Haridy Gad Haridy

2014

Salah Haridy Gad Haridy. (2014). Attribute control charts for effective statistical process control. Doctoral thesis, Nanyang Technological University, Singapore.

https://hdl.handle.net/10356/59545

https://doi.org/10.32657/10356/59545

NANYANG TECHNOLOGICAL UNIVERSITY

School of Mechanical and Aerospace Engineering
Division of Systems and Engineering Management

ATTRIBUTE CONTROL CHARTS FOR EFFECTIVE STATISTICAL PROCESS CONTROL

SALAH HARIDY GAD HARIDY

A thesis submitted to the Nanyang Technological University in partial fulfilment of the requirement for the degree of Doctor of Philosophy

2014

Abstract

The control chart is fast becoming a necessity rather than a fashion in different manufacturing processes and service sectors. No tool can capture the voice of a process better than the control chart. It is an effective tool to monitor a process, reduce variation, improve productivity and ensure quality. The applications of the control chart have now moved into engineering, service management, biology, health care and finance.

The control chart is considered as one of the most powerful monitoring techniques in Statistical Process Control (SPC). It is basically used to achieve the statistical control of a process and its output. SPC provides the decision maker with the ability to monitor the quality characteristics of the product, evaluate the process performance and take a quick corrective action when out-of-control statuses and abnormal conditions are going to occur in order to avoid damages and serious economic losses.

Attribute control charts play a vital role in monitoring the quality characteristics which cannot be conveniently measured in a continuous numerical scale. Nowadays, attribute charts enjoy a wide range of applications in many fields such as manufacturing processes, healthcare systems and service industries.

The main objective of this thesis is to develop new attribute control charts with high detection effectiveness. This thesis proposes five new attribute charts, namely, a synthetic & np (Syn-np) chart, an optimal np & Cumulative Sum (np-CUSUM) chart, a CUSUM chart with curtailment (Curt_CUSUM), an optimal Sequential Probability Ratio Test (SPRT) chart for monitoring p, and finally a novel attribute chart (AFV chart) for monitoring the mean and variance of a variable.

A second goal is to provide an overall effectiveness evaluation and systematic comparison among the newly developed charts and different attribute charts in the literature under the same false alarm rate for a fair comparison. The results of this evaluation give a clear conclusion on the overall detection effectiveness of the charts and provide a practical guide to both academia and industry. To achieve this goal, several types of commonly used control charts for attributes including np chart, synthetic chart, Cumulative Sum (CUSUM) chart,

Exponentially Weighted Moving Average (EWMA) chart, and Sequential Probability Ratio Test (SPRT) chart are studied in this thesis. The results of these evaluation and comparison can be used as guidelines to facilitate the selection of the attribute control charts for different SPC practitioners.

In addition, a general model for the optimal design of the attribute control charts is proposed. In this model, all the independent and dependent charting parameters are optimized using an exhaustive search algorithm in order to achieve the best overall performance. This search algorithm is simple and reliable. The Average Number of Defectives (*AND*) is adopted as an objective function to design and compare the charts subject to the same false alarm rate. Since *AND* is an overall measure of chart performance, therefore, minimizing *AND* will ensure that the control chart has an excellent overall performance across the entire shift range of interest.

The results of the quantitative comparative study reveal that the new charts developed in this thesis have achieved a significant improvement in detection effectiveness. Specifically, the Syn-np chart stands as the most effective Shewhart-type chart for attributes in current SPC literature, the np-CUSUM chart and Curt_CUSUM charts are considered as the fastest CUSUM charts for detecting p shifts and the optimal SPRT chart is able to double the overall detection speed compared with the basic SPRT chart. Although the design of the Syn-np, np-CUSUM, Curt_CUSUM and optimal SPRT charts is more complicated and their implementation is slightly more difficult than the existing counterpart charts, the application of the new charts developed in this research can be justified by the substantial improvement in performance.

Finally, the new AFV chart that employs a simple attribute inspection is found to outperform the variable $\bar{X}$&R and $\bar{X}$&S charts from an overall viewpoint, under different circumstances. As a limitation, the AFV chart is not able to detect decreasing variance shifts. Moreover, it is not quite suitable to monitor the processes parameters which change frequently.

The new charts developed in this thesis may help SPC practitioners elsewhere to make a correct and timely decision in face of critical problems, to substantially reduce damages and quality cost in the long run, and to pave the way for a new cutting-edge research in attribute SPC.

Acknowledgements

First of all, I am so grateful to Allah all mighty for giving me the guidance, patience and hope to finish my thesis. It is the mercy of Allah and my trust in Him that have made such a work to be accomplished.

I wish to immensely express my deep gratitude to my advisors, Prof. Wu Zhang and Prof. Chen Songlin. I greatly appreciate their warm supervision, valuable advice and constant encouragement that tremendously facilitate the progress of my research. Their constructive suggestions, insightful opinions, criticism and patience have been a great asset. Most importantly, I have learnt the art of research from them. Without the inspiring guidance of my advisors, the fruitful achievement of this research will never be possible.

I sincerely thank A*STAR for offering me a generous scholarship scheme (SINGA) that enabled me to pursue my Ph.D. at an inspiring and resourceful institution like Nanyang Technological University. My university, school and division provided me with a convenient environment to study and an excellent opportunity to interact locally and globally with others. In addition, special thanks for my colleagues and friends who supported me with their valuable suggestions and continuous help. Their collaboration and understanding have created a pleasant circle, where I can focus on my research whole-heartedly.

I am deeply grateful to my dearest wife, beloved kids, generous parents and relatives whose love, care, support and encouragement have been the source of inspiration and motivation to finish this research.

Finally, I would like to appreciate all of those who graciously gave me their time and assistance so that I could accomplish the requirements of this degree.

Table of Contents

List of Figures

List of Tables

Nomenclature

Notations

$\overline{X}$	Sample Mean
μ	Process mean
B	Steady-state probability vector
c	Number of nonconformities
C_t	Quality statistic for CUSUM chart
d	Number of nonconforming units
e	Constant between 1 and 3
E_t	Quality statistic for EWMA chart
$F(\ )$	Cumulative probability function
$f(\ )$	Probability density function
g	Lower control limit of SPRT chart
H	Upper control limit of CUSUM chart or SPRT chart
h	Sampling interval
H_0	Null hypothesis
H_1	Alternative hypothesis
I	Identity matrix
k	Reference parameter of CUSUM chart
K_c	Constant depends on the individual process
L	Lower control limit of synthetic chart
Lo	Loss
M	Number of transitional states
m	Number of samples
m_0	Number of conforming samples before time T
m_1	Number of conforming samples after time T
N	Number of units produced per time unit
n	Sample size
O_i	Center of state i
p	Fraction nonconforming
p_{ij}	Transition probability from state i to state j
r	Inspection rate
R	Sample range
R_0	In-control transition probability matrix for Markov Chain
R_1	Out-of-control transition probability matrix for Markov Chain
S	Sample standard deviation
S_t	Quality statistic for SPRT chart

t	Time interval
T^2	Hotelling's statistic
u	Number of nonconformities per unit
U	Vector of *ARL* for Markov Chain
V	Average number of units produced in an out-of-control case
w	Warning limit of synthetic control chart
W	Upper control limit of EWMA chart
x	Quality characteristic
α	Type I error
β	Type II error
γ	Reference value for SPRT chart
δ	Shift
Δ	Width of the interval
θ	Distance of the control limits from the center line
λ	Smoothing parameter of EWMA chart
σ	Standard deviation
σ^2	Variance
τ	Allowable minimum value of in-control *ATS*
Φ ( )	Standard normal cumulative probability function

Abbreviations

1-*CUSUM*	Single Cumulative Sum
AEQL	Average Extra Quadratic Loss
AFV	Attribute For monitoring a Variable
AL	Adjusted Loss
AND	Average Number of Defectives
ARATS	Average Ratio of Average Time to Signal
ARL	Average Run Length
ART	Adaptive Resonance Theory
ATS	Average Time to Signal
BSI	British Standard Institution
CATs	Classroom Assessment Techniques
CL	Center Line
CRL	Conforming Run Length
Curt_CUSUM	CUSUM chart with Curtailment
CUSUM	Cumulative Sum
DOE	Design of Experiments
DSVSI	Double Sampling and Variable Sampling Interval

EPC	Engineering Process Control
EQL	Extra Quadratic Loss
EWMA	Exponentially Weighted Moving Average
FCL	Fractional Control Limits
FSR	Fixed Sampling Rate
GCRL	Generalized Conforming Run Length
GWMA	Generally Weighted Moving Average
IC	Integrated Circuit
LCL	Lower Control Limit
MNS	Maxima Nomination Sampling
MP	Most Powerful
NCS	Non-central Chi-squared Statistic
QA	Quality Assurance
QC	Quality Control
RL	Run Length
SPC	Statistical Process Control
SPRT	Sequential Probability Ratio Test
SPRTFT	Sequential Probability Ratio Test Fixed-Times
SQC	Statistical Quality Control
SS-DEWMA	Sum of Squares Double Exponentially Weighted Moving Average
SXC	Sum of Xs with Curtailment
Syn	Synthetic
Syn-np	Synthetic-np
TBE	Time Between Events
TQM	Total Quality Management
UCL	Upper Control Limit
UGR	Unit and Group Runs
VSI	Variable Sampling Interval
VSS	Variable Sample Size
VSSI	Variable Sample Size and Sampling Interval
WL	Weighted Loss
WLC	Weighted Loss Cumulative Sum

List of Publications

Published or Accepted Journal Papers

(1) **Haridy S.** and Wu Z. (2009), Univariate and Multivariate Control Charts for Monitoring Dynamic-Behavior Processes: a Case Study. *Journal of Industrial Engineering and Management*, 2, 464-498.

(2) **Haridy S.**, Wu Z., and Castagliola P. (2011), Univariate and Multivariate Approaches for Evaluating the Capability of Dynamic-Behavior Processes (Case Study). *Statistical Methodology*, 8, 185-203.

(3) **Haridy S.**, Gouda S. A. and Wu Z. (2011), An Integrated Framework of Statistical Process Control and Design of Experiments for Optimizing Wire Electrochemical Turning Process. *International Journal of Advanced Manufacturing Technology*, 53, 191-207.

(4) **Haridy S.**, Wu Z., Khoo M. B. C. and Yu F. J. (2012), A Combined Synthetic & np Scheme for Detecting Increases in Fraction Nonconforming. *Computers and Industrial Engineering*, 62, 979-988.

(5) **Haridy S.**, Wu Z. and Flaig J. (2012), Chi-squared Control Chart for Multiple Attributes. *International Journal of Industrial and Systems Engineering*, 12, 316-330.

(6) **Haridy S.**, Wu Z., Yu F. J. and Shamsuzzaman M. (2013), An Optimization Design of the Combined np-CUSUM Scheme for Attributes. *European Journal of Industrial Engineering*, 7, 16-37.

(7) **Haridy S.**, Wu Z., Lee C. K. and Bhuiyan N. (2013), Optimal Average Sample Number of the SPRT Chart for Monitoring Fraction Nonconforming. *European Journal of Operational Research*, 229, 411-421.

(8) **Haridy S.**, Wu Z., Lee C. K. and Rahim M. A. (2014), An Attribute Chart for Monitoring the Process Mean and Variance. Accepted for publication by *International Journal of Production Research*, 52, 3366-3380.

(9) **Haridy S.**, Wu Z., Chen S. and Knoth S. (in press), Binomial CUSUM Chart with Curtailment. *International Journal of Production Research*.

(10) **Haridy S.**, Wu Z., Abhary K., Castagliola P. and Shamsuzzaman M. (in press), Development of a Multiattribute Synthetic-np Chart. *Journal of Statistical Computation and Simulation*.

Submitted Journal Papers

(1) **Haridy S.**, Ou Y., Wu Z. and Khoo M. B. C., A Single X Chart Outperforming the Joint $\bar{X}$&R and $\bar{X}$&S Charts for Monitoring Mean and Variance. Submitted to *European Journal of Industrial Engineering*.

(2) Flaig J., Wu Z. and **Haridy S.**, A Comparison Test for Net Sensitivity. Submitted to *Journal of Industrial Engineering and Management* (Editorial decision: revision).

(3) Shamsuzzaman M., Khoo M. B. C., **Haridy S.** and Alsyouf I., An Optimization Design of the Combined Shewhart-EWMA Control Chart. Submitted to *International Journal of Quality & Reliability Management*.

(4) Ou Y., Hu J., Li X. and **Haridy S.**, Real-Time Anomaly Detection Approach Based on Condition-Based Statistical Process Control. Submitted to *Journal of Intelligent Manufacturing*.

Conference Papers

(1) **Haridy S.** and Wu Z. (2011), Synthetic-np Chart for Attributes. *IEEE International Conference on Industrial Engineering and Engineering Management*, Singapore.

(2) **Haridy S.**, Wu Z., Ker D. and Chen S. L. (2012), A Challenging X Chart for Monitoring the Mean and Variance. *Engineering Lean & Six Sigma Conference*, Louisville, KY, USA.

(3) **Haridy S.** (2012), An Attribute Control Chart for Monitoring A variable. *World Congress in Probability and Statistics*, Istanbul, Turkey.

(4) **Haridy S.**, Wu Z., Chen S. L. and Bhuiyan N. (2012), Optimal np-CUSUM Scheme for Monitoring Fraction Nonconforming. *IIE Asian Conference*, Singapore.

(5) Qu L., **Haridy S.**, Wu Z. and Bhuiyan N. (2012), Monitoring Multiattribute Processes Using Synthetic-type Control Charts. *IIE Asian Conference*, Singapore.

(6) **Haridy S.** (2013), An Application of Curtailment in Control Charts. *Quality and Productivity Research Conference*, Niskayuna, NY, USA.

List of Awards

(1) Mary G. and Joseph Natrella Scholarship by the Quality and Productivity Section of the American Statistical Association for academic excellence, teaching, leadership and service to the statistical community and the abstract entitled "An Application of Curtailment in Control Charts".

(2) Research grant for Doctoral Candidates and Young Scientists by the German Academic Exchange Service (DAAD) for the research proposal entitled "Advanced Statistical Process Control Charts for Monitoring Attributes".

(3) Grant by the European Mathematical Society, Bernoulli Society, Biometrika and International Mathematical Union for the abstract entitled "An Attribute Control Chart for Monitoring A variable".

(4) Singapore International Graduate Award (SINGA) by the Agency for Science, Technology and Research (A*STAR).

Chapter 1

Introduction

Quality Control (QC) is nowadays one of the most important activities in modern industries and service sectors. Customers are usually very concerned with the quality of products. Producing good quality to satisfy customers' requirements is critical to the survival of a company both now and in the future. Essentially, QC covers the monitoring, examination and improvement of the quality and productivity of a product, service, or process.

Statistical Process Control (SPC) is one of the most popular and important topics in QC. The stability of a process is achieved through the application of SPC. SPC assists the decision maker in drawing conclusions from data representing process status in order to maintain the process and quality characteristics on target and within boundaries of natural variation. SPC focuses on controlling both the process and product. Effective and practical SPC approaches are essential. A successful process control approach needs to provide on-line real time monitoring of quality related characteristics. An approach that analyses quality related data only after the product is produced is no longer acceptable.

SPC effectively monitors the process and reports trouble spots before defective items are produced. It is essential to help avoid damages and serious economic losses. Among the major well-known tools of SPC technology such as histogram, check sheet, Pareto chart, cause-and-effect diagram, defect concentration diagram and scatter diagram, the control chart is absolutely the most sophisticated and powerful one. It is an effective graphical device widely used to monitor the process and thereby to assure the quality of products. SPC has been adopted and widely employed in manufacturing and service industries. For example, Friedman and Albin (1991) proposed a method for constructing defect control charts for monitoring clustered defects in Integrated Circuit (IC) fabrication. Ngo (1995) developed a Defects Per Million Opportunities (DPMO) chart for assembly operations in electronics industry. Dhafr *et al*. (2006) presented an attribute chart to monitor the defects and improve the quality performance in manufacturing

organizations. Kaya and Engin (2007) determined the optimal sample size of attribute charts to effectively monitor an engine piston manufacturing process.

Jones and Dent (1994) applied SPC charts in staff restaurant to identify the problems in this service industry. Wood (1994) proposed a set of guidelines for the statistical monitoring of service processes. Hart *et al*. (2003) developed a new class of control charts for monitoring and improving the service quality in health care. Duclos and Voirin (2010) provided key elements to enhance the service quality in clinical practice using a *p* chart. Jumah *et al*. (2012) discussed the use of QC techniques including the control charts in the improvement of the trading, finance, banking, and service industries. The applications of SPC have now moved into many other different sections such as health care (Woodall *et al*. 2006, Coory *et al*. 2008, Albers 2011, Cannon *et al*. 2012), service management (Herbert *et al.* 2003, Pettersson 2004, Tao *et al*. 2012), finance (Shin and Sohn 2007), environmental science (Schneider *et al*. 1992, Anderson and Thompson 2004, Morrison 2008, Luo *et al*. 2010) and biology (Abdurrahman *et al*. 2008, De Vries and Reneau 2010, Dokouhaki and Noorossana 2012).

There are two main categories of the control charts, variable charts for monitoring the quality characteristics which can be measured on a continuous numerical scale, and attribute charts for monitoring the quality characteristics which can only be classified as conforming or nonconforming. The applications of attribute control charts cover a wide variety of manufacturing processes and other sectors in which quality characteristics cannot be measured on a numerical or quantitative scale.

This thesis investigates the effectiveness of different types of attribute control charts including np chart, synthetic chart, Cumulative Sum (CUSUM) chart, Exponentially Weighted Moving Average (EWMA) chart and Sequential Probability Ratio Test (SPRT) chart. Meanwhile, it develops five new effective attribute charts; namely, synthetic & np (Syn-np) chart, optimal np & Cumulative Sum (np-CUSUM) chart, CUSUM chart with curtailment (Curt_CUSUM), optimal Sequential Probability Ratio Test (SPRT) chart and an attribute chart for monitoring the mean and variance of a variable (AFV chart).

The results of the performance comparison show that the five new charts have achieved a significant improvement in the overall detection effectiveness compared with the other charts under the same false alarm rate which is used as a common ground for the evaluation. Specifically, the Syn-np chart outperforms the np chart and synthetic chart by 100% and 29%, respectively. The np-CUSUM chart is more effective than the np chart, EWMA chart and CUSUM chart by 213%, 15% and 5%, respectively. The Curt_CUSUM chart is superior to the conventional CUSUSM chart by 36%. The optimal SPRT chart is able to double the average detection speed compared with the basic SPRT chart and excels the np chart and CUSUM chart by 221% and 171%, respectively. The AFV chart outdoes the $\bar{X}$&R chart and $\bar{X}$&S charts by 7% and 6% for detecting shifts in both mean and variance.

1.1 Background

Quality always has a pragmatic interpretation as the superiority of something. It is defined as fitness for use or conformance to requirements (Crosby 1979). Quality is a subjective attribute. Different people may define or understand the quality differently. The quality of a service or product is a reflection of the degree of the customer's satisfaction. Quality Control (QC) has become a driving force in the struggle for competitive position in the world marketplace. Organizations are clearly more cognizant that QC must be not only a central metric in the evaluation of performance of products and services, but also an essential design criterion. The basic role of QC is to fulfil the customer satisfaction and ensure a continual improvement in order to substantially reduce variability and economic loss (Donnell and Singhal 1996). QC should be able to provide the organization with a systematic structure and way of thinking for managing its processes and activities consistently. It is commonly known that QC usually uses some statistical techniques such as Statistical Process Control (SPC) to fulfil quality and improve productivity.

Montgomery (2013) explained that the SPC philosophy integrates an array of quality tools designed to solve the problems that result in process variation. He pointed out that "SPC can be applied to any process". He listed seven major technical tools to sustain an SPC program. Since the control chart is probably the most technically sophisticated and effective tool among these seven tools to detect the problems, the primary focus of this Ph.D. thesis is the control chart. The control chart in the metrology emphasizes the application of operations research methodology to problems in manufacturing systems and has become one of the most important factors for consumers in the selection of competing products and services (Krumwiede and Chwen 1996).

Dasgupta (2003) proposed a comprehensive framework for the use of control charts with an emphasis on the detection of assignable causes. Woodall *et al.* (2006) presented many applications of control charts in healthcare monitoring and public-health surveillance. Hsieh and Tong (2007) proposed a control chart that applies fuzzy theory and engineering experience to monitor wafer defects with the consideration of defect clustering. The widespread availability of powerful microcomputers and the excellent SPC software has made the implementation of SPC at the workplace a standard practice in many businesses (Montgomery 2013). It is a key factor leading to business success, growth and competition. Haridy and Wu (2009) presented adjustment methodologies for the use of univariate and multivariate control charts in monitoring dynamic behaviour processes. De Vries and Reneau (2010) provided a review of control chart applications in animal production systems found in the literature from 1977 to 2009. Noorossana *et al*. (2011) developed a control chart for monitoring rare infections. Ozkul and Karaoglan (2011) proposed a regression control chart to determine Young's modulus from a particular region on stress-strain curve. Castagliola *et al*. (2012) developed a variable sample size t control chart for monitoring short production runs. Yi *et al*. (2012) developed a control chart for detecting displacement shifts in Global Position System (GPS) monitoring.

In this thesis, different typical attribute control charts including np chart, CUSUM chart, EWMA chart, synthetic chart and SPRT chart are investigated. Meanwhile, five new attribute

charts (the Syn-np chart, np-CUSUM chart, Curt_CUSUM chart, optimal SPRT chart and AFV chart) are proposed. Their optimal design algorithms are developed. The key methods to optimize the charting parameters are studied and the comparisons among different control charts are presented in detail as well.

The control chart should be designed appropriately for an effective use. The design of the control chart is to determine its charting parameters such as the sampling interval, sample size and control limits (Montgomery *et al.* 1996). The control chart may be designed statistically or economically. While the economic design aims at minimizing the cost, the main objective of the statistical design is to minimize the out-of-control Average Time to Signal (*ATS*). The statistical design is widely used in organizations to improve the quality, reduce variability and control unexpected failure. The statistical design of the attribute charts is the focus of this thesis, as it makes the SPC more scientific and practical compared with the economic design.

The variable control charts are mainly used for detecting shifts in mean (δ_μ) and standard deviation (δ_σ). On the other hand, the attribute control charts are basically used for detecting shifts in the defective rate or fraction nonconforming (p). Considering the fact that attribute control charts are most often used to detect an increase in fraction nonconforming or deterioration in quality (Lucas 1985*a*, Reynolds and Stoumbos 1999, Wu *et al.* 2008*a*), the focus of the research in this thesis is to detect increasing p shifts. The reduction in fraction nonconforming p is usually due to a process improvement. Therefore, decreasing p shifts doesn't jeopardize the process quality directly and is often much less critical than increasing p shifts. However, if detecting decreasing p shifts is really desired and of interest, a corresponding symmetric lower-sided chart can be built and implemented.

In a process, there are two types of shifts, i.e., sustained shift and transient shift (Reynolds and Stoumbos 2004*a*). The sustained shift lasts until it is detected by the control chart. On the other hand, the transient shift lasts for a short time. Most of the control charts are designed under the assumption of a sustained shift.

The performance of the control charts are usually measured by in-control and out-of-control Average Time to Signal (*ATS*). The out-of-control *ATS* is the average time required to detect the out-of-control case. It is commonly used as an indicator of the power or effectiveness of the control chart. When a process is out of control, the smaller the out-of-control *ATS*, the more quickly the shift is signalled and the less loss in product quality. On the other hand, the in-control ATS_0 indicates the false alarm rate. Another measure of the detection effectiveness is the Average Number of Defectives (*AND*) (Haridy *et al*. 2012*a*). It is an overall measure of performance that evaluates the average number of defectives (nonconforming units) produced in out-of-control cases over a wide range of shifts. In current SPC practice, it is quite hard to identify the most efficient control chart from a large number of various control charts since there is not a unique performance measure that is commonly used as a standard to compare the chart performance.

1.2 Motivation

In reality, many quality characteristics cannot be measured on a numerical scale or even a quantitative scale. They can only be classified as conforming or nonconforming. Attribute control charts have been successfully used for monitoring such quality characteristics in a wide variety of manufacturing processes and service sectors. The widespread application of the attribute charts is due to many factors, such as the simple handling of attribute characteristics, the ease of communication between people at different levels, the capability of checking multiple quality requirements, and the prevalence of count data in many applications, especially in non-manufacturing sectors.

In the literature, less attention has been paid to attribute control charts compared with variable control charts. This thesis mainly focuses on developing new effective attribute control charts. These new control charts will increase the detection speed to a significant degree and meanwhile maintain the false alarm rate at a predetermined level. More specifically, these charts

will help SPC practitioners and decision makers elsewhere to make a prompt and correct decision in face of critical problems and substantially reduce serious damages and economic losses in the long run.

The new charts will continuously monitor the collected data or information from the process, and decide in time whether the system is normal (in control) or in danger (out of control) so that immediate and prompt actions can be taken. The new charts are developed to achieve the highest detection effectiveness for SPC.

A general model for the optimal design of the attribute control charts is proposed. In this model, the Average Number of Defectives (*AND*) is adopted as the objective function to be minimized. All of the independent and dependent charting parameters of the control charts are optimized in order to minimize the Average Number of Defectives (*AND*) which is an overall measure of performance. The optimal values of the independent charting parameters are determined by a search algorithm, while the values of the dependent charting parameters are determined based on the values of the independent parameters and constraint functions. Finally, overall comparison of the new charts with other existing charts is conducted under an identical false alarm rate. The results of this comparative study can provide SPC users with some useful guidelines for the selection of the attribute charts.

The results of this research may lay a foundation and pave the way for designing and developing advanced attribute control charts to detect problems timely and cost-effectively, and will ultimately advance the research in this area to a new cutting edge.

1.3 Research Objectives and Scope

SPC can be defined as a collection of tools which tracks the statistical behavior of processes, in order to maintain and improve the product quality. In recent decades, many quality philosophies like Total Quality Management (TQM) and Six Sigma has been developed (Cheng and Dawson 1998). SPC is expected to play an even greater role in the future. The control chart developed in SPC is an effective monitoring technique widely used in production lines and

manufacturing processes. In recent years, many new charts have been proposed for both variable and attribute SPC (Wu and Jiao 2007, Khoo *et al.* 2008, Costa *et al.* 2009, Huang *et al.* 2010, Teh *et al*. 2011, Yang *et al*. 2012, Haridy *et al*. 2012*b*).

1.3.1 Developing new charts

The primary objective of this Ph.D. research is to develop new attribute control charts to achieve the highest detection effectiveness. Five new control charts have been developed. A brief description regarding the general advantages and limitations of each of them is given below:

(1) Synthetic & np (Syn-np) chart

This chart has both the strength of the synthetic chart for quickly detecting small p shifts and the advantage of the np chart of being sensitive to large p shifts. As a result, it has a better and more uniform overall performance. The Syn-np chart is more effective than the np chart and synthetic chart by 100% and 29%, respectively, in terms of the Average Number of Defectives (*AND*) over a wide range of p shifts under different conditions. Although the design of the Syn-np chart is more complicated and its implementation is slightly more difficult than the np and synthetic charts, its application can be justified by the substantial improvement in performance.

(2) Optimal np & CUSUM (np-CUSUM) chart

This chart is an optimal version of the np & CUSUM scheme. The design algorithm not only optimizes the charting parameters of the np chart element and the CUSUM chart element, but also optimizes the allocation of detection power between the two chart elements, so that the best overall performance can be achieved. On average, the np-CUSUM chart outperforms the np chart, EWMA chart and CUSUM chart by 213%, 15% and 5%, respectively, under different settings. Even though the design and implementation of the np-CUSUM chart is not as simple as those of the np and CUSUM charts, the former is more preferable as it results in a considerable gain in the detection effectiveness.

(3) CUSUM chart with curtailment (Curt_CUSUM)

This chart applies the curtailment technique to improve the overall detection effectiveness of the conventional CUSUM chart. In the Curt_CUSUM chart, the inspection of a sample is terminated or curtailed if the number of nonconforming units exceeds the control limit. While the general idea of the curtailment is very simple, the results of the comparative studies show that the Curt_CUSUM chart excels the CUSUM chart without curtailment by 36% in terms of Average Number of Defectives (*AND*) under different circumstances. The interpretation of the Curt_CUSUM chart is slightly more difficult than the conventional CUSUM chart as a curtailment threshold needs to be defined and the count of nonconforming units has to be updated during the inspection of each sample and compared with the curtailment threshold. The Curt_CUSUM chart can be used for both 100% inspection and random sampling inspection.

(4) Optimal SPRT chart

This chart is an optimal version of the basic SPRT chart. By optimizing the charting parameters, the overall detection effectiveness of the basic SPRT chart is improved by more than 100%. Meanwhile, the optimal SPRT chart outperforms the np and CUSUM charts by 221% and 171%, respectively, in terms of Average Number of Defectives (*AND*) under different circumstances. While the optimal design algorithm significantly enhances the overall performance of the SPRT chart, it does not increase the difficulty for implementing the SPRT chart. The implementation of the SPRT chart is usually more difficult than the Fixed Sampling Rate (FSR) charts. The in-control sample number of the SPRT chart may be quite long occasionally in a particular sample. Some special procedure may have to be adopted to handle this problem.

(5) Attribute chart for monitoring a variable (AFV chart)

This chart employs an attribute inspection to monitor both the mean and variance of a variable. The salient feature of the AFV chart is its ability to determine if the process is in control or out of control by inspecting only a single unit in each sample. By selecting its

inspection limits appropriately, the AFV chart fairly outperforms the $\bar{X}$&R and $\bar{X}$&S charts by 7% and 6%, respectively, from an overall viewpoint under different circumstances. In general, the AFV chart is simpler to be designed and implemented than the $\bar{X}$&R and $\bar{X}$&S charts, and meanwhile more effective than the latter to detect out-of-control cases. As a result, it lends itself to be a pragmatic replacement of the latter two charts and may be adopted for many SPC applications, in which both the mean and variance of a variable need to be monitored. The AFV chart is not quite suitable to monitor the processes whose parameters change frequently and also unable to detect decreasing variance shifts.

The first four charts (Syn-np, np-CUSUM, Curt_CUSUM and optimal SPRT charts) are mainly used to monitor the fraction nonconforming p. Consequently, they are designed based on the following assumptions and conventions:

(1) The number d of nonconforming units in a sample is assumed to follow a binomial distribution with known in-control fraction nonconforming p_0.

(2) When a process shift in fraction nonconforming occurs, the fraction nonconforming p changes to

$$p = \delta \times p_0 \tag{1.1}$$

where the index δ ($1 \le \delta \le \delta_{max}$) indicates the increasing p shift in terms of p_0. The process is in control when $\delta = 1$ (i.e., $p = p_0$) and out of control when ($1 < \delta \le \delta_{max}$) with a maximum fraction nonconforming of $p = \delta_{max} \times p_0$.

(3) Considering the fact that control charts for attributes are most often used to detect an increase in fraction nonconforming or deterioration in quality (Lucas 1985, Reynolds and Stoumbos 1999), the focus of these new charts is to detect increasing p shifts. The reduction in fraction nonconforming p is usually due to a process improvement. Therefore, decreasing p shifts doesn't jeopardize the process quality directly and is often much less critical than increasing p shifts. However, if detecting decreasing p shifts is

really desired and of interest, a corresponding symmetric lower-sided chart can be built and implemented.

(4) The steady-state *ATS* is used rather than the zero-state *ATS* to evaluate the performance of the charts, because the former is more realistic than latter as will be explained in Section (2.7.3).

While the first four charts used to monitor the fraction nonconforming p, the fifth chart (AFV chart) is used to monitor the mean and variance of a variable. Therefore, the following assumptions and conventions are considered for its design:

(1) The variable quality characteristic x is assumed to follow an identical and independent normal distribution with a known in-control mean μ_0 and standard deviation σ_0. In practice, μ_0 and σ_0 may be estimated from the observed field records, or historical data. When a process shift occurs, the mean μ_0 and standard deviation σ_0 of x will change to:

$$\mu = \mu_0 + \delta_\mu \sigma_0 \qquad \sigma = \delta_\sigma \sigma_0 \tag{1.2}$$

where δ_μ and δ_σ are the mean shift and standard deviation shift, respectively, in terms of σ_0. When the process is in control, $\delta_\mu = 0$ and $\delta_\sigma = 1$.

(2) For convenience of discussion, x is converted to z, which follows a standard normal distribution when the process is in control, that is

$$z = \frac{x - \mu_0}{\sigma_0} \tag{1.3}$$

(3) The out-of-control *ATS* is still computed under the steady-state mode. This assumes that the process has reached its steady state or stationary distribution at the random time when the shift occurs (Reynolds *et al*. 1990).

(4) Since deterioration in product quality is often the main concern in most of the applications (Reynolds and Glosh 1981, Wu *et al*. 2002), this research only handles the increasing variance shift, together with the increasing and decreasing mean shifts.

1.3.2 Evaluating the overall performance of charts

Another objective of this research is to evaluate and compare the overall performance of all major attribute control charts. To achieve this objective, a broad literature survey on the control charts is carried out and the attributions of different control charts are studied. A systematic performance comparison among different control charts is conducted under an identical false alarm rate for a fair evaluation. The comparison is conducted based on two criteria. One is the overall effectiveness for detecting shifts and another is the simplicity in understanding, design and implementation. The results can be used as guidelines to facilitate the selection of the attribute control charts for different SPC users.

This research proposes and adopts the Average Number of Defectives (*AND*) as the objective function to be minimized. *AND* is an overall measure of performance that evaluates the average number of defectives (nonconforming units) produced in out-of-control cases over a wide range of shifts and takes into account different contributors to the product quality (such as the time to signal and the magnitude of the shift).

The *AND* is more informative and practical than the *ATS* as it aims at improving the overall performance of the control chart across the entire shift range of interest, rather than the performance just at a specified shift point. *AND* is actually a weighted average of *ATS*. Moreover, *AND* directly relates the chart performance to the economic outcome. In view of this, *AND* is used as the basic criterion for the design, optimization and comparison of different control charts in this research.

1.3.3 Proposing a general model for the design of charts

The final objective is to propose a general model for the optimal design of the control charts. This optimal design model aims at increasing the speed of detecting the out-of-control status and controlling the false alarm rate at a specific level. In SPC terminology, the goal of the optimal design is to minimize the Average Number of Defectives (*AND*) and satisfy the

requirement on false alarm rate which is indicated by the in-control Average Time to Signal (ATS_0). The optimal values of the independent and dependent charting parameters are identified by an exhaustive search algorithm so that the best overall performance can be obtained.

1.4 Organization of Thesis

The organization of this thesis is as follows:

Chapter 2 "*Literature Review*": This chapter presents a review of SPC literature. More particularly, it provides a broad research survey of the basic variable control charts and attribute control charts, as well as the recent important developments in this area. The research gaps addressed by this research are listed in Section (2.9).

Chapter 3 "*Synthetic & np* (*Syn-np*) *Chart*": This chapter proposes a new chart (Syn-np chart) that comprises a synthetic chart and an np chart. In Section (3.3), details of the design of the Syn-np chart are presented. In Section (3.4), the performance of the Syn-np chart is evaluated and compared with that of the individual np chart and synthetic chart.

Chapter 4 "*Optimal np & CUSUM* (*np-CUSUM*) *Chart*": This chapter presents an algorithm to design the optimal version of the np & CUSUM scheme. Section (4.3) presents the design of the optimal np-CUSUM chart. In Section (4.4), the performance of the np-CUSUM chart is evaluated and compared with that of the np chart, CUSUM chart, EWMA chart and np-CUSUM scheme proposed by Morias and Pacheco (2006).

Chapter 5 "*CUSUM Chart with Curtailment* (*Curt_CUSUM*)": This chapter proposes a new chart (Curt_CUSUM chart) that makes use of the curtailment technique to enhance the detection effectiveness of the CUSUM chart. Section (5.3) explains the design procedure of the Curt_CUSUM chart. In Section (5.4), the detection effectiveness of the Curt_CUSUM chart is evaluated and compared with that of the conventional CUSUM.

Chapter 6 "*Optimal SPRT Chart*": This chapter presents an optimal SPRT chart. Section (6.3) demonstrates the design of the optimal SPRT chart. In Section (6.4), the detection speed of

this optimal SPRT chart is evaluated and compared with that of the np chart, CUSUM chart, and SPRT chart proposed by Reynolds and Stoumbos (1998).

Chapter 7 "*Attribute Chart for Monitoring a Variable* (*AFV Chart*)": This chapter proposes a novel AFV chart that employs an attribute inspection to monitor both the mean and variance of a variable. Section (7.3) highlights the design of the AFV chart. In Section (7.4), the performance of the AFV chart is evaluated and compared with that of the $\bar{X}\&R$, $\bar{X}\&S$ and X&MR charts that have traditionally been used for detecting shifts in the mean and variance of a variable.

Chapter 8 "*Conclusions and Future Research*": This chapter concludes the contributions made in this thesis and provides some visions for the future research.

Chapter 2

Literature Review

This chapter conducts review on the major topics in quality control, including basic variable control charts, various types of attribute control charts, single and combined control charts, and different performance measures of control charts. Moreover, it highlights the relevant research conducted in these topics and presents the main concepts and conventions used in developing the statistical control charts.

2.1 Statistical Process Control (SPC)

Statistical Process Control (SPC) is a collection of statistical techniques useful in achieving process stability and improving capability by monitoring the variability of the quality characteristics of a product. Every product possesses a number of parameters that jointly describe what the user or customer thinks of as quality. These parameters are called quality characteristics (Montgomery 2013). Statistical techniques have been widely used since 1940s. During the mid-1980s, statistical methodology became the most important topic under the title of SPC (Klyatis and Klyatis 2005).

SPC is a systematic study of a process through control charts and other statistical methods in order to discover whether the process is behaving naturally or unnaturally (AT&T 1985). Montgomery (2013) explained that SPC philosophy integrates an array of quality tools designed to solve the problems that result in process variation and stated that "SPC can be applied to any process". SPC is a methodology and philosophy for monitoring a process to identify the assignable causes of variation and signal the need to take a corrective action when appropriate. SPC can be defined as "the application of statistical techniques to monitor and adjust an operation" (APICS 1995). SPC is a subset of the more inclusive term statistical quality control (SQC). However, the terms SPC and SQC are often used interchangeably (APICS 1995).

It is necessary to distinguish SPC from another term called Engineering Process Control (EPC). EPC is to adjust the process without detecting and removing the assignable causes. It originated from the idea of process compensation and regulation, in which a manipulable process variable is adjusted to keep the process output on target (Montgomery 2013). Unlike SPC which will adjust the process variables only when assignable causes are detected, EPC adjusts the process continuously whenever the variable of interest deviates from the target value without removing the assignable causes. The difference between EPC and SPC comes from the fundamental models constructed for them (Crowder *et al.* 1997, Stoumbos *et al.* 2000).

The purpose of SPC is to determine if a process is in control or, conversely, out of control. A process is defined as "any combination of machines, tools, methods, materials and people employed to attain the desired quality of a product or service" (Bicking and Gryna 1979). Leitnaker and Cooper (2005) pointed out the need to use SPC as a tool for active process study, rather than simply as a method for maintaining and controlling processes. SPC includes many different monitoring techniques and charts. SPC charts have several different functions (Kolesar 1993, Wheeler 2004). At first, they are used at the start of an SPC implementation to determine if a process is in control. This helps in understanding the process, removing assignable causes and measuring in-control variability. Later, the prospective monitoring function of SPC charts is to detect the out-of-control cases in the process. SPC charts will have the most benefit when management is committed to continual process improvement (Wheeler 2004, Montgomery 2013).

MacCarthy and Wasusri (2002) reviewed the non-standard applications of SPC charts reported in the literature from the period 1989 to 2000. They highlighted the critical fundamentals and technical issues that are needed to be addressed when applying SPC chart techniques in a range of non-standard applications. Koshy and Koshy (2004) provided a new management charting technique along the lines of the SPC chart. Grygoryev and Karapetrovic

(2005) illustrated a model for measuring classroom performance, which makes use of SPC in combination with classroom assessment techniques (CATs).

Wu and Tian (2005) proposed a single weighted-loss function (WL) chart for monitoring the process mean and variance simultaneously. Thor *et al.* (2007) systematically reviewed the literature regarding how SPC has been applied to healthcare quality improvement and demonstrated the benefits, limitations, barriers and facilitating factors related to such applications. Wu *et al.* (2009*a*) presented an SPC method for simultaneously monitoring the time interval *t* and magnitude *x*. It, essentially, combines a t chart and an X chart. Du and Xi (2011) provided guidelines for developing selective neural network ensemble and SPC-based fault diagnosis systems with integration of engineering knowledge in assembly processes. Haridy *et al.* (2011) proposed an integrated framework of SPC and Design of Experiments (DOE) for optimizing the wire electrochemical turning process. Nezhad and Niaki (2010) employed an iterative approach to analyze and classify the states of univariate quality control systems. Mataragas *et al*. (2012) proposed an integrated SPC approach to monitor and improve carcasses quality in slaughterhouses. Singh *et al*. (2012) applied SPC techniques to improve the quality management of technical staff in the educational institutions.

2.2 Sources of Product Variation

The ideal manufacturing process is one that produces products that are identical (i.e., same size, shape, etc.). However, in reality, this is not possible. Products will always vary from one to another. As a result, manufacturers have learned to accept variation as part of the manufacturing process (Chase and Stewart 1995). When products are designed, their specifications include tolerances. This is the amount or the range of variation that can be tolerated. When the product variation exceeds the tolerance range, problems can result (e.g., parts that are supposed to fit together with each other may not fit, thereby resulting in product defects).

The aforementioned sources of product variation can be grouped into two categories, assignable and chance causes (Grenier *et al.* 1997). The former refers to causes that can be avoided, such as human error or broken tools, while the latter refers to causes that are often random in nature and are beyond human control, such as the variation in the hardness of steel. When only chance causes exist, the process is said to be in control. In other words, variation due to chance causes is variation that must be 'lived with' unless one is willing and able to change the technology or process design (Evans and Lindsay 2002). A process that is in control is expected to have some minor variation. The variation resulting from the presence of chance causes is random and follows no discernible pattern (Delmar and Sheldon 1988). On the other hand, the variation due to assignable causes introduces non-random variation, which follows a pattern.

Much of the effort in quality control is dedicated to isolating assignable causes by detecting the existence of patterns in the data. The presence of assignable causes leads to an increase in product variation, resulting in defects. Chance causes are innate to the production process and are due to causes that are not well understood. Assignable causes of variation are other forms of variability that are not considered to be part of the normal system. These assignable causes of variation are not random in nature and therefore can be detected, investigated and eliminated. When a process is operating in the presence of assignable causes, it is said to be out of control (Montgomery 2013). Evans and Lindsay (2002) explained the two sources of variation in a manufacturing process:

(1) Inherent or chance causes of variation: these chance causes are the result of slight variations in machine performance, material composition, temperature and humidity of the work environment, etc.

(2) Assignable causes of variation: these assignable causes usually produce a large amount of process variation, and as such are readily detectable. Typical examples are inexperienced operators, faulty process setups, defective material and machine malfunction.

SPC charts are built on the principle of allocating the observed variation in performance to these two categories of sources: chance causes and assignable causes (Shewhart 1931, Deming 1986, Montgomery 2013). Often, production processes will operate in an in-control state, producing acceptable products for relatively long periods of time. Assignable causes will occasionally occur, resulting in a shift to an out-of-control state where a larger proportion of the process output does not conform to requirements. A main objective of control charts is to quickly detect the occurrence of assignable causes or process shifts so that the investigation and the appropriate corrective action may be undertaken before many nonconforming units are manufactured.

2.3 Rational Subgroups

Another important concept behind SPC is what Shewhart called the rational subgroup concept. A rational subgroup is a group or sample in which all of the observations are generated under conditions in which only random effects are responsible for the observed variation (Nelson 1988, Hawkins and Olwell 1998, Wheeler 2004). A subgroup must be a representative of process performance. Subgroups or samples should be selected so that if assignable causes are present, the chance for differences between subgroups will be maximized, while the chance for differences within a subgroup will be minimized. Usually, time order is a good basis for the selection of subgroups because it allows detecting time related assignable causes. Sefik (1998) provided an overview on how to choose rational subgroups while using control charts to monitor processes. In general, the approaches to construct rational subgroups expressed by Montgomery (2013) are as follows:

(1) Samples consist of units produced at the same time or as closely together as possible. This approach is used to detect process shifts.

(2) Each sample is a random sample of all process output over the sampling interval. This approach is used to make decisions about the acceptance of all products that have been produced since the last sample.

(3) If several individual machines pool their output into a common stream, separate control charts should be applied to theses individual machines to avoid confusing the origin of assignable causes.

2.4 Variable Control Charts

2.4.1 Shewhart charts for variables

Walter A. Shewhart first introduced SPC in 1924 while working at Bell Laboratories "In a memorandum prepared on May 16, 1924, Shewhart made the first sketch of a modern control chart". Shewhart (1931) proposed the use of statistical control charts for quality monitoring. These charts are the present day Shewhart control charts, namely the X, $\overline{X}$, R and S charts for variable data and p, np, c and u charts for attribute data. The control chart procedure emphasizes the improvement of quality by monitoring the process rather than correcting defects in the final product.

If *w* is a sample statistic that measures a quality characteristic of interest with a mean μ_w and a standard deviation of σ_w, then the center line *CL*, upper control limit *UCL* and lower control limit *LCL* are determined by:

$$\begin{aligned} UCL &= \mu_w + \theta\sigma_w \\ CL &= \mu_w \\ LCL &= \mu_w - \theta\sigma_w \end{aligned} \qquad (2.1)$$

where θ is the "distance" of the control limits from the center line, expressed in standard deviation. A common choice is $\theta = 3$. Control charts developed according to these principles are often called Shewhart control charts.

Wheeler and Chambers (1992) emphasized that SPC is a way of thinking and that the Shewhart chart is a catalyst for that thinking. In order to have a stable process and to consistently avoid the state of chaos, it is necessary to use Shewhart charts. They built upon the original writings of Shewhart to discuss the theory and the empirical concept that lead to the method of control charting. Devor *et al.* (1992) and Mitra (1998) presented information summarizing the current use of the Shewhart style of SPC charts. Wu *et al*. (2006*b*) employed the curtailment to develop a new SXC (sum of *x*s with curtailment) chart. The curtailment technique has been widely used in acceptance sampling plans where a lot can be rejected without completing the inspection of the whole sample (Montgomery 2013). Recently, Hung and Hong (2010) developed Shewhart-type control charts for monitoring the variance components of two-factor mixed effect model. Schafer *et al*. (2011) described Shewart charts and provided examples of their applications to monitor quality in testing programs. Celano *et al*. (2012) evaluated the economic performance of Shewhart charts.

More details about the construction and operation of Shewhart control charts can be found in most statistical quality control books (Grant and Leavenworth 1996, Montgomery 2013). The Shewhart control chart is one of the most popular statistical tools for monitoring a quality characteristic of interest. This arises from its simplicity and effectiveness (Montgomery 2013). Other more sophisticated charts are not as widely used (Saniga and Shirland 1977). Several authors (Wheeler and Chambers 1992, Grant and Leavenworth 1996, Wheeler 2004, Montgomery 2013) presented the excellent theory and practical applications of control charts. These authors typically wrote from a manufacturing perspective, but usually made it clear that Shewhart charts can be used for any process.

2.4.2 Variable CUSUM, EWMA and SPRT charts

Three other sophisticated control chart methods for monitoring variables are the Cumulative Sum (CUSUM) chart, Exponentially Weighted Moving Average (EWMA) chart and

Sequential Probability Ratio Test (SPRT) chart. Rapid detection of changes in the quality characteristic of interest and ease of computation through recursive equations are some of the many good properties of the CUSUM, EWMA and SPRT charts that make them attractive.

The first CUSUM chart was introduced by Page (1954) to monitor the mean of a quality characteristic. The quality statistic C_t for the tth sample in an upper one-sided CUSUM chart is formed as follows (Hawkins and Olwell 1998):

$$\begin{aligned} C_0 &= 0 \\ C_t &= \max\left(0, C_{t-1} + (x_t - \mu_0) - k\right) \end{aligned} \tag{2.2}$$

where μ_0 is the in-control mean of the quality characteristic x and k is the reference parameter.

The basic principle of this chart is to take samples from the process at fixed sampling intervals and use a control statistic based on a cumulative sum of differences between the sample means and the target value (Lucas 1985*b*, Reynolds *et al.* 1990, Lu and Reynolds 2001, Zhang and Wu 2007).

EWMA chart was first introduced by Roberts (1959) to achieve faster detection of small changes in the mean. The EWMA chart is used extensively in time series modeling and forecasting for processes with gradual drift (Box *et al*. 1994). It provides a forecast of where the process will be in the next instance of time. It thus provides a mechanism for dynamic process control (Hunter 1986). The statistic E_t in an upper one-sided EWMA chart is defined as:

$$\begin{aligned} E_0 &= \mu_0 \\ E_t &= \lambda x_t + (1-\lambda) E_{t-1} \end{aligned} \tag{2.3}$$

where μ_0 is the in-control mean and λ is the smoothing parameter.

Stoumbos and Reynolds (1997*a*) employed the idea of Sequential Probability Ratio Test (SPRT) (Wald 1947) in developing a variable SPRT control chart for monitoring the process mean. They conducted systematic performance comparison between the variable SPRT chart and many other charts (such as the $\overline{X}$ chart and CUSUM chart) and their variable sampling rate versions. The results revealed that the variable SPRT chart detects most mean shifts substantially

faster than all other charts. The basic idea of the SPRT chart is changing the sampling rate based on the process status. A high sampling rate should be used when there is an indication of a shift in the process while a low sampling rate should be used when the process is stable. Within a sample of an upper one-sided SPRT chart, the statistic S_i is updated for each observation as follows:

$$\begin{aligned} S_0 &= 0 \\ S_t &= S_{t-1} + x_t - \gamma \end{aligned} \tag{2.4}$$

where γ is the reference value.

The CUSUM and EWMA charts usually outperform Shewhart charts (Radaelli 1994, White *et al*. 1997, Reynolds and Arnold 2001, Yang *et al*. 2012). Vargas *et al.* (2004) presented a comparative study of the performance of CUSUM and EWMA control charts. The objective of their study is to clarify when CUSUM and EWMA control charts are good choices for process control. Reynolds and Stoumbos (2005) showed that an EWMA or CUSUM chart combination with Shewhart chart is very effective for detecting small or large shifts in mean μ or variance σ^2. The SPRT chart is substantially more effective than Shewhart, CUSUM and EWMA charts (Stoumbos and Reynolds 1997*a*, Stoumbos and Reynolds 2001, Ou *et al*. 2012*b*). Since automatic measuring and distributed computing systems become a norm in SPC applications, the CUSUM, EWMA and SPRT charts have been widely used across industries for monitoring process shifts (Lucas 1989, Zhao *et al.* 2005, Shu *et al.* 2008, Li *et al*. 2009, Li *et al.* 2010).

2.4.3 Single charts for monitoring mean and variance

The variable quality characteristic is often characterized by two distribution parameters: the mean and variance. Thus, many variable control charts are designed to detect shifts in both mean and variance. Usually, two separate charts are needed; one chart for detecting mean shifts and another for detecting variance shifts. However, much research efforts have also been made to use a single chart only for detecting both mean and variance shifts. White and Schroeder

(1987) first developed a single chart for monitoring the mean and variance of an electronic component. Domangue and Patch (1991) developed some omnibus EWMA quality-monitoring schemes to detect changes in both mean and variance. Chen and Cheng (1998) also designed a single chart to monitor both the mean and variance. The proposed chart is shown to be as effective as the joint $\bar{X}\&S$ chart.

Chen *et al.* (2001) proposed a single EWMA chart to monitor the mean and variance, and indicate the direction of the shift. Wu and Tian (2005) developed a Weighted Loss CUSUM (WLC) chart to monitor both mean and variance of a variable. It is found that the new WLC chart is, on average, more effective than Shewhart $\bar{X}\&S$ chart by about 30%. Wu *et al*. (2005) proposed a single chart with Variable Sample Sizes and Sampling Intervals (VSSI) to monitor the process shifts in mean and variance simultaneously. This chart is based on Adjusted Loss function (AL) and is able to outperform the VSSI $\bar{X}\&R$ and $\bar{X}\&S$ charts by 10% from an overall viewpoint. Cheng and Thaga (2006) conducted an overview on using single charts to monitor both mean and variance. They concluded that the single charts are more applicable and appealing than simultaneous charts because they are easy to interpret and clearly show the direction of the shift when an out-of-control signal occurs. They also emphasized that it is impossible to identify whether the change in the process has actually occurred due to a mean shift or variance shift.

In recent years, Costa and De Magalhães (2007) used a Non-central Chi-square Statistic (NCS) chart to monitor both mean and variance. It is found that the NCS chart is more sensitive than the $\bar{X}\&R$ chart for detecting shifts in mean and variance. Wu and Wang (2007) established a single CUSUM (1-CUSUM) chart to detect two-sided mean shifts and increasing variance shift by checking samples of a single observation (i.e., sample size $n = 1$). This 1-CUSUM scheme outperforms many other control charts for detecting shifts in mean and variance. Teh *et al*. (2011) designed a sum of squares double EWMA (SS-DEWMA) chart to simultaneously monitor the process mean and variance in a single chart. Teh *et al*. (2012) further developed a new Generally

Weighted Moving Average (GWMA) chart for a simultaneous monitoring of the process mean and variance. Zhang *et al*. (2012) proposed a new adaptive single control chart which integrates EWMA procedure with the generalized likelihood ratio test statistics to jointly monitor both the mean and variability of a process. This new chart is effective in detecting the disturbances that shift the process mean and variance, or lead to a combination of both effects.

2.5 Attribute Control Charts

Attribute data, or data taking the form of counts, play a vital role in quality improvement. Many quality characteristics cannot be conveniently represented numerically, but can be represented as conforming or nonconforming (Montgomery 2013). Generally speaking, most manufacturing plants using attribute control charting are paying close attention to nonconformance. This data is counted and plotted as discrete events. The most popular attribute control charts are p chart (for fraction nonconforming), np chart (for number of nonconforming items), c chart (for number of nonconformities) and u chart (for number of nonconformities per unit). Brassard and Ritter (1994) detailed a flow diagram (Figure 2.1) for selecting a chart from these four charts based on the type of the attribute data. This outline illustrates the difference between defect and defective data.

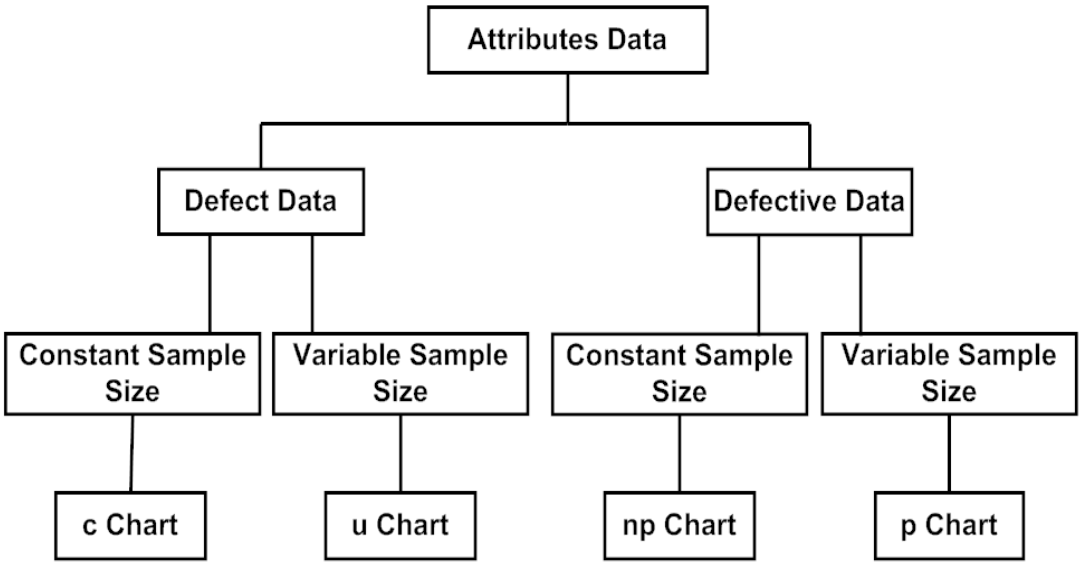

Figure 2.1: Attribute Data Control Chart Selection

2.5.1 p, np, c and u charts

The p chart is used to monitor the fraction nonconforming. The fraction nonconforming is the ratio of number of defectives to the total number of items. For example, in a hospital, the fraction nonconforming may be the ratio of number of unsatisfied patients to the total number of patients. The center line and control limits are calculated as follows:

$$\begin{aligned} CL &= p_0 \\ UCL &= p_0 + 3\sqrt{p_0(1-p_0)/n} \\ LCL &= p_0 - 3\sqrt{p_0(1-p_0)/n} \end{aligned} \tag{2.5}$$

where p_0 is the in-control value of the fraction nonconforming and n is the sample size.

To use the p chart, users have to convert the number of defectives in a sample to a fraction nonconforming. In this case, it may be more convenient to switch to the np charts since numbers of defectives from samples are plotted directly instead of the fraction nonconforming. One disadvantage of the np chart is that the sample size should be constant, otherwise the control limits and center line will change. The center line and control limits formulas are given below:

$$\begin{aligned} CL &= np_0 \\ UCL &= np_0 + 3\sqrt{np_0(1-p_0)} \\ LCL &= np_0 - 3\sqrt{np_0(1-p_0)} \end{aligned} \tag{2.6}$$

The nonconformity is usually a minor defect in a unit. One or a few nonconformities may not cause the entire unit to be scrapped. However, the nonconforming item (defective) is a unit that fails to meet the function or design requirement and therefore must be rejected. A c chart is used to monitor the number of nonconformities in a sample of n units. The c chart usually requires a constant sample size. This control chart assumes that the occurrences of the nonconformities follow a Poisson distribution. The center line and control limits are given below:

$$\begin{aligned} CL &= c_0 \\ UCL &= c_0 + 3\sqrt{c_0} \\ LCL &= c_0 - 3\sqrt{c_0} \end{aligned} \tag{2.7}$$

where c_0 is the in-control value of the average number of nonconformities.

The u chart is used instead of the c chart when the sample size is not constant. u chart is used to monitor the number of nonconformities per unit. The center line and control limits are determined as follow:

$$\begin{aligned} CL &= u_0 \\ UCL &= u_0 + 3\sqrt{u_0 / n} \\ LCL &= u_0 - 3\sqrt{u_0 / n} \end{aligned} \tag{2.8}$$

where u_0 is the in-control value of the average number of nonconformities per unit.

The sample size of the charts is critical and should be determined appropriately for an effective monitoring. Usually, a large sample size is required when the fraction nonconforming is very small. However, the sample size depends on the available resources. Rocke (1990) gave a simple procedure for constructing a control chart for fraction nonconforming or number of nonconformities when sample sizes vary. Su and Tong (1997) suggested using a Neyman-based chart or fuzzy Adaptive Resonance Theory (ART) chart instead of c chart when the occurrence of defects in an item of a process does not follow the Poisson distribution. One drawback of the Neyman-based control chart is that it cannot be applied to the cases of large sample sizes. Acosta-Mejia (1999) analyzed the performance of several charts for monitoring increases and decreases in p based on their run length (RL) distribution. The results showed that replacing the lower control limit by a simple runs rule can result in an improvement in the overall chart performance. Schwertman and Ryan (1999) developed a dual np chart that comprises two charts. The first chart monitors the quality deterioration and the second gives a final decision on the process status.

Wu *et al.* (2001*c*) presented a Fractional Control Limits (FCL) scheme for the np control charts. The FCL scheme enables the quality engineers to have more control on the designs of the np charts. Wu and Luo (2003) investigated an algorithm for designing the np control charts based on their statistical performance (3-triplet np chart). The new chart is designed by seeking an optimal combination of the sample size and the control limits. Khoo (2003) discussed an approach for increasing the sensitivity of the p chart by incorporating runs rules. Wu and Luo

(2004) developed an algorithm for the optimal designs of the adaptive np control charts. Khoo (2004) discussed a more efficient alternative to the standard p chart based on the construction of a moving average control chart for fraction nonconforming *p*.

Gadre and Rattihalli (2005) proposed a Unit and Group Runs (UGR) chart to detect an increase in fraction nonconforming *p*. The proposed chart starts with unit-level inspection and switches to the group-level inspection and back to the unit-level inspection according to a specified rule. Wu and Jiao (2007) further improved the overall performance of the UGR chart. Chakrabortiand and Human (2006) examined the effect of fraction nonconforming estimation on p chart. The results are useful in the study of the reliability of systems that involve binary data. Wu *et al.* (2006*a*) presented an algorithm for the optimal design of the np control chart with curtailment. The np chart with curtailment doubles the detection effectiveness of the conventional np charts. Wu and Jiao (2008) proposed an attribute chart, the MON chart, for monitoring the mean of a variable. Wu *et al*. (2009*b*) also proposed an np chart to monitor the mean of a variable. This chart uses the statistical warning for the classification of conforming or nonconforming units. Ho and Costa (2011) designed an np chart to monitor the wandering behaviour of the process mean.

Recently, Zhou and Lian (2011) proposed a new Variable Sample Size (VSS) np chart. The result shows that the performance of the new VSS np chart is considerably better than that of the classical np chart in all scenarios. Kooli and Limam (2011) proposed an economic design of the np chart using a variable sample size. This economic design algorithm leads to a significant cost savings. Jafari and Mirkamali (2011) developed new attribute charts based on the Maxima Nomination Sampling (MNS) method. These MNS based charts substantially outperform the conventional attribute charts. Yang and Yeh (2011) developed cause selecting control charts to monitor attribute data from two dependent processes. The simulation study shows that the cause selecting control charts outperform attribute Shewhart charts. Sellers (2012) developed a flexible control chart that encompasses the traditional attribute Shewart charts based on the Bernoulli and Geometric distributions.

2.5.2 Conforming run length (CRL) chart

The CRL chart is another type of attribute charts. It is mainly based on the Conforming Run Length (*CRL*). It has received a lot of attention in SPC researches and applications (Kaminsky *et al.* 1992, Glushkovsky 1994, Bourke 2001*b*). The statistic *CRL* is defined as the number of inspected units between two consecutive nonconforming units, including all conforming units in between as well as the last nonconforming unit.

The concept of the CRL chart relies on the change of the conforming run length *CRL* when a shift occurs in the process fraction nonconforming *p* (Bourke 1991). If an observed *CRL* value becomes smaller than the lower limit of the CRL chart, the process is considered to be out of control. Moreover, Xie *et al.* (1995) mentioned that the change of *CRL* is easier to detect than the change in *p* itself. Woodall (1997) highly recommended the CRL control chart in a review paper, especially when the fraction nonconforming *p* is very small.

The CRL chart is quite informative Shewhart-like charting technique. In Figure 2.2, the white and black dots denote conforming units and nonconforming units, respectively. A process starts at $t = 0$. Three samples of *CRL* are displayed: $CRL_1 = 4$, $CRL_2 = 5$ and $CRL_3 = 3$. In order to implement the CRL chart, one usually inspects every unit in the process (i.e., using 100% inspection).

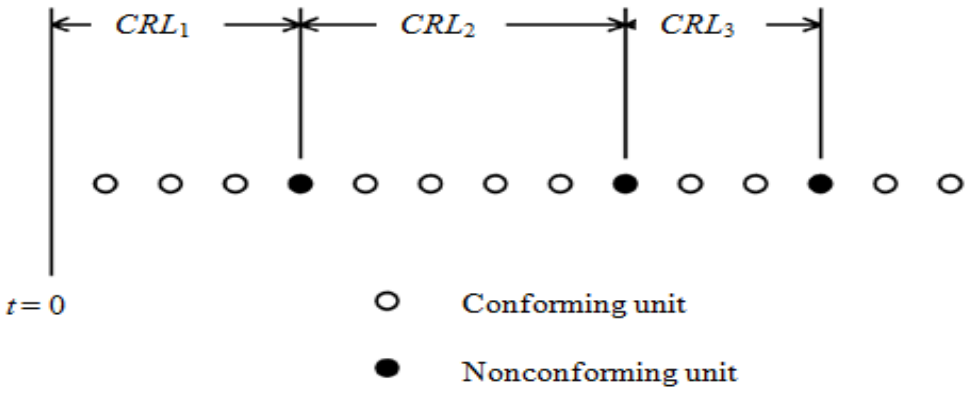

Figure 2.2: Conforming Run Length

The lower control limit *LCL* and the upper control limit *UCL* of a CRL chart are calculated as follows (Xie *et al.* 1995):

$$LCL = \frac{\ln(1-\alpha/2)}{\ln(1-p_0)}$$
$$UCL = \frac{\ln(\alpha/2)}{\ln(1-p_0)} \qquad (2.9)$$

where p_0 is the in-control, or nominal, value of the process fraction nonconforming and α is the specified probability of type I error. In using the CRL chart, each observed *CRL* value serves as a sample. If the sample value is smaller than the lower limit *LCL* (when $p > p_0$) or larger than the upper limit *UCL* (when $p < p_0$), the process is considered out of control. Otherwise, it is deemed under control.

For the CRL chart, the random variable *CRL* follows a Geometric distribution (Dudewicz and Mishra 1988). Consequently, the mean value of *CRL* (the average number of the inspected units in a *CRL* sample) is:

$$\mu_{CRL} = \frac{1}{p} \qquad (2.10)$$

and the cumulative probability function of *CRL* is

$$F_p(CRL) = 1-(1-p)^{CRL}, \qquad CRL = 1, 2, ... \qquad (2.11)$$

If detecting the increase in p is the only concern, a single lower control limit (L) is sufficient for the CRL chart. L can be derived easily from Equation (2.12) (Xie *et al.* 1995):

$$\alpha_{CRL} = F_{p_0}(L-1) = 1-(1-p_0)^{L-1}$$
$$L = \frac{\ln(1-\alpha_{CRL})}{\ln(1-p_0)} + 1 \qquad (2.12)$$

where α_{CRL} is the Type I error of the CRL chart. L must be rounded down to an integer. If a sample *CRL* is smaller than L, it is very likely that the fraction nonconforming p has increased and, therefore an out-of-control status is signaled.

Wu and Spedding (1999) derived the accurate formulae for calculating the out-of-control *ATS* (Average Time to Signal) of the CRL chart. These formulae take into account the steady-state model of fraction nonconforming p, in which the p value may shift at any point during a

conforming run length. Wu *et al.* (2001*b*) presented the general formulae for designing the control limits and evaluating the out-of-control *ATS* of the sum of CRLs chart. Recently, Wu *et al.* (2010*b*) proposed a Generalized CRL chart (GCRL chart) for monitoring the mean of a measurable quality characteristic *x* under 100% inspection.

2.5.3 Synthetic chart

Based on the general idea of the CRL chart, two synthetic control charts using warning limits to decide the status of samples were proposed, one for variables (Wu and Spedding 2000) and another for attributes (Wu *et al.* 2001*a*). The synthetic chart is actually an integration of the np chart and the CRL chart and it is able to provide the quality engineer with more freedom to adjust the charting parameters of the control chart, so that the out-of-control *ATS* and the Average Number of Defectives (*AND*) can be reduced significantly. Unlike the np chart that uses the information about the number *d* of nonconforming units in the last sample, the synthetic chart makes use of the information of the time interval between two consecutive nonconforming samples. A sample is nonconforming, if *d* falls beyond the warning limits.

The synthetic control chart consists of both np-based and CRL-based procedures. To run a synthetic chart, the following four charting parameters need to be determined: (1) the warning limit *w* of the np chart, (2) the sample size *n*, (3) the lower control limit *L* of the CRL chart, and (4) the upper control limit *U* of the CRL chart. The synthetic chart checks the conforming run length (*CRL*) which is defined as the number of inspected samples between two consecutive nonconforming samples, including all conforming samples as well as the last nonconforming sample (Bourke 1991, Xie *et al.* 1995). The operation of a synthetic chart is outlined in Figure 2.3.

Basically, a synthetic control chart functions the same way as an ordinary CRL chart, except that each unit in the CRL chart is replaced by a sample of *n* units in the synthetic chart. Referring to Figure 2.2, for a synthetic chart, the white and black dots will now represent the

conforming and nonconforming samples, respectively. In a conventional CRL chart, the fraction nonconforming p is the probability that the nonconforming unit occurs. However, in the synthetic chart, this probability refers to the probability that the nonconforming sample occurs.

In the following years, many extensions of the synthetic chart were proposed (Wu and Yeo 2001, Davis and Woodall 2002, Wu and Jiao 2007, Khoo *et al.* 2008). Researchers are interested in the applications and optimization of the synthetic chart and a lot of new types of synthetic charts have been proposed. Sim (2003) discussed the combined $\overline{X}$ and CRL charts under the assumption that the quality characteristic of interest follows a gamma distribution. The synthetic chart for exponential data was proposed by Scariano and Calzada (2003). However, while the synthetic chart for exponentials outperforms the Shewhart chart for individuals, the EWMA and CUSUM charts are shown to be superior in detecting decreases in the exponential mean. A special synthetic chart based on the non-central chi-square statistic is proposed using a Markov chain model (Costa and Rahim 2006). Chen and Huang (2006) developed a variable sampling interval synthetic chart for detecting the shifts in mean and variance. It has been found that varying the sampling intervals of a synthetic chart is able to improve the detection effectiveness significantly. Bourke (2008) re-evaluated the performance of the synthetic chart and compared it with other charts.

Castagliola and Khoo (2009) proposed a synthetic scaled weighted variance control chart to monitor the process mean of skewed populations. This control chart is an improvement of the synthetic weighted variance chart suggested by Khoo *et al.* (2008), for detecting a negative shift in the mean. Machado *et al.* (2009) proposed a synthetic chart based on the sample variances of two quality characteristics to control the covariance matrix of bivariate processes. The proposed chart is always more efficient than the chart based on the generalized variance. Costa *et al.* (2009) proposed a synthetic control chart with two-stage testing to control the process mean and variance. Aparisi and De Luna (2009) developed the synthetic-T^2 control chart which consists of a CRL chart and a Hotelling's T^2 chart. Khilare and Shirke (2010) presented a synthetic control

chart for detecting shifts in the process median. Pawar and Shirke (2010) provided a nonparametric Shewhart-type synthetic control chart based on the signed-rank statistic to monitor shifts in the known in-control median of a process. Here, the synthetic control chart is a combination of a signed-rank chart (Bakir 2004) and CRL chart (Bourke 1991). Most recently, Khilare and Shirke (2012) proposed a nonparametric synthetic chart for controlling the fraction nonconforming p in a process.

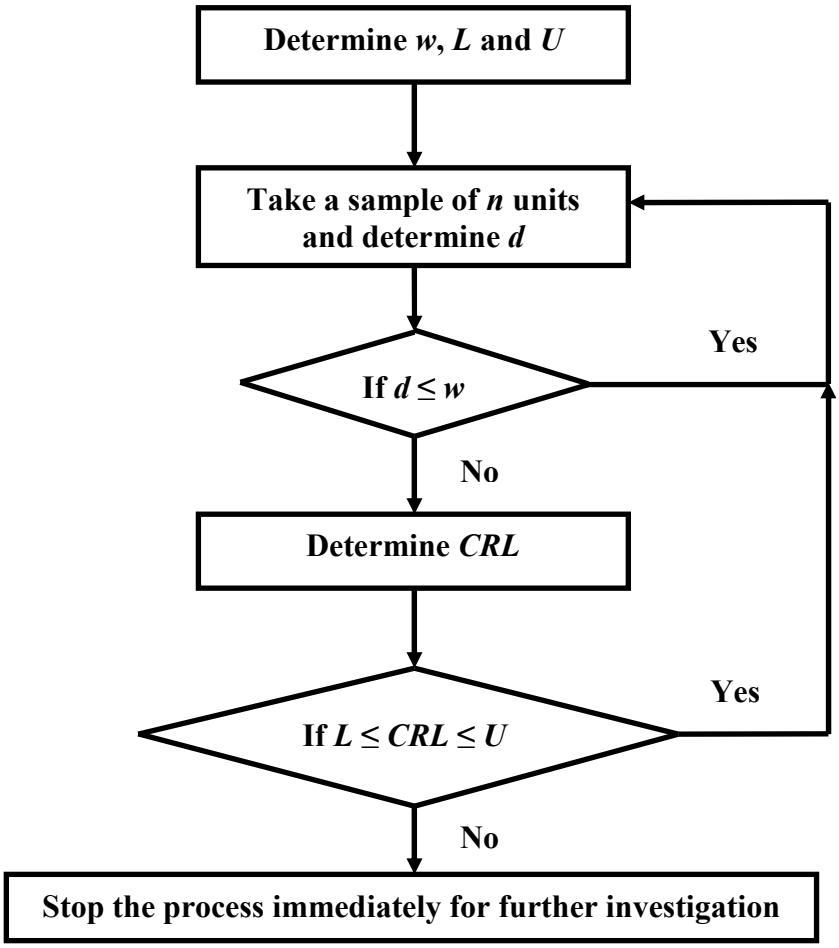

Figure 2.3: Operation of a Synthetic Chart

2.5.4 CUSUM chart

A typical CUSUM chart for monitoring the number d of nonconforming units is the binomial CUSUM chart. This chart is so named because of the assumption that d follows a binomial distribution. The binomial CUSUM chart examines the cumulative number of nonconforming units in sequential samples (Lucas 1985*a*). The first CUSUM chart was

introduced by Page (1954) to monitor the mean of a quality characteristic. The statistic to be updated and plotted for the *t*th sample in an upper one-sided binomial CUSUM chart is C_t.

$$\begin{aligned} C_0 &= 0 \\ C_t &= \max\left(0, C_{t-1} + (d_t - d_0) - k\right) \end{aligned} \tag{2.13}$$

where d_t is the number of nonconforming units in the *t*th sample, d_0 is the in-control value equal to (np_0) and k is the reference parameter. The choice of k depends on the in-control fraction nonconforming p_0 and a specified out-of-control fraction nonconforming p_1 (Gan 1993):

$$k = \frac{n \ln\left[(1-p_0)/(1-p)\right]}{\ln\left[(1-p_0)/(1-p)\right] - \ln\left[(p_0)/(p)\right]} \tag{2.14}$$

In Equation (2.13), the statistic C_t may increase or decrease depending on whether the sample shift $(d_t - d_0)$ is larger or smaller than zero. However, C_t is always shrunk toward zero by the reference parameter k. When an increasing p shift occurs, C_t tends to become larger and larger. Sooner or later, a sample point will exceed the control limit H of the CUSUM chart, and thereby a signal is produced. The CUSUM chart provides the quality assurance (QA) engineers with more freedom to adjust the control parameters (e.g., k and H), so that the out-of-control *ATS* can be minimized. The CUSUM chart incorporates all the information in the sequence of observed sample data. While the CUSUM chart is more sensitive to small and moderate shifts in fraction nonconforming p, it is not effective for detecting large p shifts, because the CUSUM chart does not make a decision merely based on the latest sample and is unable to respond promptly to a sudden and large p shift.

Kemp (1962) described the use of the CUSUM chart for controlling the percentage of defective items being produced. Woodall (1984) extended the Markov chain representation of the one-sided CUSUM procedure proposed by Brook and Evans (1972) to the two-sided CUSUM procedure. Lucas (1985*b*) detailed the design of the CUSUM chart. Lucas (1989) also studied the performance of the binomial CUSUM chart when the defect level is very low. Hawkins (1992) proposed a general algorithm for evaluating the *ARL* of this chart. Gan (1993)

further developed an optimal design of the binomial CUSUM chart to minimize *ATS* at a particular *p* shift value. Radaelli (1994) examined the Poisson approximation to the binomial CUSUM chart. White and Keats (1996) developed a computer program to calculate the *ARL* for the Poisson CUSUM scheme. Woodall (1997) provided a comprehensive review of the control charts for attributes including the binomial CUSUM chart. Some researchers compared the performance of the binomial CUSUM chart with other charts such as the c chart (White *et al.* 1997) and the Bernoulli CUSUM chart (Reynolds and Stoumbos 2000).

Bourke (2001*a*) investigated the operating characteristics of the binomial CUSUM chart under 100% inspection and steady-state mode. Wu and Tian (2005) proposed a CUSUM chart based on the weighted loss function. Wu *et al.* (2008*a*) studied a unique feature of the binomial CUSUM chart in which the difference $(d_t - d_0)$ is replaced by $(d_t - d_0)^w$ in the formulation of the cumulative sum. A large exponential *w* should be adopted if the size of process shifts is generally large and vice versa. The results revealed that this new feature can enhance the detection effectiveness when fraction nonconforming *p* becomes three to four times as large as the in-control value p_0. Szarka and Woodall (2012) mathematically proved that the steady-state properties of the Bernoulli CUSUM chart are the same as those of the Geometric CUSUM chart.

2.5.5 EWMA chart

Another effective tool for detecting small and moderate shifts in fraction nonconforming *p* is the binomial EWMA chart. This chart also uses cumulative information from all samples up to the last one and has quite similar operating characteristics as the CUSUM chart (Reynolds and Stoumbos 2004*b*). The EWMA chart was first introduced by Roberts (1959) to achieve faster detection of small changes in the mean. The EWMA chart is used extensively in time series modeling and forecasting for processes with gradual drift (Box *et al*. 1994). It provides a forecast of where the process will be in the next instance of time. Thus, it provides a mechanism for

dynamic process control (Hunter 1986). A statistic E_t is updated and plotted for the tth sample in an EWMA chart for detecting upward p shifts.

$$E_0 = 0$$
$$E_t = \lambda(d_t - d_0) + (1-\lambda)E_{t-1} \qquad (2.15)$$

The parameters of an EWMA chart include the smoothing parameter λ ($0 < \lambda \leq 1$) and the control limit W. Lucas and Saccucci (1990) gave tables to select the value of λ. The EWMA chart produces an out-of-control signal when E_t becomes larger than W.

As in the CUSUM chart, the EWMA control chart is also based on the intuition of accumulating information over time. However, the main difference between the CUSUM and the EWMA chart is the weights applied to previous data. The CUSUM chart uses equal weights for the data from the last reinitialization time to the current time and forgets the data before that since a reinitialization is a decision in favor of statistical control. On the contrary, a EWMA chart uses exponentially discounted weighting of the previous observations.

Gan (1990) proposed a Markov chain approach to calculate the *ARL* of the binomial EWMA control chart. Testik *et al*. (2006) studied the effect of estimating the mean on the performance of the Poisson EWMA control chart. Arthur *et al.* (2008) developed EWMA charts based on non-transformed geometric, binomial and Bernoulli counts. The proposed EWMA control charts outperform, in numerous cases, the CUSUM control charts developed by Chang and Gan (2001) for monitoring high-yield processes. Epprecht *et al.* (2010) proposed an optimal design for the EWMA chart with variable sampling interval. Spliid (2010) proposed an EWMA control chart for Bernoulli data. The proposed chart is well suited for surveillance of a great variety of activities in production and service industries.

2.5.6 SPRT chart

A distinguishing feature of the variable sampling interval (VSI) and variable sample size (VSS) control charts developed by many authors (Rendtel 1990, Prabhu *et al.* 1994, Costa 1997)

is their ability to vary the sampling interval and/or sample size of the next sample based of the value of the monitoring statistic at the current sample. This approach to vary the sampling rate requires the knowledge of the sampling interval and sample size to use at the next sampling point before reaching this point. Another approach to vary the sampling rate can be used for situations in which the sample size of the current sampling point is not determined beforehand, but instead it can be determined by the data in the current sample as it is taken. The concept of determining the sample size based on the data in the current sample is the basic principle of sequential analysis (Wald 1947, Ghosh 1970).

This concept was employed by Daudin (1992) for developing a control chart for monitoring the mean of a process by using two different sample sizes. This concept was also used by Stoumbos and Reynolds (1996) in developing a Sequential Probability Ratio Test (SPRT) chart for monitoring a general process parameter and also by Stoumbos and Reynolds (1997*a*) in developing a variable SPRT control chart for monitoring the process mean. Stoumbos and Reynolds (1997*b*) employed the Corrected Diffusion Theory (CDT) to evaluate the properties and statistical design of SPRT charts. Reynolds and Stoumbos (1998) extended the generalized SPRT chart presented in Stoumbos and Reynolds (1996) to monitor the process fraction nonconforming p and proposed an SPRT chart. The SPRT is a general sequential test introduced by Wald (1947). It can be applied to test a simple null hypothesis against a simple alternative hypothesis. For the case of a test involving the fraction nonconforming p, the SPRT is used to test the null hypothesis H_0: $p = p_0$ against the alternative hypothesis H_1: $p = p_1$. In the context of monitoring p, p_0 would be the in-control value of p, and p_1 would usually be a value larger than p_0. The fraction nonconforming p_1 is the result of an assignable cause that should be detected quickly. The SPRT requires the specification of two control limits g and H where $g < H$. For an upper one-sided SPRT chart (where $-\infty < g < H < \infty$),

$$\begin{aligned} S_0 &= 0 \\ S_t &= S_{t-1} + x_t - \gamma \end{aligned} \qquad (2.16)$$

where $0 < \gamma < 1$, and x_t is a Bernoulli random variable which is defined as $x_t = 1$ if the tth item is defective and $x_t = 0$ otherwise. The reference value (γ) depends on p_0 and p_1 (Reynolds and Stoumbos 1998):

$$\gamma = \left(-\ln\left(\frac{1-p_1}{1-p_0}\right)\right) \Big/ \left(\ln\left(\frac{p_1(1-p_0)}{p_0(1-p_1)}\right)\right) \tag{2.17}$$

In the SPRT chart, a sampling point is taken for every sampling interval h. At each sampling point, an SPRT is applied in which items from the process are inspected one by one. If $S_t < g$, H_0 is accepted and the process is thought to be in control. On the other hand, if $S_t > H$, H_0 is rejected and the process is thought to be out of control. Otherwise (i.e., $g \leq S_t \leq H$), the inspection is continued sequentially.

The sample size used at each sampling point depends on the SPRT that is applied at that point. If the inspection rate is very high, then the items can be inspected consecutively as they come from the production line. On the other hand, if the inspection rate is very slow compared with the production rate, then the items can be accumulated from the production line and inspected whenever possible. Alternately, the items still can be inspected as they come from the production line with some items skipped.

Stoumbos and Reynolds (2001) proposed the SPRT Fixed-Times (SPRTFT) chart in which each individual observation is too long to be neglected and observations in group are considered. The advantages of this chart are the high efficiency and the ease to be administrated in industry. Recently, Li *et al.* (2009) studied the double SPRT chart which applies a 2-SPRT at each sampling point. Approximate performance measures of the 2-SPRT control chart are obtained by the backward method with the Gaussian quadrature using a computer program. Ou *et al.* (2010) proposed a design algorithm for the SPRT chart in which the reference value (γ) of the SPRT chart is optimized. The design algorithm increases the overall effectiveness of the SPRT chart by more than 10%, on average. Ou *et al*. (2011) developed a new SPRT chart (ABS SPRT chart) to monitor the mean and variance of a variable simultaneously. The ABS chart is faster

than VSS CUSUM chart by about 30%. Ou *et al.* (2012*b*) further proposed an effective SPRT chart for detecting mean shifts. The new SPRT chart outperforms the $\bar{X}$ and CUSUM charts. The SPRT charts have also been applied to different areas, such as attribute sampling plan (Bagchi 1992), quality monitoring in robotized short arc welding (Stefan *et al.* 1996), monitoring for multiple quality categories (Yu *et al.* 2003), failure analysis for electronic products (Kwon *et al.* 2008) and radiation (Luo *et al.* 2010).

2.6 Combined Schemes of Control Charts

One possible approach for increasing the detection effectiveness of a control chart in broad situations is to combine it with other charts. Many researches have considered this approach for developing new schemes of control charts that combine the advantages and strengths of individual chart elements.

Lucas (1982) proposed a Shewhart-CUSUM control scheme that combines the key features of the Shewhart chart and CUSUM chart. In this scheme, the CUSUM component will quickly detect small process shifts while the addition of Shewhart component increases the speed of detecting large shifts. Lucas (1982) also commented that the new combined Shewhart-CUSUM scheme is almost as easy to use as a single CUSUM chart. Yashchin (1985) considered combined CUSUM–Shewhart schemes for detecting one- and two-sided process shifts. Abel (1990) addressed the use of combined CUSUM-Shewhart control schemes for count data when the data follow a Poisson distribution. He and Grigoryan (2006) proposed a combined scheme of double sampling $\bar{X}$ chart and S chart. The performance studies indicated that the new scheme has a better statistical efficiency than the combined EWMA and CUSUM schemes over certain shift ranges. Morias and Pacheco (2006) proposed a combined CUSUM-Shewhart scheme for binomial data. They commented that the combined np-CUSUM scheme may not be necessarily better than the individual charts from an overall viewpoint.

Recently, Wu *et al.* (2008*b*) presented the optimal design of Lucas's combined Shewhart-CUSUM scheme ($\overline{X}$ & CUSUM chart). While the optimal design effectively improves the overall performance of the $\overline{X}$ & CUSUM chart over the entire process shift range, it does not increase the difficulty for understanding and implementing this combined chart. Wu *et al.* (2010*a*) proposed a combined synthetic chart and X chart for monitoring the process mean. The performance study shows that this combined scheme is more effective than both the X chart and the variable synthetic chart over a wide range of mean shifts. Lee *et al*. (2012) proposed combined Double Sampling and Variable Sampling Interval s chart (DSVSI s chart) based on the idea of Carot *et al*. (2002). The performance evaluation shows that the DSVSI s chart is effective for detecting small shifts.

2.7 Measures of Performance

2.7.1 Type I and type II errors

Two typical types of response errors occur when using a traditional SPC chart. A type I error (or false alarm) is made when the process is judged to be out of control when it is, in fact, in control. A type II error is made when the process is judged to be in control when it is actually out of control. Both types of errors incur economic loss.

Type I error and Type II error are the bases to evaluate the performance of a control chart. Suppose a random variable d has a binomial distribution with an in-control fraction nonconforming p_0 and sample size n as shown in Figure 2.4. During operation, a process shift changes the fraction nonconforming to a larger out-of-control value p_1. The in-control probability curve with ($p = p_0$) is depicted in a solid line while the curve of the shifted or out-of-control process with ($p = p_1$) is plotted by a dashed line.

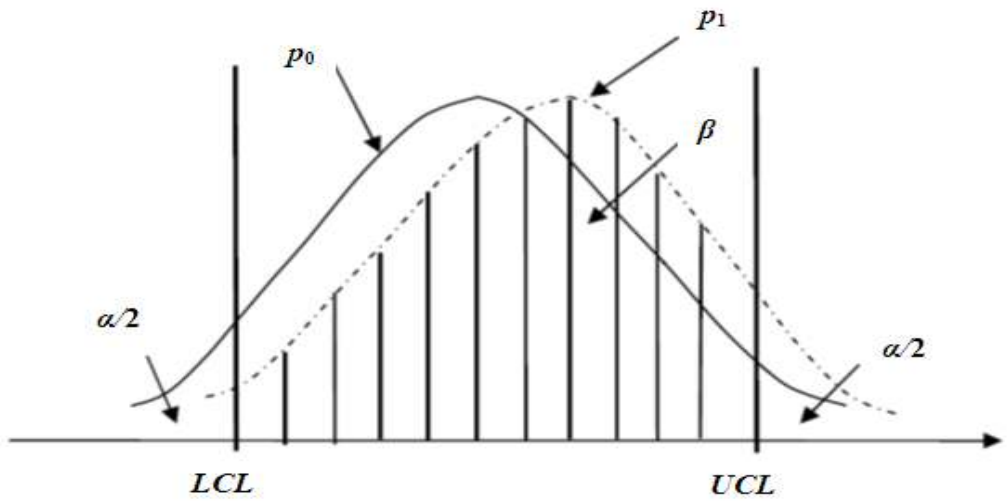

Figure 2.4: Binomial Distribution of a Random Variable

Type I error probability α is the area beyond *LCL* or *UCL* under the in-control curve. Type II error probability β is the area within *LCL* and *UCL* under the out-of-control curve. The probabilities of these two types of errors are determined as follows:

$$\alpha = \left(1 - P_r\left(d \le UCL\big|_{p_0}\right)\right) + P_r\left(d < LCL\big|_{p_0}\right) \tag{2.18}$$

$$\beta = P_r\left(d \le UCL\big|_{p_1}\right) - P_r\left(d < LCL\big|_{p_1}\right) \tag{2.19}$$

where the binomial cumulative probability function $P_r(D)$ of d can be calculated as follows:

$$P_r(D) = \Pr(d \le D) = \sum_{i=0}^{D} C_i^n p^i (1-p)^{n-i} \tag{2.20}$$
$$C_i^n = n!/i!\,(n-i)!$$

2.7.2 Average run length (*ARL*) and average time to signal (*ATS*)

Quality practitioners often make a decision concerning which control chart or what values of control limits to use for monitoring a quality characteristic of interest. The most accepted performance criterion is the Average Run Length (*ARL*), which is first introduced by Aroian and Levene (1950). *ARL* is the expected or average value of the random Run Length (*RL*) which can be classified into two types: in-control RL_0 and out-of-control *RL*.

In-control RL_0 is the number of samples from the start of a control chart until the time an alarm is triggered falsely when a process is in control. Out-of-control *RL* is the number of

samples from the time of the occurrence of an assignable cause (i.e., a shift from the in-control state to an out-of-control state) to the time that the control chart triggers an alarm. Consequently, the in-control ARL_0 is the average number of sample points that are plotted until a false alarm is produced while the out-of-control *ARL* is the average number of sample points that are plotted until an out-of-control case is detected. Usually, a control chart with a smaller out-of-control *ARL* has a better performance. The out-of-control *ARL* is commonly used as an indicator of the power (or effectiveness) of the control chart, whereas the in-control ARL_0 relates to the false alarm rate (Shu *et al*. 2007, Wu *et al.* 2008*a*).

The run length *RL* follows a Geometric probability distribution for given control limits when observations are independently and identically distributed (Quesenberry 1997). The distribution of *RL* is not a Geometric for the CUSUM charts or the Shewhart charts with supplementary runs tests. The distribution of CUSUM run lengths may be approximated by a Geometric distribution unless there is a low probability of extremely short run lengths (Lucas 1985*b*).

In SPC, a performance comparison among various control charts is often conducted. A common method is to compare the out-of-control Average Run Length (*ARL*) of the control charts on the condition that the in-control Average Run Length (ARL_0) of all charts is set equal to or larger than a specified value. There is always a trade-off between a larger in-control ARL_0 and a smaller out-of-control *ARL*. For a control chart, the *ARL* is calculated as:

$$ARL = \frac{1}{P} \tag{2.21}$$

where *P* is the power of the chart or the probability that a sample point exceeds the control limits. So the in-control ARL_0 and out-of-control *ARL* can be expressed in terms of Type I error (α) and Type II error (β), respectively:

$$ARL_0 = \frac{1}{\alpha} \tag{2.22}$$

$$ARL = \frac{1}{1-\beta} \tag{2.23}$$

For a two-sided chart, Type I error α and Type II error β are calculated using Equations (2.18) and (2.19), respectively.

Another performance measure is the Average Time to Signal (*ATS*). The out-of-control *ATS* is the average time required to detect the out-of-control case while the in-control ATS_0 is the average time to produce a false alarm. Figure 2.5 shows the in-control period (ATS_0), out-of control period (*ATS*) and sampling interval (*h*) of a typical control chart. The relationship between *ARL* and *ATS* can be expressed as:

$$ATS = ARL \times h \tag{2.24}$$

where *h* is the sampling interval between two consecutive sample points.

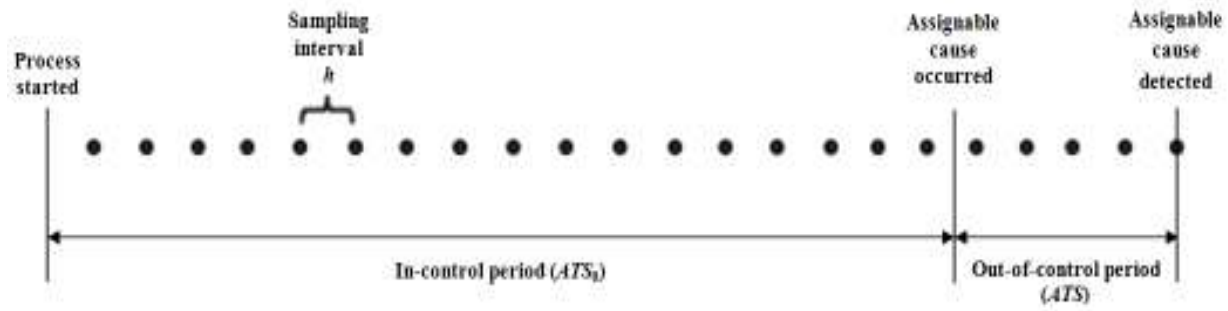

Figure 2.5: In-control Period, Out-of-control Period and Sampling Interval of a Typical Control Chart

2.7.3 Zero-state and steady-state mode

In calculating *ARL* or *ATS*, it is important to distinguish between the zero-state mode and steady-state mode of a process. In SPC literature, many researchers have used the zero-state mode to evaluate *ATS* (Saccucci *et al*. 1992, Borror *et al*. 1998, Davis and Woodall 2002). For the zero-state mode, the process may fall out of control from the beginning (Bourke 2008). In recent years, the steady-state mode has been increasingly adopted for evaluating *ATS* (Reynolds and Stoumbos 2005, Khoo *et al.* 2010, Lee 2010, Yang *et al*. 2011). This mode implies that the process starts and stays in an in-control condition for a long time and then a process shift occurs at some random time. This random time is assumed to have a uniform distribution between two

samples (Reynolds *et al*. 1990). The steady-state *ARL* (or *ATS*) is computed assuming that the quality statistic has reached its steady-state or stationary distribution condition by the random time point when the process change occurs (Reynolds and Stoumbos 2004*a*).

It is commonly accepted that the *ARL* or *ATS* values calculated under the steady-state mode are more realistic, as the steady-state mode allows the shift to occur randomly (Nenes and Tagaras 2008). Furthermore, since production processes often operate in an in-control condition for most or relatively long periods of time (Montgomery 2013), the steady-state mode is therefore more realistic than the zero-state mode. In alignment with this, the research in this thesis adopts the steady-state mode to calculate *ARL* and *ATS*.

2.7.4 Average extra quadratic loss (*AEQL*)

As mentioned before, the performance of a control chart can be measured by *ARL*. The out-of-control *ARL* at one or a few specified shift levels is often used as the objective function to be minimized in the design of a control chart (Morias and Pacheco 2006, Shu *et al*. 2007).

It is usually difficult to predict the magnitudes or sizes of process shifts in most applications (Reynolds and Stoumbos 2004*a*). Therefore a control chart should produce a small out-of-control *ARL* (or *ATS*) for process shifts of different sizes, or have an excellent overall performance across the entire shift range of interest. As a result, it is more applicable to make control charts efficient at signaling a range of process shifts and the objective function of the optimization should measure the holistic performance of the charts across the shift range rather than the effectiveness at one or a few particular points (Zhao *et al.* 2005). Recently, many researchers (Reynolds and Stoumbos 2004*b*, Wu *et al.* 2005, Wu *et al.* 2008*b*, Yang *et al*. 2012) used the Average Extra Quadratic Loss function (*AEQL*) to measure and compare the overall performance of the variable charts. When a process shift occurs, the in-control mean μ_0 and standard deviation σ_0 of a variable quality characteristic x will change:

$$\mu = \mu_0 + \delta_\mu \sigma_0 , \qquad \sigma = \delta_\sigma \sigma_0 \tag{2.25}$$

where δ_μ and δ_σ represent the shift in mean and standard deviation, respectively, in terms of σ_0.

The process is in control when $\delta_\mu = 0$ (i.e., $\mu = \mu_0$) and $\delta_\mu = 1$ (i.e., $\sigma = \sigma_0$). The quadratic loss function developed by Taguchi and Wu (1980) is widely used as a design criterion for the design of many control charts (Elsayed and Chen 1994, Chou *et al*. 2000, Chen and Chen 2007, Serel and Moskowitz 2008, Yang and Rahim 2009). The loss *Lo* incurred during an out-of-control case due to a mean shift δ_μ and/or a standard deviation shift δ_σ is calculated by

$$Lo(\delta_\mu, \delta_\sigma) = \ell(\delta_\mu, \delta_\sigma) \times V(\delta_\mu, \delta_\sigma) \tag{2.26}$$

where V is the average number of units produced in an out-of-control case and ℓ is the extra quadratic loss (the quadratic loss due to (δ) minus the quadratic loss when the process is in control) per unit.

$$V(\delta_\mu, \delta_\sigma) = N \times ATS(\delta_\mu, \delta_\sigma) \tag{2.27}$$

$$\begin{aligned} \ell(\delta_\mu, \delta_\sigma) &= K_c \left[\sigma^2 + (\mu - \mu_0)^2 \right] - K_c \sigma_0^2 \\ &= K_c \left[(\delta_\sigma \sigma_0)^2 + (\delta_\mu \sigma_0)^2 \right] - K_c \sigma_0^2 \\ &= K_c \sigma_0^2 \left(\delta_\mu^2 + \delta_\sigma^2 - 1 \right) \end{aligned} \tag{2.28}$$

where N is the production rate (i.e., number of units produced per unit time) and K_c is a constant depending on individual process. By taking all different δ_μ and/or δ_σ within the shift range ($0 < \delta_\mu \le \delta_{\mu,\max}$ and/or $1 < \delta_\sigma \le \delta_{\sigma,max}$) into consideration, *AEQL* can be calculated as an integration:

$$AEQL = \int_0^{\delta_{\mu,max}} \int_1^{\delta_{\sigma,max}} Lo(\delta_\mu, \delta_\sigma) \cdot f(\delta_\mu) \cdot f(\delta_\sigma) d\delta_\sigma d\delta_\mu \tag{2.29}$$

$$AEQL = NK_c \sigma_0^2 \int_0^{\delta_{\mu,max}} \int_1^{\delta_{\sigma,max}} (\delta_\mu^2 + \delta_\sigma^2 - 1) \cdot ATS(\delta_\mu, \delta_\sigma) \cdot f(\delta_\mu) \cdot f(\delta_\sigma) d\delta_\sigma d\delta_\mu \tag{2.30}$$

where $f(\delta_\mu)$ and $f(\delta_\sigma)$ are the probability density functions of δ_μ and δ_σ, respectively.

The constant term of $NK_c\sigma_0^2$ can be omitted for the sake of simplicity as it has no influence on the performance comparison and the optimal solution. As such,

$$AEQL = \int_{0}^{\delta_{\mu,max}} \int_{1}^{\delta_{\sigma,max}} (\delta_\mu^2 + \delta_\sigma^2 - 1) \cdot ATS(\delta_\mu, \delta_\sigma) \cdot f(\delta_\mu) \cdot f(\delta_\sigma) d\delta_\sigma d\delta_\mu \quad (2.31)$$

The index *AEQL* based on loss function is a comprehensive measure of the overall performance of variable control charts as it considers all the contributors to the quality cost including the time to signal and the magnitude of shift. It is noted that the index *AEQL* is actually a weighted average of *ATS* over the shift domain of ($0 < \delta_\mu \leq \delta_{\mu,max}$, $1 < \delta_\sigma \leq \delta_{\sigma,max}$), using the extra loss $(\delta_\mu^2 + \delta_\sigma^2 - 1)$ as the weight (Reynolds and Stoumbos 2004*b*). It is justifiable as quality is inversely proportional to variability (Montgomery 2013). If a chart has a smaller *AEQL* value, its out-of-control *ATS* value at each (δ_μ, δ_σ) point is generally smaller compared with other charts. Consequently, a minimum *AEQL* will achieve the best overall statistical performance.

In any process, a probability distribution of the process shift δ must exist. In almost all of the research works, it is assumed explicitly (Domangue and Patch 1991, Sparks 2000, Castagliola *et al*. 2011) or implicitly (Reynolds and Stoumbos 2004*a*) that all process shifts δ occur with equal probability, and a uniform distribution is used to characterize the process shifts. As pointed out by Siddall (1983), if one has complete uncertainty about a random variable except for its bounds, then it leads to a uniform distribution -- as it should. Other distributions such as Rayleigh distribution (Wu *et al*. 2002) and beta distribution (Wu *et al*. 2010*a*) have also been used to describe the process shift δ.

Both the Rayleigh and beta distributions are more appropriate than the uniform distribution to model the random δ shifts. The beta distribution is quite flexible to fit various types of the probability distributions of δ in many applications. The Rayleigh distribution is also considered as a suitable delegation of the distributions of many process shifts.

2.7.5 Average ratio of *ATS* (*ARATS*)

The Average Ratio of *ATS* (*ARATS*) is another index for evaluating the overall detection effectiveness of variable control charts (Wu *et al*. 2010*a*). It is a more heuristic measure of the

overall performance. It directly calculates the average of the ratios between the out-of-control *ATS* of a chart to be evaluated and the $ATS_{benchmark}$ of a benchmark chart.

$$ARATS = \int_0^{\delta_{\mu,max}} \int_1^{\delta_{\sigma,max}} \frac{ATS(\delta_\mu, \delta_\sigma)}{ATS(\delta_\mu, \delta_\sigma)_{benchmark}} \cdot f(\delta_\mu) \cdot f(\delta_\sigma) d\delta_\sigma d\delta_\mu \tag{2.32}$$

If a chart has an *ARATS* larger than one, this chart should have larger *ATS* values at larger portion of the shift domain and/or to a greater degree compared to the benchmark, and *vice versa*. In fact, both *AEQL* and *ARATS* usually give a similar conclusion regarding the comparative study of the overall performance of variable control charts (Ou *et al*. 2012*a*).

2.7.6 Average number of defectives (*AND*)

In a similar vein to *AEQL* and *ARATS*, the Average Number of Defectives (*AND*) can be adopted to measure the overall performance of attribute control charts (Shamsuzzaman and Wu 2006, Haridy *et al*. 2012*a*). It is the average number of defectives (nonconforming units) produced in different out-of-control cases across a range of shifts in fraction nonconforming *p*. When a process shift occurs, the fraction nonconforming *p* will change to:

$$p = \delta \times p_0 \tag{2.33}$$

The index δ ($1 \le \delta \le \delta_{max}$) indicates the increasing *p* shift in terms of p_0. The process is in control when $\delta = 1$ (i.e., $p = p_0$) and out of control when ($1 < \delta \le \delta_{max}$) with a maximum fraction nonconforming at $\delta = \delta_{max}$ (i.e., $p = p_{max} = \delta_{max} \times p_0$).

If *N* is the number of units produced per time unit and $ATS(\delta)$ is the *ATS* value that corresponds to a particular shift δ, then the *AND* produced by the control charts across the *p* shift range ($1 < \delta \le \delta_{max}$) can be calculated by the following formula:

$$\begin{aligned} AND &= \int_1^{\delta_{max}} N \times \delta \times p_0 \times ATS(\delta) \times f_\delta(\delta) \; d\delta \\ &= N \int_1^{\delta_{max}} \delta \times p_0 \times ATS(\delta) \times f_\delta(\delta) \; d\delta \end{aligned} \tag{2.34}$$

where $f_\delta(\delta)$ is the probability density function of δ and δ_{max} is the maximum shift in fraction

nonconforming p. In Equation (2.34), the term (N) is a constant and has no effect on the performance comparison and the optimal solution. Therefore, without loss of generality, N is assumed to be 100 units in this thesis. Then,

$$AND = 100 \int_{1}^{\delta_{max}} \delta \times p_0 \times ATS(\delta) \times f_{\delta}(\delta) \; d\delta \tag{2.35}$$

The integration in Equations (2.31), (2.32) and (2.35) can be computed quickly and accurately by a numerical method such as Legendre-Gauss Quadrature. In this thesis, Equation (2.35) is used to design and compare the charts. In all the comparative studies conducted in this research, the ratio $AND/AND_{new\ developed\ chart}$ is calculated to evaluate the relative performance and the superiority degree of the new developed charts over the existing charts.

The index *AND* directly relates the chart performance to the number of nonconforming units or the economic outcome. That is to say, a chart that produces smaller *AND* (less average number of nonconforming units) for different shifts δ is thought to be more economical. Meanwhile, *AND* can be considered as a weighted average of *ATS* that uses δ as the weight. If *AND* is used as the objective function to be minimized, then the larger the δ (or the more serious the shift) is, the smaller the corresponding $ATS(\delta)$ will result from the optimal design. It is justifiable, as a larger p shift will lead to a greater loss in quality and should be detected at a higher speed. It is noteworthy that both *AEQL* and *AND* are a weighted average of *ATS* to measure and evaluate the overall performance. The only difference is that while the former uses the extra loss $(\delta_{\mu}^2 + \delta_{\sigma}^2 - 1)$ as the weight, the latter uses δ. In the past, many researchers have used the out-of-control *ATS* at one or a few specified process shifts (δ) as the objective function to be minimized in the optimal design of a control chart. However, this approach does not guarantee that the resultant control chart will perform well over a wide range of process shifts.

2.8 Summary

The literature review in this chapter summarizes the development and widespread applications of the control charts for monitoring different quality characteristics. The review covers the major variable control charts and focuses on different types of attribute control charts. The following can be drawn from this literature review:

(1) Depending on the nature of the process parameters, either variable or attribute control charts may be used. The attribute charts are less informative, and generally require a higher sampling rate in order to achieve the same level of the detection effectiveness as the variable charts. However, the attribute charts are easier in design and implementation by different level of personnel including operators.

(2) The Shewhart charts are usually inferior to the CUSUM and EWMA charts, and the latters are less effective than the SPRT charts. However, each control chart can find its application in SPC practice, because the detection effectiveness is not the only criterion for selecting the control chart. Some users may give priority to other considerations such as the ease for design, understanding and implementation. Generally, the higher the detection effectiveness is, the more complicated the design and the implementation of the chart. For instance, the SPRT chart is considered as the most effective monitoring technique but, it is also quite difficult to design compared with other charts. The SPRT chart is a VSS chart. As a result, the sample size of each sample is a random number and unpredictable. This may cause some operational and managerial problems and make the SPRT chart unsuitable for some applications. Despite that the fact that the CUSUM chart is not as powerful as the SPRT chart, it is the most effective Fixed Sample Size (FSS) chart. Therefore, it may be adopted to monitor some processes.

(3) Usually, no control chart can produce the smallest *ATS* for all shifts. Each chart may be most powerful for detecting the process shifts in a particular range. For example, the np chart is effective for detecting large p shifts while the synthetic chart and the binomial

CUSUM chart are more sensitive to detect small p shifts. As a result, selecting the best chart for a specific application or situation is a difficult and tedious process for most SPC practitioners.

(4) According to the previous research on adaptive charts, the performance of some charts may be increased by on-line adaption of their sample sizes and sampling intervals.

(5) The performance evaluation of the control charts remains a challenge. The commonly used measures are *ARL* and *ATS* which consider only a particular shift point. Using a measure of the overall performance such *AEQL* is highly desirable for designing variable control charts that perform well over the entire range of shifts. The ranking of charts' superiority may be quite different, if different assessment indices are used.

(6) The steady-state mode is more realistic than the zero-state mode for calculating *ATS* as it allows the shift to occur randomly after the process operates in an in-control condition for relatively long periods of time.

(7) Usually, two charts are needed to monitor a variable (one for monitoring the mean and another for the variance), while one chart is required to monitor an attribute. However, some single charts have been developed to monitor both the mean and variance of a variable simultaneously. Many of them have better performance than the two-chart schemes.

2.9 Research Gaps

A lot of effort and enormous SPC researches have been conducted with endless stimulation to develop new or improved control charts with high detection effectiveness. This is justifiable as even a 10% improvement in the detection speed may lead to a significant savings in quality cost and considerable reduction of economic losses in different manufacturing and service industries. This thesis is an inherent part of this research effort. The literature review in this chapter shows some of the research gaps that may be filled in order to improve the

performance of the attribute control charts by increasing the detection speed or effectiveness, and therefore to promote the applications of these charts in practice. These research gaps can be listed as follows:

(1) In general, relatively less attention has been paid to attribute charts compared with the variable charts. This research focuses on the development of new attribute control charts which are significantly more highly effective than the existing counterparts that can be found in literature.

(2) One possible approach to enhance the detection effectiveness of a control chart is to combine it with other charts in order to make it more sensitive to a broad shift domain. However, most of the combined charts in the literature have been developed by simply combining the individual charts without optimizing the charting parameters (Lucas 1982, Morias and Pacheco 2006). In this research, the design algorithm of the proposed combined schemes doesn't only optimize the parameters of the individual charts, but also optimizes the allocation of detection power between the individual chart elements, so that the best overall performance can be achieved.

(3) Although the SPRT chart developed by Reynolds and Stoumbos (1998) has been found to have an excellent performance over a wide range of shifts, it is not optimized for the best overall performance. Much research work has found that more significant gain in detection effectiveness can be obtained by improving the design algorithm of an existing chart rather than proposing a completely new chart (Wu *et al*. 2008*b*, Ou *et al*. 2012*b*). Therefore, optimizing the charting parameters of the SPRT chart is considered in this research to achieve the best performance of this chart without increasing the difficulty of its implementation.

(4) The out-of-control *ARL* at a particular shift is often used as the objective function to be minimized in the design of a control chart (Shu *et al*. 2007, Wu *et al*. 2008*a*). However, this approach is no longer considered feasible since it is usually difficult to predict the

sizes of process shifts (Reynolds and Stoumbos 2004*a*). The control chart should have an excellent overall performance across the entire shift range of interest. In alignment with this, this research proposes and adopts an overall measure of performance (*AND*) as the objective function to be minimized. Minimizing *AND* guarantees that the control chart will have the best overall performance across the entire shift range of interest.

(5) There is no general model for the optimal design or systematic evaluation of the overall performance of the attribute control charts. This research suggests a general model for the optimal design of the attribute charts. This model uses *AND* as an objective function to design and compare the charts subject to the same false alarm rate. In this model, all of the independent and dependent charting parameters are optimized so that the best overall performance of the charts can be achieved.

(6) The distribution of the process shift is usually represented implicitly (Reynolds and Stoumbos 2004*a*) or explicitly (Castagliola *et al*. 2011) as a uniform distribution. This research studies the performance of the charts under different distributions of the process shift such as uniform, Rayleigh and Beta distributions.

(7) In attribute charts, the curtailment has only been employed to improve the performance of the simple Shewhart np chart (Wu *et al*. 2006*a*). This research explores the incorporation of the curtailment technique into a more advanced and sophisticated chart, namely the binomial CUSUM chart, to further enhance its detection effectiveness.

(8) There are limited studies that considered using the attribute charts to monitor the mean of a variable due to the simplicity of these charts (Wu *et al*. 2009*b*, Ho and Costa 2011). So far, there is no attribute charts for monitoring both the mean and variance in the literature. Consequently, it is worthwhile in this research to investigate the possibility of developing an attribute chart that is able to effectively monitor both the mean and variance of a variable.

Chapter 3

Synthetic & np (Syn-np) Chart

This chapter proposes a new chart, the *Syn-np chart*, which comprises an np chart and a synthetic chart. The np control chart is a typical attribute chart used to monitor the fraction nonconforming p of a process. This chart is effective in detecting large process shifts in p. The synthetic chart is also proposed to detect p shifts. It utilizes the information about the time interval or the Conforming Run Length (*CRL*) between two nonconforming samples. During the implementation of a synthetic chart, a sample is classified as nonconforming if the number d of nonconforming units falls beyond a warning limit. Unlike the np chart, the synthetic chart is more powerful to detect small and moderate p shifts. Since the Syn-np chart has both the strength of the synthetic chart for quickly detecting small p shifts and the advantage of the np chart of being sensitive to large p shifts, it has a better and more uniform overall performance. Specifically, it is shown to be more effective than the np chart and synthetic chart by 100% and 29%, respectively, in terms of Average Number of Defectives (*AND*) over a wide range of p shifts under different conditions.

3.1 Introduction

The np control chart is one of the most popular charts for attributes, used to monitor the fraction nonconforming of a process. For the np chart, the process is considered to be in control if d satisfies $LCL \leq d \leq UCL$; here, *LCL* and *UCL* are the lower and upper control limits of the np chart. However, if $d < LCL$, a downward p shift is signaled, and if $d > UCL$, then an upward p shift is signaled. In many cases, especially when the in-control fraction nonconforming p_0 is small, the lower control limit *LCL* is equal to zero.

The synthetic control chart proposed by Wu *et al.* (2001*a*) is a combination of an np-like chart and a Conforming Run Length (CRL) chart. Basically, the random variable *CRL* is the

number of inspected samples between two consecutive nonconforming samples, inclusive of the nonconforming sample at the end. Here, a sample is nonconforming if d in this sample falls beyond a warning limit w. The *CRL* of a synthetic chart will change when the fraction nonconforming p of a process shifts. When an increasing p shift takes place, d is more likely to fall beyond w. This will lead to a decrease in *CRL*. If a *CRL* value is smaller than the lower control limit L of the synthetic chart, the process is thought to be out of control. It provides the quality assurance (QA) engineers with some freedom to adjust the control parameters (e.g., w and L), so that the out-of-control Average Time to Signal (*ATS*) can be minimized.

The synthetic chart does not only use the information about the number d of nonconforming units in the last sample, but also makes use of the information of the time interval between two consecutive nonconforming samples. While the synthetic chart is more sensitive to small shifts in fraction nonconforming p, it is less effective than the np chart for detecting large p shifts, because the synthetic chart does not make a decision merely based on the latest sample and is unable to respond promptly to a sudden and large p shift. In recent years, many extensions of the synthetic chart have been proposed for both variable and attribute SPC (Khoo *et al*. 2008, Khilare and Shirke 2010, Khoo *et al*. 2011).

This research proposes a new chart comprising a synthetic chart and an np chart, called the Syn-np chart. The results of performance studies show that this new chart is quite effective for detecting both small and large p shifts, and always has a better overall performance than the individual synthetic chart and individual np chart. The high effectiveness of the Syn-np chart is attributable to its capability to make a decision based on both the information regarding the number d of nonconforming units in the last sample and the information about the time interval (or distance) between the last two nonconforming samples.

The detection effectiveness of a control chart is usually measured by the out-of-control *ARL* or *ATS* which has been introduced in Section (2.7.2). Wu *et al*. (2001*a*) proposed a formula for calculating the zero-state *ARL* of the synthetic chart. Davis and Woodall (2002) developed a

Markov approach to calculate both the zero- and steady-state *ARL* of the variable synthetic chart. Similarly, Bourke (2008) used a Markov approach to evaluate both the zero- and steady-state *ATS* of the synthetic chart. In this research, a new set of non-Markov formulae for calculating the steady-state *ATS* of the synthetic chart, and the zero- and steady-state *ATS* of the Syn-np chart are derived and presented in Section (3.5). This provides SPC practitioners with some diversity for evaluating the performance of the synthetic-type control charts. The non-Markov method is considerably simpler than the Markov approach. It does not only simplify the calculation of *ATS* of the synthetic chart, but also facilitates the further development of other synthetic-type control charts with more advanced features.

While some attribute control charts are developed based on the 100% inspection (Bourke 2001*a*, Wu *et al*. 2001*b*), sampling inspection is adopted in this research to account for the restrictions of the resources such as manpower, cost and measurement instruments. The sampling interval h is determined by using the rational subgroup concept. It assumes that the p shift can only occur between samples rather than within a sample. A sample is a group of n units which are produced at the same time (or as closely together as possible) and under a condition that only random effects are responsible for the observed variation (Nelson 1988). In other words, the time required to inspect the n units in a sample is negligible compared to the duration of the sampling interval h. As a result, if assignable causes are present, the chance for differences between samples due to these assignable causes will be maximized, while the chance for differences within a sample will be minimized (Montgomery 2013).

The remainder of this chapter is organized as follows. Firstly, the implementation and design of the Syn-np chart are presented in Sections (3.2) and (3.3), respectively. Next, a comparison of three control charts is conducted in Section (3.4). Subsequently, the calculation of the *ATS* is performed in Section (3.5). Finally, the concluding remarks are presented in Section (3.6).

3.2 Implementation of the Syn-np Chart

A Syn-np chart consists of a synthetic chart element and an np chart element. It has three parameters: the warning limit w and lower limit L for the synthetic element and the upper limit UCL for the np element. A Syn-np chart is implemented as follows:

(1) Take a sample of n units.

(2) Determine the number d of nonconforming units in this sample.

(3) If $d > UCL$, the process is thought to be out of control. Go to step (6); otherwise go to the next step.

(4) If $d \leq w$, this sample is a conforming one. Go back to step (1) to take the next sample. Otherwise (i.e., if $w < d \leq UCL$), the current sample is nonconforming and go to the next step.

(5) Determine the CRL (i.e., the number of conforming samples between the current and last nonconforming samples plus one). If $CRL \geq L$, the process is still considered to be in control; go back to step (1). Otherwise (i.e., $CRL < L$), go to the next step.

(6) Stop the process immediately for further investigation.

It is noted that step (3) is the only additional step for the implementation of a Syn-np chart compared with the individual synthetic chart. While the synthetic chart produces an out-of-control signal only when ($CRL < L$) in step (5), a Syn-np chart signals when ($CRL < L$) and/or ($d > UCL$). Checking the condition of ($d > UCL$) only slightly increases the difficulty in implementation, but it significantly enhances the capability of the Syn-np chart for detecting large p shifts.

3.3 Design of the Syn-np Chart

3.3.1 Objective function

As mentioned in Chapter (2), an efficient control chart should produce a small out-of-control *ATS* for process shifts of different sizes, or have an excellent overall performance across the entire shift range of interest (Reynolds and Stoumbos 2004*b*). As a result, the Average Number of Defectives (*AND*) is used as the objective function in designing the Syn-np chart.

$$AND = 100 \int_{1}^{\delta_{max}} \delta \times p_0 \times ATS(\delta) \times f_\delta(\delta) \; d\delta \tag{3.1}$$

This equation has been discussed in Equations (2.34 - 2.35). The index *AND* directly relates the chart performance with the economic outcome. That is, a chart producing smaller *AND* will produce fewer defectives, on average, when out-of-control cases occur.

Since the distribution of the p shift differs for different processes and under different conditions, it is hard to use a special distribution in a general performance study. Therefore, the random shift δ in fraction nonconforming p is firstly assumed to follow a uniform distribution. The probability density function $f_\delta(\delta)$ of the uniform distribution is expressed as follows:

$$f_\delta(\delta) = \frac{1}{\delta_{max} - 1} \tag{3.2}$$

A later study shows that if the p shift follows another probability distribution, the Syn-np chart designed based on an assumed uniform distribution of the p shift will still outperform the other charts.

3.3.2 Specifications

To design a Syn-np chart, the following four specifications need to be determined beforehand: (1) the allowable minimum value τ of ATS_0, (2) the in-control fraction nonconforming p_0, (3) the maximum shift δ_{max} in fraction nonconforming, and (4) the sample size n.

The value of τ is decided with regards to the tolerable false alarm rate. The value of p_0 is usually estimated from the historical data observed when the process is in control. The maximum shift δ_{max} is required for the calculation of the Average Number of Defectives (*AND*). The value of δ_{max} may be chosen based on the knowledge about a process (e.g., the maximum possible p shift in a process) or taken as the shift range the users are interested in. The sample size n is usually determined according to the available resources such as manpower, instruments, and the requirements on detection effectiveness (Gan 1993, Morias and Pacheco 2006, Subramani and Balamurali 2012). A large sample size generally increases the detection effectiveness of the control charts, but make the inspection more costly. BSI Handbook 24 (1985) suggested determining n by:

$$n = \frac{e}{p_0} \tag{3.3}$$

where e is a constant between 1 and 3 when $p_0 \geq 0.03$; and e should be made smaller along with the decrease of p_0, otherwise the sample size will be prohibitively large.

The sample size plays a critical role in the overall performance of any control chart. There are many research studies on the sample sizes of different control charts (Reynolds and Stoumbos 2004*a*, Wu *et al*. 2011). Although Montgomery (2013) commented "In designing a control chart, we must specify both the sample size to use and the frequency of sampling", the sample size n can be considered as an adjustable charting parameter rather than a predetermined design specification if there is no constraint on the available resources. The adjustment of n increases the flexibility of the control charts, especially for those with a limited number of charting parameters such as the np chart, so that their ATS_0 can be closer to the allowable τ and their control limits become tighter. This may, in turn, enhance the detection effectiveness of the control charts. However, the choice of the sample size always remains a decision-making preference. As a future work, a user-friendly and intelligent computer program can be developed to suggest an alternative sample size if the user entered an unsuitable one.

3.3.3 Design model

The design of the Syn-np chart is carried out based on the following model using *AND* as the objective function:

Objective: Minimize *AND* (3.4)

Constraint: $ATS_0 \geq \tau$, (3.5)

Design variables: *UCL, w, L*.

The objective of the design model is to identify the optimal values of *UCL*, *w* and *L* that minimize *AND* over a shift range of ($1 < \delta \leq \delta_{max}$) and meanwhile ensure that $ATS_0 \geq \tau$. The minimization of *AND* in turn results in a smaller out-of-control *ATS* over the entire range of *p* shifts. It is noted that *UCL*, *w* and *L* are all integers. The warning limit *w* (for the synthetic element) is always smaller than the upper control limit *UCL* (for the np element); otherwise the synthetic element of the Syn-np chart will be inactive.

3.3.4 Optimal search

The optimal design is implemented by a two-level search as outlined below:

(1) Specify parameters τ, p_0, δ_{max}, and n.

(2) Initialize a variable AND_{min} as a very large number, say 10^7 (AND_{min} is used to store the minimum value of *AND*).

(3) At the first level, search the optimal value of *UCL* by increasing it one by one with a starting value of UCL_{np}, where UCL_{np} is the upper control limit of the np chart under the same design specifications. It is noted that the *UCL* of the Syn-np chart cannot be smaller than UCL_{np}, otherwise the constraint of ($ATS_0 \geq \tau$) will be violated. The search at this top level is terminated when *AND* cannot be further reduced.

(4) At the second level, with each given value of *UCL*, search the optimal value of *w* within the range of ($0 \leq w \leq UCL - 1$). For each given set of values of (*UCL*, *w*),

(4.1) Determine the lower limit L as a function of UCL and w (Equation (3.25)) in Section (3.5). The resultant L satisfies the constraint $ATS_0 \geq \tau$.

(4.2) When the values of all three charting parameters, UCL, w and L, are preliminarily determined, calculate the objective function AND by Equation (3.1).

(4.3) If the calculated AND is smaller than the current AND_{min}, replace the latter by the former and the current values of UCL, w and L are stored as a temporary optimal solution.

(5) At the end of the entire two-level search, the optimal Syn-np chart that produces the minimum AND and satisfies the constraint ($ATS_0 \geq \tau$) is identified. The corresponding optimal values of UCL, w and L are also finalized.

The above grid search approach is very reliable and can complete the optimal design of a Syn-np chart in a few seconds of CPU time on a personal computer. The heuristic search used in this optimization can be allegorically considered as a global optimization because of the discrete nature of attributes which allows searching all the possible values of the two independent integer variables (UCL and w) in a short CPU time.

3.4 Comparative Studies

The detection effectiveness of three control charts (the np chart, the synthetic chart and their combination Syn-np chart) is studied and compared in this section. The charts are studied only for detecting increases in fraction nonconforming. The sampling interval h is taken as the time unit (i.e., $h = 1$).

The design of an np chart aims to adjust the upper control limit UCL so that the resultant ATS_0 is no smaller than τ, while the design of a synthetic chart aims to find the best combination of the warning limit w and the lower limit L so that the chart produces the minimum AND (Equation (3.1)) and with an ATS_0 larger than or at least equal to τ.

3.4.1 Comparison under a general case

The three charts are first studied under a general case. This general case concerns the quality of the chips manufactured in a photolithography process in the semiconductor company. This company produces 300 chips per hour (N = 300). A control chart is to be designed to monitor the fraction nonconforming of the process. The in-control p_0 is estimated as 0.01 from historical records. Based on the requirement on quality and the experience of the quality engineer on the process, the maximum shift δ_{max} is set as 10. A sample size n of 100 is selected based on the available manpower and working shift. The allowable value of ATS_0 is set as 650. The specifications are summarized as follows:

$$\tau = 650, p_0 = 0.01, \delta_{max} = 10 \text{ and } n = 100 \qquad (3.6)$$

The three charts are designed for this case and the results are as follows:

np chart: $UCL = 5$.

Synthetic chart: $w = 3$, $L = 5$.

Syn-np chart: $w = 3$, $L = 4$, $UCL = 5$.

The values of the in-control ATS_0 (when $\delta = 1$) and out-of-control ATS (when $1 < \delta \leq 10$) of the three charts are calculated within the process shift range, and the results are displayed in Table 3.1. The normalized ATS curves (i.e., $ATS/ATS_{Syn\text{-}np}$) of the np and synthetic charts are illustrated in Figure 3.1.

It is interesting to observe the following from Table 3.1 and Figure 3.1:

(1) Firstly, the three charts generate ATS_0 values close to or larger than τ when the process is in control. This ensures that the three charts satisfy the requirement on the false alarm rate.

(2) As expected, the synthetic chart outperforms the np chart for small p shifts (when $\delta \leq 4$), but it is less sensitive than the latter to larger p shifts.

(3) The Syn-np chart achieves a sound balance for detecting process shifts of different sizes. The Syn-np chart is always more effective than both the np and synthetic charts for any p

shift within ($1 < \delta \leq 10$). The superiority of the Syn-np chart over the synthetic chart increases with the increase in δ. When $\delta = 10$, the synthetic chart produces an *ATS* larger than that of the Syn-np chart by 160%. On the other hand, the Syn-np chart becomes more superior to the np chart at small p shifts. When $\delta = 2$, the *ATS* of the np chart is larger than that of the Syn-np chart by 207%.

(4) The fact that the Syn-np chart always produces an *ATS* smaller than that of the np and synthetic charts for any p shift manifests that the Syn-np chart will outperform the other two charts regardless of the probability distribution of p shift. The distribution of p shift may only slightly influence the degree of the superiority of the Syn-np chart.

(5) It is noted that the np chart with $UCL = 5$ generates an in-control ATS_0 (= 1871) much larger than the specified τ (= 650) and, thus, has lower effectiveness (Reynolds and Stoumbos 1999). However, an attempt to tighten the *UCL* (i.e., reducing *UCL* to four) will make the resultant ATS_0 equal to 291 that seriously violates the constraint ($ATS_0 \geq \tau$). It reflects an intrinsic limitation of the np charts due to the discrete nature of the attribute characteristics. Unlike the np chart, the synthetic chart is able to adjust w and L, and the Syn-np chart has even more flexibility for adjusting *UCL*, w, and L in an optimal manner. As a result, the ATS_0 for these two charts is usually larger than τ and the potential effectiveness of the control charts is fully utilized.

The *AND* values (calculated by Equation (3.1)), as well as the ratios of ($AND/AND_{Syn\text{-}np}$), of the three charts are enumerated in case 0 in Table 3.2. As shown, the Syn-np chart can result in a higher overall detection effectiveness in terms of *AND* compared with the np chart and synthetic chart. The values of ($AND/AND_{Syn\text{-}np}$) indicate that, when $\tau = 650$, $p_0 = 0.01$, $\delta_{max} = 10$ and $n = 100$, the Syn-np chart reduces the average number of nonconforming units by 118% and 41% compared with the np chart and synthetic chart, respectively, over the range of p shift.

Table 3.1: *ATS* of the Three Charts

δ	*ATS*		
	np chart	Synthetic chart	Syn-np chart
1	1870.787	761.235	666.699
2	64.084	21.808	20.871
3	11.871	5.620	5.014
4	4.225	2.961	2.365
5	2.104	2.112	1.472
6	1.288	1.754	1.052
7	0.911	1.585	0.820
8	0.719	1.503	0.684
9	0.617	1.463	0.603
10	0.561	1.444	0.556

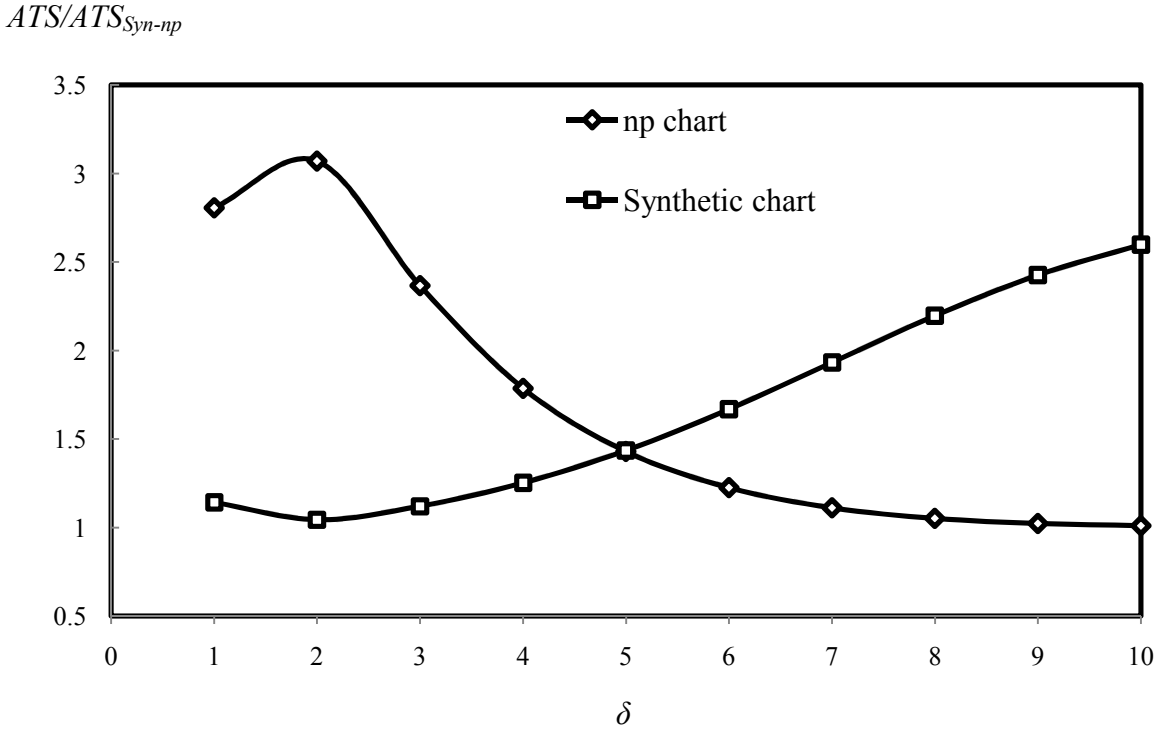

Figure 3.1: Normalized *ATS* of the np and Synthetic Charts

If the Syn-np chart is selected for this general case, the number d of nonconforming units is plotted for every sample as shown in Figure 3.2. Whenever $d > w$, CRL is counted. If $d > UCL$ and/or $CRL < L$, the Syn-np chart signals an upward process shift in fraction nonconforming. Figure 3.2 shows a sample run of this Syn-np chart. The process is in control up to the 12th sample. Then an increasing p shift occurs. The 14th and 16th samples are nonconforming as ($d > w$). They result in a CRL equal to two. Since this CRL is smaller than the lower control limit L (= 4) shown on the top-left corner of the Syn-np chart, an out-of-control signal is produced by the synthetic chart element of the Syn-np chart. This p shift will also be detected at the 20th sample by the np chart element of the Syn-np chart as ($d > UCL$). In the sample run shown in Figure 3.2, the synthetic chart element is the first one that signals the out-of-control status.

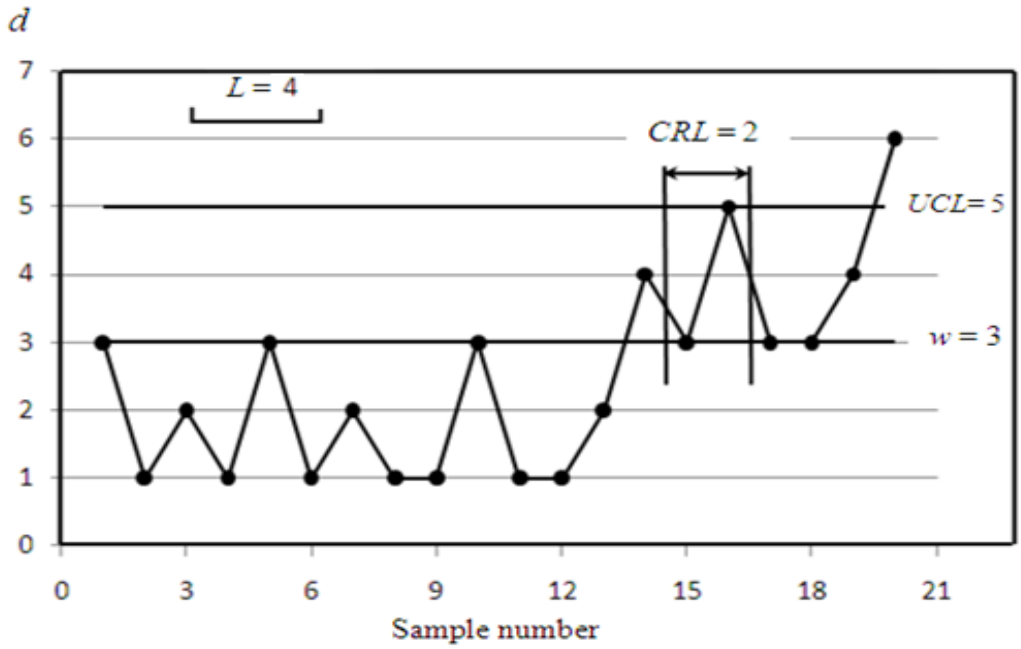

Figure 3.2: A Sample Run of the Syn-np Chart

3.4.2 Comparison under a factorial experiment

Next, the three charts are further studied under different conditions through a 2^4 factorial experiment in which the four specifications (τ, p_0, δ_{max}, and n) are used as the input factors and each of them is varied at two levels as follows:

τ: 300, 1200.

p_0: 0.005, 0.03.

δ_{max}: 5, 15.

n: $0.6 / p_0$, $1.2 / p_0$.

The levels are determined with reference to those commonly used by many authors (Bourke 2008, Wu *et al.* 2008*a*). The sample size n is expressed in terms of p_0 (BSI Handbook 24 1985)

This results in 16 different cases or combinations of τ, p_0, δ_{max}, and n as shown in Table 3.2 (in cases 1 to 16). For each case, the three control charts are designed and each of them produces an ATS_0 no smaller than τ. In all these 16 cases, the relative detection effectiveness of the charts is similar to that revealed in Table 3.1. Namely, the Syn-np chart is more effective than the other two charts across the p shift range.

The charting parameters and overall performance, as reflected by *AND*, are listed in Table 3.2 for the 16 cases. The values of $AND_{np}/AND_{Syn\text{-}np}$ and $AND_{synthetic}/AND_{Syn\text{-}np}$ are always larger than one. The Syn-np chart always outperforms the np chart to a significant degree, especially when τ is large and δ_{max} is small. The ratio of $AND_{np}/AND_{Syn\text{-}np}$ has its maximum value of 3.75 as in case 15. Similarly, the Syn-np chart is often considerably more effective than the synthetic chart. For example, in case 16, when both τ and δ_{max} are large, the ratio of $AND_{synthetic}/AND_{Syn\text{-}np}$ is equal to 1.71. The rightmost column in Table 3.2 displays the reduction ratio (*RR*) that can be obtained when the Syn-np chart is adopted.

Finally, a grand average $\overline{AND/AND_{Syn\text{-}np}}$ is calculated for each chart. It indicates the average of the $AND/AND_{Syn\text{-}np}$ values encompassing all the 16 cases in Table 3.2. The results are $\overline{AND_{np}/AND_{Syn\text{-}np}} = 2.00$ and $\overline{AND_{synthetic}/AND_{Syn\text{-}np}} = 1.29$. This indicates that, from the most comprehensive viewpoint (covering all different values of τ, p_0, δ_{max}, and n), the Syn-np chart is more effective than the np chart and synthetic chart by 100% and 29%, respectively.

It is noteworthy that neither the np chart nor the synthetic chart can have higher overall effectiveness than the Syn-np chart under any circumstances (for any set of specifications τ, p_0, δ_{max} and n), because each of the np chart and synthetic chart is just a special case of the Syn-np chart. If the L of a Syn-np chart is set infinitely large and its w and UCL are made equal to the UCL of an np chart, then this Syn-np chart will perform exactly as that np chart. Similarly, if the upper limit UCL of the Syn-np chart is set infinitely large and its L and w are made equal to the L and w of a synthetic chart, then the Syn-np chart works as the synthetic chart. Consequently, one can always design a Syn-np chart that will surely perform better than, or at least equally well as, the best np chart or the best synthetic chart.

Moreover, the np chart is a special case of the synthetic chart. They are equivalent to each other if the lower limit L of the synthetic chart is set infinitely large and its warning limit w is made equal to the UCL of the np chart. This means that the synthetic chart will always have a higher or equal overall detection effectiveness compared with the np chart. As shown in Table 3.2, there are a few cases in which the synthetic chart and the np chart are equivalent and both produce the same results. In all other cases, the synthetic chart outperforms the np chart.

Table 3.2: Comparison of the Three Charts in the 2^4 Factorial Design

Case	τ	p_0	δ_{max}	n	Chart	w	L	UCL	AND	$AND/AND_{Syn\text{-}np}$	RR
0	650	0.01	10	100	np	-	-	5	24.69	2.175	0.540
					Synthetic	3	5	-	16.01	1.411	0.291
					Syn-np	3	4	5	11.35	1.000	0.000
1	300	0.005	5	120	np	-	-	3	14.25	1.301	0.232
					Synthetic	2	7	-	12.13	1.108	0.097
					Syn-np	2	7	4	10.95	1.000	0.000
2	300	0.005	15	120	np	-	-	3	6.71	1.105	0.095
					Synthetic	3	$+\infty$	-	6.71	1.105	0.095
					Syn-np	2	7	4	6.07	1.000	0.000
3	300	0.005	5	240	np	-	-	5	11.28	1.793	0.442
					Synthetic	3	4	-	6.71	1.067	0.063
					Syn-np	3	4	7	6.29	1.000	0.000
4	300	0.005	15	240	np	-	-	5	5.27	1.338	0.252
					Synthetic	5	$+\infty$	-	5.27	1.338	0.252
					Syn-np	3	2	5	3.94	1.000	0.000
5	300	0.03	5	20	np	-	-	3	93.94	1.429	0.300
					Synthetic	2	9	-	68.62	1.044	0.042
					Syn-np	2	8	4	65.72	1.000	0.000
6	300	0.03	15	20	np	-	-	3	41.87	1.182	0.154
					Synthetic	3	$+\infty$	-	41.87	1.182	0.154
					Syn-np	2	8	4	35.41	1.000	0.000
7	300	0.03	5	40	np	-	-	5	73.91	2.156	0.536
					Synthetic	3	4	-	40.29	1.175	0.149
					Syn-np	3	3	5	34.28	1.000	0.000
8	300	0.03	15	40	np	-	-	5	33.19	1.527	0.345
					Synthetic	5	$+\infty$	-	33.19	1.527	0.345
					Syn-np	3	3	5	21.74	1.000	0.000
9	1200	0.005	5	120	np	-	-	4	52.39	1.814	0.449
					Synthetic	2	2	-	31.91	1.105	0.095
					Syn-np	2	2	5	28.88	1.000	0.000
10	1200	0.005	15	120	np	-	-	4	18.60	1.554	0.357
					Synthetic	2	2	-	15.60	1.303	0.233
					Syn-np	2	2	5	11.97	1.000	0.000
11	1200	0.005	5	240	np	-	-	6	30.74	3.118	0.679
					Synthetic	4	16	-	10.88	1.103	0.094
					Syn-np	4	12	6	9.86	1.000	0.000
12	1200	0.005	15	240	np	-	-	6	11.01	2.215	0.549
					Synthetic	4	16	-	8.48	1.706	0.414
					Syn-np	4	12	6	4.97	1.000	0.000
13	1200	0.03	5	20	np	-	-	4	396.78	2.726	0.633
					Synthetic	2	2	-	200.13	1.375	0.273
					Syn-np	2	2	4	145.56	1.000	0.000
14	1200	0.03	15	20	np	-	-	4	134.14	2.269	0.559
					Synthetic	2	2	-	94.68	1.602	0.376
					Syn-np	2	2	4	59.11	1.000	0.000
15	1200	0.03	5	40	np	-	-	6	220.24	3.752	0.734
					Synthetic	4	20	-	65.20	1.111	0.100
					Syn-np	4	17	6	58.70	1.000	0.000
16	1200	0.03	15	40	np	-	-	6	75.95	2.586	0.613
					Synthetic	4	20	-	50.34	1.714	0.417
					Syn-np	4	17	6	29.37	1.000	0.000

3.4.3 Performance comparison under different probability distribution

In any process, the p shift must follow a particular probability distribution. However, as aforementioned, it is usually unknown and one may have to design the control charts based on an assumed uniform distribution over the shift domain. A test is carried out in this research for the general case (i.e., $\tau = 650$, $p_0 = 0.01$, $\delta_{max} = 10$ and $n = 100$) to study how the charts will perform if the actual distribution of the random shift δ is quite different from a uniform one.

The three control charts (the np, synthetic and Syn-np charts) have already been designed based on the uniform distribution and the charting parameters can be found from case 0 in Table 3.2 and are displayed again in case 1 of Table 3.3. Now, these three charts are applied to three different cases in which δ follows different beta distributions (Equation (3.8)) as shown in cases 2, 3 and 4 of Table 3.3. The probability density function of the beta distribution is as follows:

$$f_{\delta}(\delta) = \frac{\Gamma(a+b)}{\Gamma(a)\Gamma(b)} \cdot \frac{(\delta-1)^{a-1} \cdot (\delta_{max}-\delta)^{b-1}}{(\delta_{max}-1)^{a+b-1}} \qquad (3.8)$$

The skewness of a beta distribution depends on the parameters a and b. If ($a < b$), the shift δ will have a probability distribution skewed to right (Figure 3.3(a)). This represents the situations where most of the shifts cluster to the lower end within the shift range. If ($a > b$), δ will have a probability distribution skewed to left (Figure 3.3(c)). This arises when most of the shifts cluster to the upper end, or when all small shifts have been truncated to avoid over-correction that may introduce extra variability into the process (Woodall 1985). Finally, if ($a = b$), δ will have a symmetrical probability distribution (Figure 3.3(b)). In this research, three different cases or different combinations of the values of a and b for the probability distributions of δ are studied. They serve as the representatives of different types of non-uniform probability distributions of δ. Table 3.3 lists these three cases together with the uniform distribution case.

Table 3.3: Comparison of the Three Control Charts under Different Distributions of δ

Case	Distribution	Distribution parameters *a*	Distribution parameters *b*	Chart	*w*	*L*	*UCL*	*AND*	$AND/AND_{Syn\text{-}np}$	*RR*
1	Uniform	-	-	np	-	-	5	24.69	2.175	0.540
				Synthetic	3	5	-	16.01	1.411	0.291
				Syn-np	3	4	5	11.35	1.000	0.000
2	Beta skewed to right	2	4	np	-	-	5	57.19	2.620	0.618
				Synthetic	3	5	-	25.13	1.151	0.131
				Syn-np	3	4	5	21.83	1.000	0.000
3	Beta symmetrical	3	3	np	-	-	5	16.72	1.839	0.456
				Synthetic	3	5	-	13.04	1.435	0.303
				Syn-np	3	4	5	9.09	1.000	0.000
4	Beta skewed to left	4	2	np	-	-	5	8.22	1.290	0.225
				Synthetic	3	5	-	11.82	1.856	0.461
				Syn-np	3	4	5	6.37	1.000	0.000

With these given probability distributions $f_\delta(\delta)$, the *AND* produced by the control charts can be calculated by Equation (3.1).

$$AND = \int_1^{\delta_{max}} \delta \times p_0 \times ATS(\delta) \times f_\delta(\delta) \; d\delta \qquad (3.9)$$

The ratios of $AND/AND_{Syn\text{-}np}$ and *RR* in Table 3.3 show that, under any probability distributions of δ, the Syn-np chart always outperforms the np chart and the synthetic chart. The superiority of the Syn-np chart over the np chart is more significant when $f_\delta(\delta)$ is skewed to right (case 2) as the np chart is particularly powerless for detecting small *p* shifts. On the other hand, the superiority of the Syn-np chart over the synthetic chart is more significant when $f_\delta(\delta)$ is skewed to left (case 4) as the latter is most insensitive to large *p* shifts. When the beta distribution is symmetrical (case 3), the values of $AND/AND_{Syn\text{-}np}$ of the charts are close to those under the uniform distribution (case 1). It can be concluded that if the real probability

distribution of δ is different from a uniform one, the Syn-np chart designed based on a uniform distribution will still outperform the np chart and the synthetic chart.

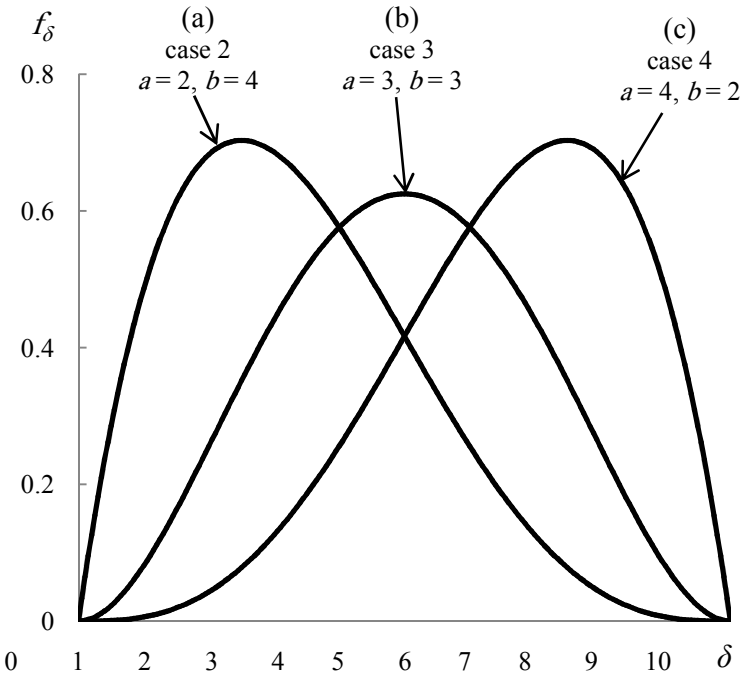

Figure 3.3: Three Beta Probability Density Functions of δ

3.5 Calculation of the *ATS*

The key formulae for computing the steady-state *ATS* of the Synthetic chart, and the zero- and steady-state *ATS* of the Syn-np chart are derived in this research.

(1) Zero-state *ATS* of the synthetic chart

The formula to calculate the zero-state ATS_{zero} for a given p was presented by Wu and Spedding (2000).

$$ATS_{zero}(p) = \frac{h}{\text{Prob}\left[\left(d > w\right) \text{ AND } \left(CRL < L\right)\right]} = \frac{h}{g(p)\cdot G(p)} \tag{3.10}$$

where,

h is the sampling interval.

$$g(p) = \text{Prob}(d > w) = 1 - \sum_{i=0}^{w} C_i^n p^i (1-p)^{n-i} \tag{3.11}$$

$$G(p) = \text{Prob}(CRL < L) = 1-(1-g(p))^{L-1} \tag{3.12}$$

The in-control Average Time to Signal ATS_0 is equal to $ATS_{zero}(p_0)$.

(2) Steady-state *ATS* of the synthetic chart

Suppose that a process shift in fraction nonconforming occurs randomly at a time moment T within an interval between two nonconforming samples. This interval is denoted as the *shifting interval*. The fraction nonconforming p is equal to p_0 before T and equal to $p_1 > p_0$ after T. Suppose that the numbers of conforming samples before and after T are m_0 and m_1, respectively, in the shifting interval. If the *CRL* for the shift interval is denoted as CRL^*, then

$$CRL^* = m_0 + m_1 + 1 \tag{3.13}$$

Here CRL^* includes the nonconforming sample at the end of the shifting interval. The probability mass function of *CRL** is (Wu and Spedding 1999)

$$\begin{aligned} f_{CRL*}(i) &= \text{Prob}(CRL* = i) = \sum_{j=1}^{i}\left[\text{Prob}(m_0 = i-j)\times\text{Prob}(m_1 = j-1)\right] \\ &= \sum_{j=1}^{i}\left[\left(q_0^{i-j}g_0\right)\left(q_1^{j-1}g_1\right)\right] = \frac{q_0^i g_0 g_1\left[1-\left(q_1/q_0\right)^i\right]}{q_0-q_1} \end{aligned} \tag{3.14}$$

where

$$g_0 = g(p_0),\ g_1 = g(p_1),\ q_0 = 1 - g_0,\ q_1 = 1 - g_1 \tag{3.15}$$

The cumulative distribution function $F_{CRL^*}(S)$ is equal to

$$\begin{aligned} F_{CRL*}(S) &= \text{Prob}(CRL* \le S) = \sum_{i=1}^{S} f_{CRL*}(i) \\ &= \frac{g_1 q_0\left(1-q_0^S\right)-g_0 q_1\left(1-q_1^S\right)}{q_0-q_1} \end{aligned} \tag{3.16}$$

It is noted that $F_{CRL^*}(S)$ depends on both p_0 and p_1. If the process shift is detected at the end of the shifting interval (or by the first nonconforming sample after the p shift), *ATS* is equal to $[h \cdot (1/g_1 - 0.5)]$. Here, the random time of process shift is assumed to have a uniform

distribution between two samples (Reynolds *et al*. 1990). The probability G_s of this event is equal to $F_{CRL^*}(L-1)$, that is

$$G_S = F_{CRL*}(L-1) = \frac{g_1 q_0 \left(1-q_0^{L-1}\right) - g_0 q_1 \left(1-q_1^{L-1}\right)}{q_0 - q_1} \tag{3.17}$$

On the other hand, if the process shift has not been detected by the first nonconforming sample but by a following one, *ATS* equals [$h \cdot (1/g_1 - 0.5) + ATS_{zero}(p_1)$]. The probability of this complementary event is ($1 - G_s$). It is noted that, after the process shift occurs, p always takes the out-of-control value p_1, and therefore the zero-state mode comes to play after the shifting interval. Now, the steady-state *ATS* can be calculated by

$$\begin{aligned} ATS &= h \cdot G_S \cdot \left(\frac{1}{g_1} - 0.5\right) + (1-G_S) \cdot \left(h \cdot \left(\frac{1}{g_1} - 0.5\right) + ATS_{zero}(p_1)\right) \\ &= h \cdot \left(\frac{1}{g_1} - 0.5\right) + (1-G_S) \cdot ATS_{zero}(p_1) \end{aligned} \tag{3.18}$$

where ATS_{zero} is calculated by Equation (3.10).

$$ATS_{zero}(p_1) = \frac{h}{g_1\left(1-q_1^{L-1}\right)} \tag{3.19}$$

(3) Zero-state *ATS* of the Syn-np chart

The zero-state ATS_{zero} of a Syn-np chart can also be calculated by Equation (3.10), except that the formula for the probability $G(p)$ (Equation (3.12)) needs to be modified. For a Syn-np chart,

$G(p)$ = Prob[(($w < d \le UCL$) AND ($CRL < L$)) OR ($d > UCL$)]

$$= \frac{a(p)}{g(p)}\left(1-(1-g(p))^{L-1}\right) + \frac{b(p)}{g(p)} \tag{3.20}$$

where $a(p)$ is the probability of ($w < d \le UCL$) and $b(p)$ is the probability of ($d > UCL$).

$$a(p)=\sum_{i=w+1}^{UCL} C_i^n p^i (1-p)^{n-i}$$
$$b(p)=1-\sum_{i=0}^{UCL} C_i^n p^i (1-p)^{n-i} \tag{3.21}$$

Equation (3.20) indicates that the Syn-np chart will produce a signal under any of the following two scenarios: (1) when ($w < d \leq UCL$) and ($CRL < L$), or (2) when ($d > UCL$).

The in-control ATS_0 of the Syn-np chart is

$$ATS_0 = ATS_{zero}(p_0) = \frac{h}{g(p_0)\cdot G(p_0)} \tag{3.22}$$

(4) Steady-state *ATS* of the Syn-np chart

The steady-state *ATS* of a Syn-np chart can be calculated by Equation (3.18), except that the probability G_s that the process shift is detected by the first nonconforming sample after the p shift is determined by

$$G_s = \frac{a(p_1)}{g(p_1)} F_{CRL*}(L-1) + \frac{b(p_1)}{g(p_1)} \tag{3.23}$$

(5) Determination of the lower control limit L of the Syn-np chart for given w and UCL

When w and UCL are given, $g(p_0)$, $a(p_0)$, and $b(p_0)$ can be calculated by Equations (3.11) and (3.21). In Equation (3.22), if ATS_0 is set as τ and $G(p_0)$ is replaced by expression (3.20), then

$$\tau = \frac{h}{g(p_0)\left[\frac{a(p_0)}{g(p_0)}\left[1-\left(1-g(p_0)\right)^{L-1}\right]+\frac{b(p_0)}{g(p_0)}\right]} \tag{3.24}$$

It leads to

$$L = \frac{\ln\left(1-\frac{(h/\tau)-b(p_0)}{a(p_0)}\right)}{\ln\left(1-g(p_0)\right)}+1 \tag{3.25}$$

This L value should be rounded down to the closest integer in order to ensure that $ATS_0 \geq \tau$.

3.6 Concluding Remarks

This research presents the rationale, design, operation, and performance assessment of the Syn-np chart which comprises an np chart element and a synthetic chart element. This chart is able to utilize the information of the number of nonconforming units in the last sample, as well as the information of the distance between two nonconforming samples. While the first type of information makes the Syn-np chart very sensitive to large shifts in fraction nonconforming, the second type of information enables this chart to detect small shifts effectively.

The results of the comparative studies show that the Syn-np chart always outperforms the np and synthetic charts regardless of the probability distribution of p shift. Specifically, it is more effective than the np chart and synthetic chart by 100% and 29%, respectively, in terms of Average Number of Defectives (*AND*) over a wide range of p shifts under different conditions.

In spite of the discrete nature of the attribute characteristics, the resultant ATS_0 of the Syn-np chart is usually close to the allowable value τ. This advantage enables the users of the Syn-np chart to control the false alarm rate accurately and, at the same time, to make full use of the potential of the detection speed of the chart.

Even though the design of the Syn-np chart is more complicated than that of the np chart and the synthetic chart, its application can be justified by the significant improvement in the detection effectiveness. The whole optimal design can be simply carried out by a computer program. Once the Syn-np chart is designed, it can be used continually (until the process settings change) and the enhancement in performance can be reaped on a long-term basis.

Chapter 4

Optimal np & CUSUM (np-CUSUM) Chart

This chapter proposes a new chart, *the np-CUSUM chart*, which is an optimal version of the np & CUSUM scheme. The np control chart is an attribute chart that checks the number *d* of nonconforming units in samples of size *n*. This chart is effective for detecting large process shifts in fraction nonconforming *p*. The binomial Cumulative Sum (CUSUM) chart is also proposed to monitor *p*. It is a more powerful procedure for detecting small and moderate *p* shifts and has higher overall detection effectiveness than the np chart. An optimal algorithm for the design of the new np-CUSUM chart is presented in this chapter. This design algorithm not only optimizes the charting parameters of the np chart element and CUSUM chart element, but also optimizes the allocation of detection power between the two chart elements, so that the best overall performance can be achieved. Since the np-CUSUM chart comprises a CUSUM chart and an np chart, it has both the strength of the CUSUM chart for quickly detecting small *p* shifts and the advantage of the np chart of being sensitive to large *p* shifts. The performance of the np-CUSUM chart is compared with that of other charts in a systematic and quantitative manner. The results show that the np-CUSUM chart always outperforms, or at least performs as well as, the individual np chart, CUSUM chart and EWMA chart, in terms of Average Number of Defectives (*AND*). On average, the np-CUSUM chart is more effective than the np chart, EWMA chart and CUSUM chart by 213%, 15% and 5%, respectively, under different conditions. While the optimal design effectively improves the overall performance of the np & CUSUM scheme over the entire process shift range, it does not increase the difficulty for understanding and implementing this scheme.

4.1 Introduction

The np control chart introduced in Chapter (3) is a simple attribute chart used to monitor the number d of nonconforming units found in a sample. Unlike the np chart that only uses the information about d in the last sample, the binomial Cumulative Sum chart (CUSUM chart in short) incorporates all the information in the sequence of observed values of d (Lucas 1985*a*). The first CUSUM chart was introduced by Page (1954) for monitoring the mean of a quality characteristic in a production process.

While the CUSUM chart is more sensitive to small and moderate shifts in fraction nonconforming p, it is less effective than the np chart for detecting large p shifts. The reason is that the CUSUM chart does not make a decision merely based on the data in the latest sample and is therefore unable to respond promptly to a sudden and large p shift. A statistic C_t is updated and plotted for the tth sample in a CUSUM chart for detecting upward p shifts.

$$\begin{aligned} C_0 &= 0 \\ C_t &= \max\left(0,\ C_{t-1} + (d_t - d_0) - k_0\right) \\ &= \max\left(0,\ C_{t-1} + d_t - (d_0 + k_0)\right) \end{aligned} \tag{4.1}$$

where d_t is the number of nonconforming units found in the tth sample, d_0 is the in-control value of d equal to (np_0), and k_0 is the initial reference parameter. In Equation (4.1), the constant term (d_0+k_0) can be replaced by a single reference parameter k so that Equation (4.1) can be simplified as follows:

$$\begin{aligned} C_0 &= 0 \\ C_t &= \max(0,\ C_{t-1} + d_t - k) \end{aligned} \tag{4.2}$$

When an increasing p shift occurs, C_t tends to increase. Eventually, a sample point will exceed the control limit H of the CUSUM chart, and an out-of-control signal is produced.

Another effective tool for detecting small and moderate shifts in fraction nonconforming p is the binomial Exponentially Weighted Moving Average (EWMA) chart (Roberts 1959). This chart also uses cumulative information from all samples up to the last one and has quite similar

operating characteristics as the CUSUM chart (Reynolds and Stoumbos 2004*b*). A statistic E_t is updated and plotted for the tth sample in an EWMA chart for detecting upward p shifts.

$$E_0 = 0$$
$$E_t = \lambda(d_t - d_0) + (1-\lambda)E_{t-1} \qquad (4.3)$$

The parameters of an EWMA chart include the smoothing parameter λ ($0 < \lambda \leq 1$) and the control limit W. This chart produces an out-of-control signal when E_t becomes larger than W.

The CUSUM and EWMA charts have been increasingly promoted across industries for SPC applications (Zhao *et al*. 2005, Shu *et al.* 2008). The rapid evolution of these charts is mainly attributed to the fact that online measurement and distributed computing systems become a norm in today's SPC applications (Woodall and Montgomery 1999, Chan *et al.* 2009).

Morias and Pacheco (2006) discussed the upper one-sided combined CUSUM–Shewhart scheme for binomial data (referred as the *M-P np-CUSUM scheme* in this research). However, they did not develop a systematic procedure to design the combined scheme. An np chart and a CUSUM chart are simply combined together without optimizing the charting parameters or allocating the detection power between the np chart element and the CUSUM chart element. Moreover, the design aims at minimizing the out-of-control *ATS* at a specified p shift. However, it is usually difficult to predict the magnitudes or sizes of process shifts in most SPC applications (Reynolds and Stoumbos 2004*a*). A control chart should be designed to produce a small out-of-control *ATS* for p shifts of different sizes, and have an excellent overall performance across the entire shift range of interest. Even though the performance of the M-P np-CUSUM scheme was compared with some other charts, a clear conclusion has not been reached. Morias and Pacheco (2006) mentioned that the M-P np-CUSUM scheme is better than np chart for detecting smaller p shifts and outperforms the single CUSUM chart for detecting larger p shifts, but they didn't infer which chart is better from an overall viewpoint and to what degree. They concluded that the combined np & CUSUM scheme may not necessarily outperform the individual np and CUSUM

charts from an overall viewpoint. Another problem with the M-P np-CUSUM scheme is that it often fails to satisfy the requirement on the false alarm rate.

This research proposes a new optimal np & CUSUM scheme comprising an np chart and a CUSUM chart, called the *np-CUSUM chart*. The design algorithm used to develop this new chart not only optimizes the charting parameters of each of the np chart element and the CUSUM chart element, but also optimizes the allocation of detection power between the two chart elements. The objective is to achieve the best overall performance. The performance of the np-CUSUM chart is compared with other charts in a systematic and analytical manner. The results show that this np-CUSUM chart is quite effective for detecting both small and large p shifts, and its overall performance is always better than, or at least as good as, that of the individual np chart, CUSUM chart and EWMA chart. The high effectiveness of the np-CUSUM chart is attributable to the optimal design of the combined np & CUSUM scheme as well as the concurrent use of the information regarding the last sample and the information from the series of the previous sample points. In this research, the sampling interval h is taken as the time unit (i.e., $h = 1$) and determined based on the rational subgroup concept that has been introduced in earlier chapters.

The remainder of this chapter is organized as follows. Firstly, the implementation of the np-CUSUM chart is outlined in Section (4.2). Secondly, the design of the chart is presented in Section (4.3). Next, a comparison of four charts including the M-P np-CUSUM scheme and the np-CUSUM chart is conducted in Section (4.4). Subsequently, the calculation of the *ATS* of the np-CUSUM chart is computed in Section (4.5). The concluding remarks are presented in Section (4.6).

4.2 Implementation of the np-CUSUM Chart

An np-CUSUM chart consists of a CUSUM chart element and an np chart element. It has three parameters: the control limit H and reference parameter k for the CUSUM element and the upper limit UCL for the np element. An np-CUSUM chart is implemented as follows:

(1) Initialize the statistic C_0 in Equation (4.2) as zero.

(2) Take a sample of n units at the end of each sampling interval h and count the number d_t of nonconforming units in this sample.

(3) Update C_t as follows (referring to Equation (4.2))

$$C_t = \max(0,\ C_{t-1} + d_t - k) \tag{4.4}$$

(4) If $C_t \le H$ and $d_t \le UCL$, the process is thought to be in control; go back to step (2) for the next sample.

(5) Otherwise (if $C_t > H$ and/or $d_t > UCL$), an out-of-control signal is produced and the process is stopped immediately for further investigation.

It is noted that ($d_t > UCL$) is the only addition for the implementation of an np-CUSUM chart compared with the individual CUSUM chart. While the CUSUM chart produces an out-of-control signal only when ($C_t > H$), an np-CUSUM chart signals when ($C_t > H$) and/or ($d_t > UCL$). Checking the condition of ($d_t > UCL$) increases the difficulty in implementation only slightly, but it significantly enhances the capability of the np-CUSUM chart for detecting large p shifts.

4.3 Design of the np-CUSUM Chart

4.3.1 Objective function

A sound measure of the overall effectiveness is the Average Number of Defectives (*AND*) that has been presented in Equations (2.34 - 2.35).

$$AND = 100 \int_{1}^{\delta_{max}} \delta \times p_0 \times ATS(\delta) \times f_{\delta}(\delta)\ d\delta \tag{4.5}$$

As explained earlier, minimizing *AND* ensures that the control chart has the best overall performance across the entire shift range of interest.

As different production processes are prone to a variety of shift distributions, the random shift δ in fraction nonconforming p is assumed to follow a uniform distribution (Domangue and Patch 1991, Sparks 2000, Castagliola *et al*. 2011) in this research. As mentioned in Chapter (3), the probability density function $f_\delta(\delta)$ of the uniform distribution can be represented as follows:

$$f_\delta(\delta) = \frac{1}{\delta_{max} - 1} \tag{4.6}$$

4.3.2 Specifications

The following four specifications need to be determined in designing an np-CUSUM chart: (1) the allowable minimum value τ of in-control ATS_0, (2) the in-control fraction nonconforming p_0, (3) the maximum shift δ_{max}, and (4) the sample size n. The general guidelines for selecting the values of these specifications have been discussed in Section (3.3.2).

4.3.3 Design model

The design of the np-CUSUM chart is carried out based on the following model using *AND* as the objective function:

Objective: Minimize *AND* (4.7)

Constraint: $ATS_0 \geq \tau$ (4.8)

Design variables: *UCL, k, H*

where *UCL* and *k* are treated as independent design variables. The control limit *H* is dependent on *UCL*, *k* and the specified τ. The objective of the optimal design is to identify the optimal values of *UCL* and *k* that minimize *AND* over a shift range of ($1 < \delta \leq \delta_{max}$), and meanwhile *H* is adjusted so that $ATS_0 \geq \tau$.

4.3.4 Optimal search

The optimal design is carried out by a two-level search as outlined below:

(1) Specify the parameters τ, p_0, δ_{max} and n.

(2) Initialize a variable AND_{min} as a very large number, say 10^7 (AND_{min} is used to store the minimum value of AND).

(3) At the first or top level, search the optimal value of UCL by increasing it one by one with a starting value of UCL_{np}, where UCL_{np} is the upper control limit of an np chart that satisfies $ATS_0 \geq \tau$. It is noted that the UCL of the np-CUSUM chart cannot be smaller than UCL_{np}, otherwise the constraint of ($ATS_0 \geq \tau$) will be violated. The search at this top level is terminated when AND cannot be reduced further.

(4) At the second or lower level, with the given value of UCL determined at the top level, search for the optimal value of k. For a given set of values of (UCL, k),

(4.1) Determine the control limit H so that the constraint of ($ATS_0 \geq \tau$) is satisfied within a predetermined tolerance such that $\left|\frac{ATS_0 - \tau}{\tau}\right| < 0.05$.

(4.2) When the values of all three charting parameters, UCL, k and H, are determined, calculate the objective function AND by Equation (4.5).

(4.3) If the calculated AND is smaller than the current AND_{min}, replace the latter by the former and the current values of UCL, k and H are stored as a temporary optimal solution.

(5) At the end of the entire two-level search, the np-CUSUM chart that produces the minimum AND and satisfies the constraint ($ATS_0 \geq \tau$) is identified. The corresponding optimal values of UCL, k and H are also finalized.

In the optimal design, adjusting UCL is to allocate the Type I error (or power) of the np-CUSUM chart between the np chart element and the CUSUM chart element. If UCL is tightened,

H must be relaxed for $ATS_0 \geq \tau$. This will make the np-CUSUM chart more sensitive to large p shifts. Similarly, if UCL is loosened, H can be tightened, and the np-CUSUM chart will be more powerful in detecting small p shifts. Furthermore, the reference parameter k is optimized in order to make the np-CUSUM chart most effective in signaling different p shifts.

The above search mechanism is very reliable and can complete the optimal design of a typical np-CUSUM chart within a few minutes of CPU time on a personal computer. The search algorithm used in this optimization is likely to identify a global optimal solution because one of the two independent design variables, UCL, is an integer variable, and therefore all its possible values can be examined. For every given value of UCL, the optimal value of the only remaining independent design variable k can be determined by an exhaustive search in a short CPU time. This search algorithm will at least produce a feasible solution that can achieve the desirable improvement from an engineering viewpoint.

4.4 Comparative Studies

In this section, the detection effectiveness of four control charts (the np chart, the CUSUM chart, the EWMA chart and the np-CUSUM chart) is studied and compared. The charts are studied only for detecting increases in fraction nonconforming.

The design of an np chart requires adjusting the upper control limit UCL so that the resultant ATS_0 is no smaller than τ. The design of a CUSUM chart is to find the best combination of the reference parameter k and the control limit H so that the chart produces the minimum AND (Equation (4.5)) and meanwhile has an ATS_0 equal to or larger than τ. The design of an EWMA chart is similar to the design of a CUSUM chart except that the two charting parameters to be adjusted are the smoothing parameter λ and the control limit W.

4.4.1 Comparison under a general case

Firstly, the four charts are studied under a general case. This general case concerns the quality of a surgical sponge product. A control chart is to be designed to monitor the fraction nonconforming of the product. The in-control p_0 is estimated as 0.01 from historical records. Based on the requirement on quality and the experience of the quality engineer on the process, the maximum shift δ_{max} is set as 10. The allowable minimum τ is set as 650 hours. A sample size n of 100 is selected based on the available manpower and working shift. The specifications are summarized as follows:

$$\tau = 650, p_0 = 0.01, \delta_{max} = 10 \text{ and } n = 100 \quad (4.9)$$

The four charts are designed for this case and the results are as follows:

np chart: $UCL = 5$.

CUSUM chart: $k = 1.750$, $H = 4.630$.

EWMA chart: $\lambda = 0.230$, $W = 1.275$.

np-CUSUM chart: $k = 1.500$, $H = 6.011$, $UCL = 5$.

Using the Markov formulae in Section (4.5), the values of the in-control ATS_0 (when $\delta = 1$) and out-of-control ATS (when $1 < \delta \leq 10$) of the four charts are calculated within the process shift range, and the results are displayed in Table 4.1. The normalized ATS curves (i.e., $ATS/ATS_{np\text{-}CUSUM}$) of the np, CUSUM and EWMA charts are depicted in Figure 4.1. Figure 4.1 (a) shows the full scale normalized ATS curves while Figure 4.1 (b) zooms in the curves over a smaller scale of $ATS/ATS_{np\text{-}CUSUM}$.

Table 4.1: *ATS* of the Four Charts

δ	*ATS*			
	np chart	CUSUM chart	EWMA chart	np-CUSUM chart
1	1870.787	679.463	635.193	673.341
2	64.084	11.911	11.827	11.000
3	11.871	3.857	3.759	3.926
4	4.225	2.245	2.126	2.285
5	2.104	1.566	1.484	1.507
6	1.288	1.190	1.105	1.091
7	0.911	0.949	0.884	0.844
8	0.719	0.786	0.740	0.695
9	0.617	0.676	0.645	0.608
10	0.561	0.602	0.584	0.558

It is interesting to observe the following from Table 4.1 and Figure 4.1:

(1) Firstly, the four charts generate ATS_0 values close to or larger than τ when the process is in control. This ensures that the requirement on the false alarm rate is satisfied. It is noted that, the ATS_0 values of the CUSUM chart, EWMA chart and np-CUSUM chart are fairly close to τ (= 650) because these three charts have several parameters that can be adapted to fit the constraint ($ATS_0 \geq \tau$). As a result, the potential effectiveness of these three charts can be better utilized. On the contrary, since the np chart has only one integer parameter (*UCL*), it generates an in-control ATS_0 (= 1871) much larger than τ as explained in Section (3.4.1).

(2) As expected, the CUSUM chart and EWMA chart outperform the np chart for small p shifts to a significant degree (when $\delta \leq 6$), but they are less sensitive than the latter to larger p shifts (when $\delta > 7$).

(3) The *ATS* values of the np-CUSUM chart are often either equal or close to the minimum across the p shift range. The np-CUSUM chart becomes superior to both CUSUM and

EWMA charts for large p shifts ($\delta > 5$) because the former is able to respond quickly to the change of p in the last sample. When $\delta = 8$, the *ATS* values of the CUSUM chart and EWMA chart are larger than that of the np-CUSUM chart by 13% and 7%, respectively. On the other hand, the np-CUSUM chart outperforms the np chart over the entire p shift range, especially when p is small. For example, when $\delta = 2$, the np chart produces an *ATS* larger than that of the np-CUSUM chart by 483%. Obviously, it is the combination of the np and CUSUM charts plus the optimal design that makes the np-CUSUM chart very effective from an overall viewpoint. The np-CUSUM chart is less effective than the CUSUM chart and EWMA chart only in a small region of p shifts (when δ is around 4).

The *AND* values (Equation (4.5)), as well as the ratios of ($AND/AND_{np\text{-}CUSUM}$), of the four charts are enumerated in case 0 in Table 4.2. The values of ($AND/AND_{np\text{-}CUSUM}$) indicate that, for this case (where $\tau = 650$, $p_0 = 0.01$, $\delta_{max} = 10$ and $n = 100$), the np-CUSUM chart reduces the average number of defectives by 182%, 10% and 3% compared with the np chart, CUSUM chart and EWMA chart, respectively, over the range of p shifts.

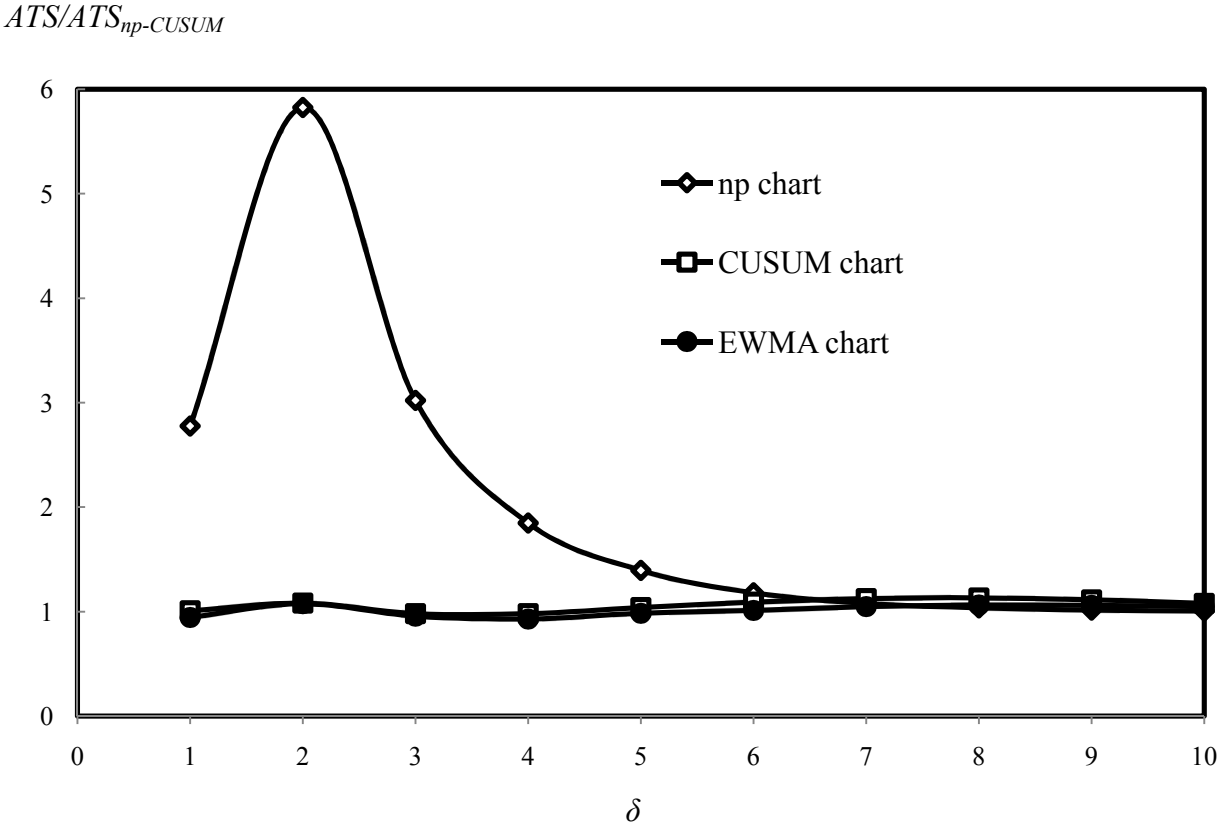

(a)

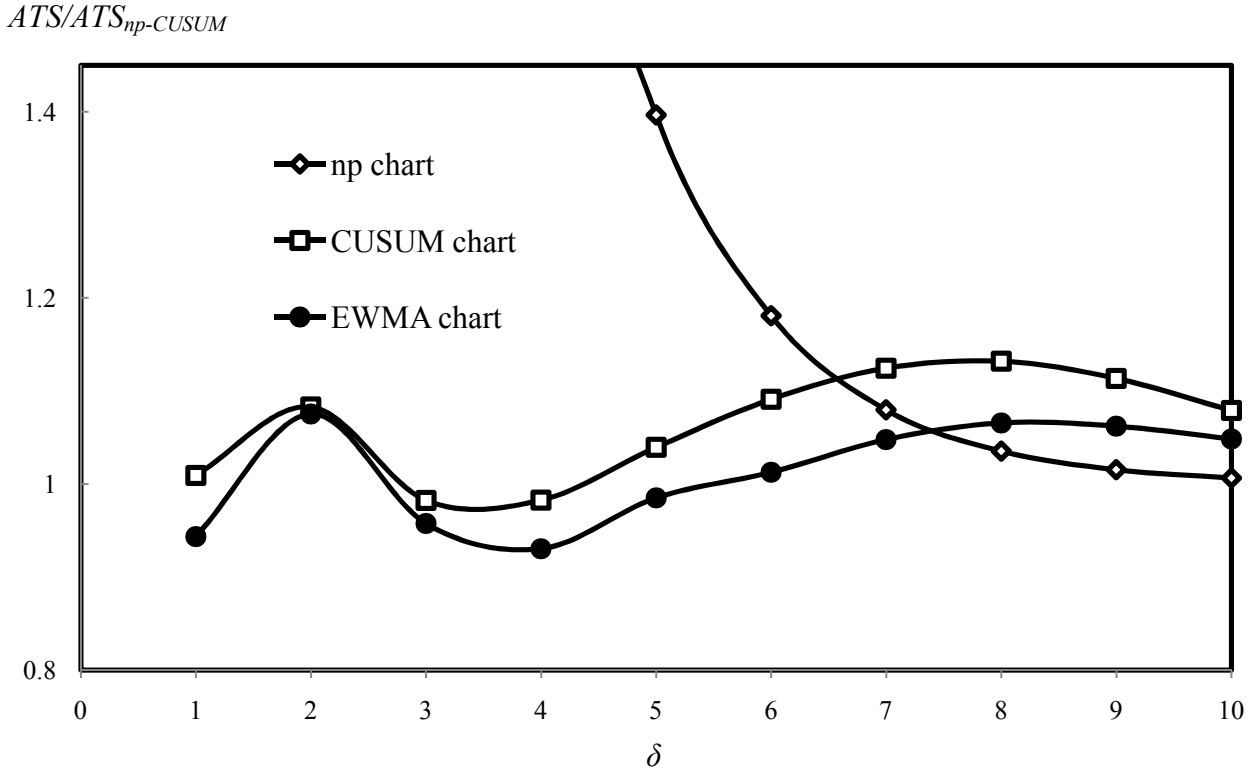

(b)

Figure 4.1: Normalized *ATS* of the np, CUSUM and EWMA Charts

4.4.2 Comparison under a factorial experiment

Next, the four charts are further studied under more different conditions through a 2^4 factorial experiment in which the four specifications (τ, p_0, δ_{max} and n) are used as the input factors and each of them varies at two levels as follows:

τ: 300, 1200.

p_0: 0.005, 0.03.

δ_{max}: 5, 15.

n: $0.6 / p_0$, $1.2 / p_0$.

This 2^4 experiment results in 16 different cases or combinations of τ, p_0, δ_{max} and n as shown in Table 4.2 (in cases 1 to 16). For each case, the four control charts are designed and each of them produces an ATS_0 no smaller than τ. In all these 16 cases, the relative detection effectiveness of the charts is similar to that revealed in Table 4.1; namely, the np-CUSUM chart is always more effective than the other three charts in terms of *AND*, with only one exception in case 5 where the np-CUSUM chart and CUSUM chart are identical and equally effective.

The charting parameters and overall performance, as reflected by *AND*, are listed in Table 4.2. The values of $AND_{np}/AND_{np\text{-}CUSUM}$, $AND_{CUSUM}/AND_{np\text{-}CUSUM}$ and $AND_{EWMA}/AND_{np\text{-}CUSUM}$ are always no smaller than one. The np-CUSUM chart always outperforms the np chart to a significant degree, especially when τ is large and δ_{max} is small. The ratio of $AND_{np}/AND_{np\text{-}CUSUM}$ has its maximum value of 6.31 in case 15. Similarly, the np-CUSUM chart is often considerably more effective than the CUSUM chart and EWMA chart, especially when τ is large and n is small. For example, in cases 13, the ratio of $AND_{EWMA}/AND_{np\text{-}CUSUM}$ is equal to 1.66 and in case 14, the ratio of $AND_{CUSUM}/AND_{np\text{-}CUSUM}$ is equal to 1.11. The rightmost column in Table 4.2 displays the reduction ratio (*RR*) that can be achieved when the np-CUSUM chart is adopted.

Table 4.2: Comparison of the Four Charts in the 2^4 Factorial Design

Case	τ	p_0	δ_{max}	n	Chart	k or λ	H or W	UCL	AND	$AND/AND_{np\text{-}CUSUM}$	RR
0	650	0.01	10	100	np	-	-	5	24.69	2.819	0.645
					CUSUM	1.750	4.630	-	9.62	1.098	0.089
					EWMA	0.230	1.275	-	9.01	1.029	0.028
					np-CUSUM	1.500	6.011	5	8.76	1.000	0.000
1	300	0.005	5	120	np	-	-	3	14.25	1.788	0.441
					CUSUM	0.950	4.333	-	8.29	1.040	0.039
					EWMA	0.410	1.402	-	9.57	1.201	0.167
					np-CUSUM	0.950	4.204	5	7.97	1.000	0.000
2	300	0.005	15	120	np	-	-	3	6.71	1.278	0.218
					CUSUM	0.950	4.236	-	5.55	1.057	0.054
					EWMA	0.365	1.294	-	5.27	1.004	0.004
					np-CUSUM	0.950	4.270	4	5.25	1.000	0.000
3	300	0.005	5	240	np	-	-	5	11.28	2.479	0.597
					CUSUM	2.150	3.725	-	4.82	1.059	0.056
					EWMA	0.275	1.404	-	4.56	1.002	0.002
					np-CUSUM	1.900	4.651	5	4.55	1.000	0.000
4	300	0.005	15	240	np	-	-	5	5.27	1.597	0.374
					CUSUM	2.150	3.703	-	3.39	1.027	0.027
					EWMA	0.365	1.741	-	3.37	1.021	0.021
					np-CUSUM	1.900	4.616	5	3.30	1.000	0.000
5	300	0.03	5	20	np	-	-	3	93.94	2.051	0.512
					CUSUM	0.950	4.173	-	45.80	1.000	0.000
					EWMA	0.365	1.260	-	52.47	1.146	0.127
					np-CUSUM	0.950	4.173	$+\infty$	45.80	1.000	0.000
6	300	0.03	15	20	np	-	-	3	41.87	1.421	0.296
					CUSUM	1.200	2.876	-	30.22	1.025	0.025
					EWMA	0.365	1.260	-	30.25	1.027	0.026
					np-CUSUM	0.950	5.349	3	29.47	1.000	0.000
7	300	0.03	5	40	np	-	-	5	73.91	2.854	0.650
					CUSUM	1.900	4.361	-	26.70	1.031	0.030
					EWMA	0.410	1.826	-	28.28	1.092	0.084
					np-CUSUM	1.900	4.472	5	25.90	1.000	0.000
8	300	0.03	15	40	np	-	-	5	33.19	1.719	0.418
					CUSUM	2.400	2.808	-	19.90	1.031	0.030
					EWMA	0.365	1.689	-	19.68	1.019	0.019
					np-CUSUM	1.900	4.400	5	19.31	1.000	0.000

Table 4.2: Comparison of Four Charts in the 2^4 Factorial Design (cont.)

Case	τ	p_0	δ_{max}	n	Chart	k or λ	H or W	UCL	AND	$AND/AND_{np\text{-}CUSUM}$	RR
9	1200	0.005	5	120	np	-	-	4	52.39	4.846	0.794
					CUSUM	0.950	5.647	-	10.85	1.004	0.004
					EWMA	0.275	1.277	-	13.62	1.260	0.206
					np-CUSUM	0.950	5.626	5	10.81	1.000	0.000
10	1200	0.005	15	120	np	-	-	4	18.60	2.848	0.649
					CUSUM	0.950	5.602	-	7.16	1.097	0.088
					EWMA	0.410	1.735	-	7.93	1.214	0.177
					np-CUSUM	0.950	6.324	4	6.53	1.000	0.000
11	1200	0.005	5	240	np	-	-	6	30.74	5.048	0.802
					CUSUM	2.150	4.856	-	6.53	1.072	0.067
					EWMA	0.455	2.424	-	8.02	1.317	0.241
					np-CUSUM	1.900	6.389	6	6.09	1.000	0.000
12	1200	0.005	15	240	np	-	-	6	11.01	2.830	0.647
					CUSUM	2.150	4.855	-	4.13	1.062	0.058
					EWMA	0.365	2.070	-	4.18	1.075	0.069
					np-CUSUM	1.900	6.342	6	3.89	1.000	0.000
13	1200	0.03	5	20	np	-	-	4	396.7	6.189	0.838
					CUSUM	0.950	5.515	-	64.64	1.008	0.008
					EWMA	0.545	2.018	-	106.7	1.665	0.399
					np-CUSUM	0.950	5.700	4	64.11	1.000	0.000
14	1200	0.03	15	20	np	-	-	4	134.1	3.706	0.730
					CUSUM	1.450	3.118	-	40.36	1.115	0.103
					EWMA	0.275	1.238	-	40.27	1.112	0.101
					np-CUSUM	0.950	5.729	4	36.20	1.000	0.000
15	1200	0.03	5	40	np	-	-	6	220.2	6.311	0.842
					CUSUM	1.900	5.805	-	36.07	1.034	0.032
					EWMA	0.455	2.383	-	46.94	1.345	0.256
					np-CUSUM	1.900	6.003	6	34.90	1.000	0.000
16	1200	0.03	15	40	np	-	-	6	75.95	3.371	0.703
					CUSUM	1.900	5.833	-	23.32	1.035	0.034
					EWMA	0.410	2.188	-	24.69	1.096	0.087
					np-CUSUM	1.900	6.001	6	22.53	1.000	0.000

Finally, a grand average $\overline{AND/AND_{np\text{-}CUSUM}}$ is calculated for each chart. It indicates the average of the $AND/AND_{np\text{-}CUSUM}$ values encompassing all the 16 cases in Table 4.2. The results are $\overline{AND_{np}/AND_{np\text{-}CUSUM}} = 3.13$, $\overline{AND_{EWMA}/AND_{np\text{-}CUSUM}} = 1.15$ and $\overline{AND_{CUSUM}/AND_{np\text{-}CUSUM}} = 1.05$.

This indicates that, from the most comprehensive viewpoint (covering all different values of τ, p_0, δ_{max} and n), the np-CUSUM chart is more effective than the np chart, EWMA chart and CUSUM chart by 213%, 15% and 5%, respectively.

It is noteworthy that neither the np chart nor the CUSUM chart can have higher overall effectiveness than the np-CUSUM chart under any circumstances (for any set of specifications τ, p_0, δ_{max} and n), because the np and CUSUM charts are a special case of the np-CUSUM chart. If the control limit H of an np-CUSUM chart is set infinitely large and its UCL is made equal to that of an np chart, then this np-CUSUM chart will perform exactly as an np chart. Similarly, if the upper limit UCL of the np-CUSUM chart is set infinitely large and its H and k are made equal to those of a CUSUM chart, then the np-CUSUM chart works exactly as the CUSUM chart. Consequently, one can always design an np-CUSUM chart that will surely perform better than, or at least as well as, the best np chart or the best CUSUM chart. As shown in Table 4.2, there is one special case (case 5) in which the np-CUSUM chart and CUSUM chart are equivalent and both produce the same results. In all other cases, the np-CUSUM chart outperforms both the np chart and CUSUM chart.

4.4.3 Comparison with the M-P np-CUSUM scheme

Finally, the performance of the np-CUSUM chart is compared with that of the M-P np-CUSUM scheme proposed by Morias and Pacheco (2006) under the following specifications (used as an example in their paper).

$$\tau = 240, p_0 = 0.05 \text{ and } n = 100 \qquad (4.10)$$

Since Morias and Pacheco (2006) have not specified a value for the maximum shift δ_{max}, a setting of (δ_{max} = 10) is used for this study. The charting parameters of the M-P np-CUSUM scheme as determined by Morias and Pacheco (2006) are k = 5.29, H = 18.3 and UCL = 8.79. However, these parameters produce a very small ATS_0 of 15 which violates the constraint ($ATS_0 \geq \tau$). In order to ensure a fair and meaningful comparison between the charts, the UCL of the M-

P np-CUSUM scheme has been relaxed from 8.79 to 15 so that ATS_0 approaches the value of τ (=240) as specified by Morias and Pacheco (2006). In addition, the CUSUM chart and np-CUSUM chart developed in this research are also designed for this case. The charting parameters and *AND* values of the three charts are as follows:

M-P np-CUSUM scheme: $k = 5.290$, $H = 18.300$, $UCL = 15$, $AND = 19.30$.

CUSUM chart: $k = 9.750$, $H = 2.406$, $AND = 18.60$.

np-CUSUM chart: $k = 7.250$, $H = 4.971$, $UCL = 15$, $AND = 17.20$.

The ratios of $AND_{M\text{-}P\ np\text{-}CUSUM}/AND_{CUSUM}$ and $AND_{M\text{-}P\ np\text{-}CUSUM}/AND_{np\text{-}CUSUM}$ are 1.04 and 1.12, respectively. This indicates that, The CUSUM chart and np-CUSUM chart reduce the average number of defectives by about 4% and 12%, respectively, compared with the M-P np-CUSUM scheme. The fact that the M-P np-CUSUM scheme is even inferior to the single CUSUM chart reflects the importance of the optimal design. In other words, if an np chart and a CUSUM chart are simply combined together without parameter optimization, the resultant combined np-CUSUM chart may not have a better performance than the individual CUSUM chart.

4.5 Calculation of the *ATS*

The cumulative probability function $F_d(D)$ of d can be calculated as follows:

$$F_d(D) = \Pr(d \le D) = \sum_{i=0}^{D} C_i^n p^i (1-p)^{n-i}$$
$$C_i^n = \frac{n!}{i!\,(n-i)!} \tag{4.11}$$

The np-CUSUM chart is a combination of a CUSUM chart element with parameters (H and k) and an np chart element with parameter (UCL). The np-CUSUM chart can be described by a Markov chain procedure. Suppose that the statistic C_t in Equation (4.2) experiences M different transitional states before being absorbed into the out-of-control state. States 0 to (M–1)

are the in-control states and state M is an out-of-control state. The width Δ of the interval of each state is given by:

$$\Delta = H / (M - 0.5) \tag{4.12}$$

The center, O_i, of state i is given by:

$$O_i = i \cdot \Delta \qquad i = 0, 1, \ldots, M. \tag{4.13}$$

The transition probability p_{ij} from state i to state j of the np-CUSUM chart is determined as follows:

for $j = 0$,

$$p_{i0} = \begin{cases} F_d[(0.5-i)\Delta + k] & if \quad UCL > (0.5-i)\Delta + k \\ F_d[UCL] & if \quad UCL < (0.5-i)\Delta + k \end{cases} \tag{4.14}$$

for $j > 0$,

$$p_{ij} = \begin{cases} F_d[u] - F_d[l] & if \quad UCL > u \\ F_d[UCL] - F_d[l] & if \quad l < UCL < u \\ 0 & if \quad UCL < l \end{cases} \tag{4.15}$$

where $l = (j - i - 0.5)\Delta + k$ and $u = l + \Delta$

When evaluating the in-control ARL_0, p_{ij} is calculated using $p = p_0$. Based on p_{ij}, the in-control transition probability matrix $\boldsymbol{R_0}$ is established. It is a $M \times M$ matrix excluding the elements associated with the absorbing (i.e., out-of-control) state.

$$\boldsymbol{R}_0 = \begin{bmatrix} p_{00} & p_{01} & \cdots & p_{0,M-1} \\ p_{10} & p_{11} & \cdots & p_{1,M-1} \\ \vdots & \vdots & \vdots & \vdots \\ p_{M-1,0} & p_{M-1,1} & \cdots & p_{M-1,M-1} \end{bmatrix}. \tag{4.16}$$

ARL_0 is equal to the first element of vector $\boldsymbol{U}$ given by the following expression:

$$\boldsymbol{U} = (\boldsymbol{I} - \boldsymbol{R_0})^{-1}\ \mathbf{1} \tag{4.17}$$

where $\boldsymbol{I}$ is an identity matrix and $\mathbf{1}$ is a vector with all elements equal to one. Finally, ATS_0 can be calculated from ARL_0.

$$ATS_0 = ARL_0 \times h \tag{4.18}$$

The transition probability matrix $\boldsymbol{R_1}$ for calculating the out-of-control *ARL* can be established similarly as $\boldsymbol{R_0}$ except that the transition probability p_{ij} of $\boldsymbol{R_1}$ must be evaluated according to the out-of-control p. It is assumed that the statistic C_t has reached its stationary distribution at the time when the p shift occurs and that the random time of process shift has a uniform distribution within the sampling interval (Reynolds *et al*. 1990). Based on these assumptions, the steady-state *ARL* is calculated below:

$$ARL = \boldsymbol{B}^T [(\boldsymbol{I} - \boldsymbol{R_1})^{-1} \mathbf{1} - \mathbf{1} / 2], \tag{4.19}$$

where $\boldsymbol{B}$ is the steady-state probability vector under ($p = p_0$). It is obtained by first normalizing the matrix $\boldsymbol{R_0}$ (making the sum of the elements in each row equal to one), and then solving the following Equation:

$$\boldsymbol{B} = \boldsymbol{R_0^T B} \tag{4.20}$$

subjected to

$$\mathbf{1}^T \boldsymbol{B} = 1 \tag{4.21}$$

At last, *ATS* can be calculated from *ARL*.

$$ATS = ARL \times h \tag{4.22}$$

4.6 Concluding Remarks

This research presents a new optimal np & CUSUM scheme (np-CUSUM chart) which comprises an np chart element and a CUSUM chart element. The design algorithm used to develop the new np-CUSUM chart does not only optimize the charting parameters of each of the np chart element and CUSUM chart element, but also optimizes the allocation of the detection power between the two elements, so that the best overall performance can be achieved. The allocation of the detection power is optimized by adjusting *UCL*. If *UCL* is tightened, *H* must be relaxed for $ATS_0 \geq \tau$. This will make the np-CUSUM chart more sensitive to large p shifts. Similarly, if *UCL* is loosened, *H* can be tightened, and the np-CUSUM chart will be more powerful in detecting small p shifts.

The results of the comparative studies show that the optimal design makes the np-CUSUM chart always outperform, or at least perform as well as, the np chart, CUSUM chart and EWMA chart in terms of *AND*. The np-CUSUM chart is more effective than the main competitor, the CUSUM chart, by 5% on average in terms of *AND*, and it considerably outperforms both the np and EWMA charts by 213% and 15%, respectively, under different settings.

The resultant ATS_0 of the np-CUSUM chart is usually very close to the specification τ in spite of the discrete nature of the attribute quality characteristics. It is also found that the primitive combination of an np chart and a CUSUM chart without optimizing the charting parameters may be inferior even to an individual CUSUM chart. This reflects the importance of the optimization in the design of control charts.

Due to the rapid advancement in computational technology, the complexity of the implementation of the np-CUSUM chart is almost the same as that of the np chart, CUSUM chart and EWMA chart. Since the np-CUSUM chart considerably outperforms the other charts, it is recommended that the individual charts be replaced by the np-CUSUM chart for attribute SPC.

The whole optimal design of the np-CUSUM chart can be implemented with a computer program by following a well developed procedure. Once the optimal design is carried out, the designed np-CUSUM chart can be used continuously and the improvement in detection effectiveness can be realized on a long term basis.

Chapter 5

CUSUM Chart with Curtailment (Curt_CUSUM)

This chapter proposes a binomial CUSUM chart with curtailment, the *Curt_CUSUM chart*, to monitor the fraction nonconforming *p*. The curtailment technique has been widely employed in acceptance sampling plans to significantly reduce the average sample number. The binomial cumulative sum (CUSUM) chart has been widely used to monitor the fraction nonconforming *p* of a process. It is a powerful procedure for detecting small and moderate *p* shifts. The new Curt_CUSUM chart is found to always have a better overall performance than the conventional CUSUM chart. On average, it is more effective than the CUSUM chart without curtailment by 36%, in terms of Average Number of Defectives (*AND*), under different circumstances. The high effectiveness of the Curt_CUSUM chart is mainly attributable to the curtailment technique. The Curt_CUSUM chart can be used for both 100% inspection and sampling inspection.

5.1 Introduction

The control chart developed in SPC is an effective on-line monitoring technique widely used in manufacturing industries and other sectors. The binomial cumulative sum (CUSUM) chart is one of the commonly used charts for attributes. The concept and operation of the binomial CUSUM chart have been introduced in Chapter (4). A statistic C_t is updated and plotted for the *t*th sample in a binomial CUSUM chart for detecting upward *p* shifts.

$$\begin{aligned} C_0 &= 0 \\ C_t &= \max\left(0,\ C_{t-1} + d_t - k\right) \end{aligned} \tag{5.1}$$

where d_t is the number of nonconforming units found in the *t*th sample and k is a reference parameter.

CUSUM charts have been increasingly recognized across industries for variable and attribute SPC applications (Lim *et al*. 2002, Pastell and Madsen 2008, Perry and Pignatiello 2011, Lee *et al.* 2012). Their popularity is mainly attributed to the fact that they are sensitive for detecting small and moderate shifts in different SPC applications.

Because of the simplicity of the attribute inspection, the applications of attribute control charts based on 100% inspection are relatively common (Montgomery 2013). In alignment with this, this research mainly focuses on 100% inspection. Under 100% inspection, it may be impossible to divide the products into samples of n units. In addition, the working shifts may be much longer than the sampling intervals. Under such conditions, the rational subgroup concept may not be applied. The samples can be created by taking n consecutive units as a sample for administrative convenience (Duncan 1986, Reynolds and Stoumbos 1999, Montgomery 2013). In fact, Hawkins and Olwell (1998) argued that the rational subgroup concept plays a useless part in CUSUM design and use.

Under a 100% inspection, the sampling interval h is equal to the product of the sample size n and the time t required to inspect a unit. Thus, the *ATS* can be evaluated as follows:

$$ATS = h \times ARL = n \times t \times ARL \tag{5.2}$$

In this research, the interval t is always used as the time unit (or in other words, *ATS* is measured in terms of t). Therefore, for the 100% inspection,

$$ATS = n \times ARL \tag{5.3}$$

The sample size n is a critical factor to *ATS*. Traditionally, n is rarely determined analytically. Many researchers (BSI Handbook 24 1985, Saniga *et al.* 1995) have suggested different methods for determining the sample size of the attribute charts. However, a sample size determined by these approaches doesn't necessarily produce the smallest *ATS*. It is common that a small sample size n will make the chart less sensitive to process shifts and result in a large *ARL* or *ATS*. On the other hand, a large sample size n will lead to a large sampling interval which also produces a large *ATS*. Therefore, one of the two factors (n and *ARL* in Equation (5.3)) of *ATS*

will increase and the other will decrease if there is a change of n in either direction. Theoretically, there should be an optimal value of n that minimizes *ATS* or maximizes the detection effectiveness of the control chart.

This research proposes a binomial CUSUM chart with curtailment (Curt_CUSUM chart) to monitor the fraction nonconforming p. The curtailment technique has been broadly used in acceptance sampling plans where a lot can be rejected without completing the inspection of the sample (Montgomery 2013). The curtailment can substantially reduce the total amount of required inspections. The curtailment has also been employed by Wu *et al*. (2006*a*) to develop an np chart. This np chart with curtailment doubled the detection speed of the conventional np chart without curtailment.

The performance of the Curt_CUSUM chart is compared with that of the conventional CUSUM chart (i.e., the binomial CUSUM chart without using curtailment) in a systematic and analytical manner. Both charts are designed by an optimal algorithm in which *AND* is still the objective function to be minimized. The results of the comparative studies show that, thanks to the curtailment technique, the Curt_CUSUM chart always has a better overall performance than the conventional CUSUM chart.

The remainder of this chapter is organized as follows. Firstly, the implementation of the Curt_CUSUM chart is presented in Section (5.2). Secondly, the design of the Curt_CUSUM chart is detailed in Section (5.3). Then, a comparative study is conducted for a general case, and then further through a factorial experiment in Section (5.4). The conclusions are drawn in Section (5.5).

5.2 Implementation of the Curt_CUSUM Chart

Similar to the conventional CUSUM charts, a Curt_CUSUM chart for detecting increasing p shifts is characterized by the reference parameter k and upper control limit H. The determination of k and H is discussed in the next section.

For a conventional CUSUM chart, a decision regarding the process status cannot be made until all the n units in a sample are inspected. On the contrary, in a Curt_CUSUM chart, an out-of-control status is detected before all the n units in a sample are inspected. The statistic $C_{t\text{-}1}$ for the (t-1)th sample of a Curt_CUSUM chart can be found by Equation (5.1), after this sample is processed. Let g_{ti} be the count of nonconforming units i found in the tth sample. The value of g_{ti} will increase one by one from zero during the inspection of the tth sample. Referring to Equation (5.1), the process is thought to be out of control when:

$$C_{t\text{-}1} + g_{ti} - k > H \tag{5.4}$$

$$\text{or } g_{ti} > G_t \tag{5.5}$$

$$\text{where } G_t = H + k - C_{t\text{-}1} \tag{5.6}$$

G_t is defined as the threshold of curtailment for the tth sample. This means that, as soon as $g_{ti} > G_t$, the process is deemed to be out-of-control and no further inspection of the remaining units in the tth sample is necessary. Consequently, an out-of-control signal may be produced earlier. This is the basic role of curtailment.

Suppose, for a CUSUM chart, n = 100, k = 2 and H = 4. If it is a conventional chart, an out-of-control signal cannot be produced until all the 100 units are inspected. On the other hand, suppose $C_{t\text{-}1}$ is equal to 3 when running a Curt_CUSUM chart, then

$$G_t = H + k - C_{t\text{-}1} = 4 + 2 - 3 = 3 \tag{5.7}$$

Now, if the 20th unit is identified as the 4th nonconforming unit (i.e., g_{ti} = 4 after 20 units are inspected), an out-of-control signal can be produced immediately since g_{ti} (= 4) becomes larger than the threshold G_t (= 3). In other words, the out-of-control status is detected after only 20 units are inspected compared with the sample size (n = 100).

A Curt_CUSUM chart can be implemented as follows:

(1) Initialize the statistic C_0 in Equation (5.1) as zero and set t = 1.

(2) Determine the threshold G_t by Equation (5.6).

(3) At the beginning of the tth sample, set the count g_{ti} of the nonconforming units at zero.

(4) Increase g_{ti} by one whenever a nonconforming unit is found. If $g_{ti} > G_t$ at any moment, terminate the inspection immediately; go to step (8).

(5) Otherwise (i.e., $g_{ti} \leq G_t$ up to the end of the sample), the process is considered to be in control currently and make $d_t = g_{ti}$.

(6) Update C_t by Equation (5.1)

$$C_t = \max\left(0,\ C_{t-1} + d_t - k\right) \tag{5.8}$$

(7) Increase t by one. Then, go back to step (2) and take the next sample.

(8) An out-of-control signal is produced and the process is stopped for further investigation.

It is clear that curtailment mechanism may detect the out-of-control condition in step (4) before completing the inspection of the entire sample and therefore, the signalling speed is expedited. In fact, the curtailment is the distinctive feature of the Curt_CUSUM chart compared to the conventional CUSUM chart.

5.3 Design of the Curt-CUSUM Chart

5.3.1 Objective function

The Average Number of Defectives (*AND*) presented in Equations (2.34 - 2.35) is adopted as the objective function for the design of the Curt_CUSUM chart in this chapter.

$$AND = 100 \int_{1}^{\delta_{max}} \delta \times p_0 \times ATS(\delta) \times f_{\delta}(\delta)\ d\delta \tag{5.9}$$

If *AND* is minimized, then the larger the δ is, the smaller the corresponding $ATS(\delta)$ will result from the optimal design.

In any process, the shift δ in fraction nonconforming p is assumed to follow a probability distribution. However, it is usually unknown and therefore one may have to design the control charts based on an assumed distribution over the shift domain. In Chapters (3) and (4), the shift δ

is assumed to follow uniform and beta distributions. In this and the following two chapters (Chapters (6) and (7)), the random shift δ is assumed to follow a Rayleigh distribution. In a recent study, Yang *et al*. (2013) found that the design and performance of the control charts such as the X and CUSUM charts are marginally influenced by the type of the probability distributions of process shifts. In other words, the type of the shift distribution almost has no effect on the performance of the control chart. This conclusion matches the results of the study conducted in Section (3.4.3).

Rayleigh distribution is often used to characterize the positional deviation from a target in geometrical tolerance. It was also adopted to model the mean shift of a normally distributed random variable (Wu *et al*. 2002). The Rayleigh distribution is skewed to the right (i.e., δ tends to cluster to the lower end) and looks like a reasonable representative of the distributions of many process shifts. If the Rayleigh distribution is used, the probability density function of δ in Equation (5.9) is as follows:

$$f_\delta(\delta) = \frac{\pi(\delta-1)}{2(\mu_\delta-1)^2}\exp\left(-\frac{\pi(\delta-1)^2}{4(\mu_\delta-1)^2}\right) \tag{5.10}$$

As shown, $f_\delta(\delta)$ is characterized by a single parameter μ_δ (the mean of δ). Figure 5.1 displays the probability density functions of three Rayleigh distributions with different μ_δ values. The cumulative distribution function of the Rayleigh distribution is

$$F_\delta(\delta) = 1-\exp\left(-\frac{\pi(\delta-1)^2}{4(\mu_\delta-1)^2}\right) \tag{5.11}$$

The value of μ_δ can be estimated from the historical data of the out-of-control cases. Suppose an out-of-control condition is signaled and a follow-up investigation discovers that the fraction nonconforming p during the estimated fallout duration is $\hat{p}_i$. Then $\hat{p}_i / p_0$ is the estimate of the sample shift $\hat{\delta}_i$ for this out-of-control case. If m records of $\hat{\delta}_i$ are available, then μ_δ can be estimated by

$$\mu_\delta = \frac{\sum_{i=1}^{m} \hat{\delta}_i}{m} \tag{5.12}$$

The values of δ_{max} in Equation (5.9) can be determined from Equation (5.11) so that the probability of ($\delta > \delta_{max}$) is negligible (say < 0.0001).

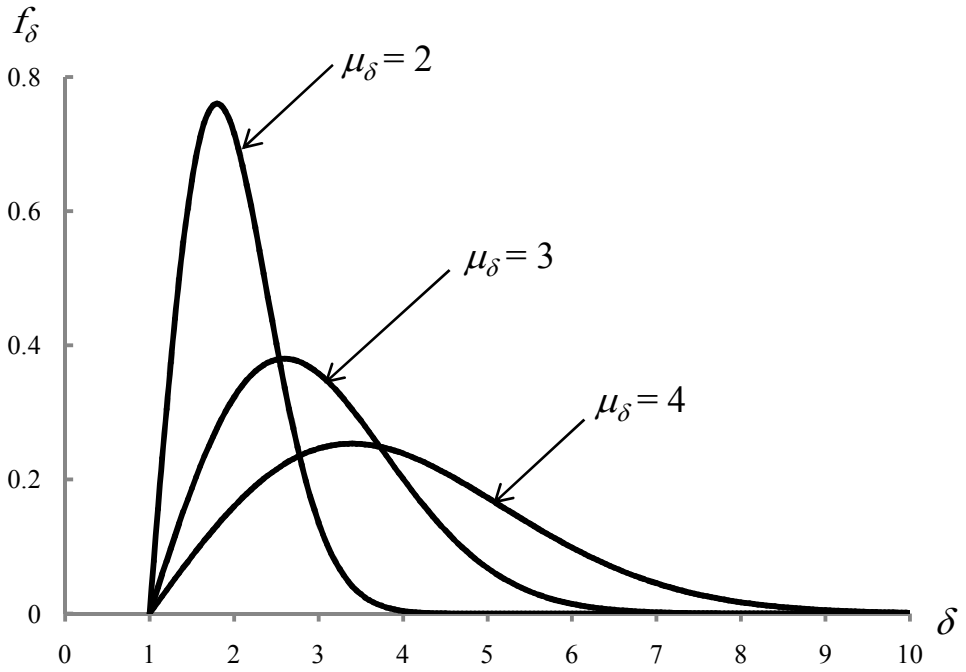

Figure 5.1: Three Rayleigh Probability Density Functions of δ

5.3.2 Specifications

To carry out the optimal design of a Curt_CUSUM chart, four specifications have to be given: (1) the minimum allowable value (τ) of the in-control ATS_0, (2) the in-control fraction nonconforming p_0, (3) the mean value (μ_δ) of the random shift δ, and (4) the sample size n.

The values of τ and p_0 are determined based on the same criteria mentioned in Section (3.3.2). The value of μ_δ is estimated from the historical data of the out-of-control cases, as presented in Equation (5.12). Finally, the value of n is specified based on the operational capability and managerial conditions. It is noteworthy that, in a 100% inspection, varying the sample size n simply means adjusting the grouping of the inspected units. In 100% inspection, every unit is inspected. As a result, the number of inspected units is always equal to the number

of produced units. A larger sample size is associated with a smaller number of samples (or less frequent sampling), and *vice versa*. For example, suppose the number of units produced per a working day is 20,000. If n is equal to 10, then 2000 samples of size 10 are required every day. On the other hand, if n is set as 1000, then 20 samples of size 1000 are taken for the same time interval.

A very small sample size n of a CUSUM chart may incur some difficulties in implementation. When n is small, it is quite difficult to handle the frequent sampling because of the troublesome updating of the statistic C_t in Equation (5.1) required by each sample. A large sample size will on the other hand, require less frequent updating of C_t (Bourke 2001*a*). For instance, if 2000 samples of size 10 have to be taken per day as in the above example, C_t has to be updated 2000 times per day. This must be exhausting and prone to error, and may encounter a serious reluctance from practitioners even if they only have to enter the number d of nonconforming units of each sample from the keyboard of a computer.

5.3.3 Design model

The design of the Curt_CUSUM chart can be formulated as follows:

Objective: Minimize AND (5.13)

Constraint: $ATS_0 \geq \tau$ (5.14)

Design variables: k, H.

where the reference parameter k is treated as an independent design variable. The upper control limit H is dependent on n, k and the specified τ.

The objective of the optimal design is to identify the optimal values of the independent design variable k that minimize the objective function AND, and meanwhile H is adjusted so that $ATS_0 \geq \tau$. The minimization of AND will in turn shorten the ATS values for different values of δ over the p shift range, or reduce the average number of nonconforming units incurred in the out-of-control cases.

5.3.4 Optimal search

The optimal design is implemented as outlined below:

(1) Specify the design parameters τ, p_0, μ_δ and n.

(2) Initialize a variable AND_{min} as a very large number, say 10^7 (AND_{min} is used to store the minimum value of AND).

(3) Search the optimal value of k. For a given value of k,

(3.1) Determine the control limit H that satisfies the constraint of ($ATS_0 \geq \tau$) within a predetermined tolerance such that $\left|\frac{ATS_0 - \tau}{\tau}\right| < 0.05$.

(3.2) When the values of the two charting parameters, k and H, are determined, the objective function AND is calculated by Equation (5.9).

(3.3) If the calculated AND is smaller than the current AND_{min}, replace the latter by the former and the current values of k and H are stored as a temporary optimal solution.

(4) At the end of the entire search, the optimal Curt_Cusum chart that produces the minimum AND and satisfies the constraint ($ATS_0 \geq \tau$) is identified. The corresponding optimal values of k and H are also finalized.

The above grid search approach is quite feasible, because there is only one independent design variable k whose optimal value can be easily determined by a search algorithm for a single variable.

In this research, the in-control ATS_0 and out-of-control ATS values of the conventional CUSUM chart and Curt_CUSUM chart are evaluated by simulation using a sample size of 100000. By using this number of iterations, the variation coefficients of ATS_0 and ATS for both the conventional CUSUM and Curt_CUSUM charts are less than 1%.

5.4 Comparative Studies

In this section, the detection effectiveness of two control charts (the conventional CUSUM chart and the Curt_CUSUM chart) is compared. Both charts are designed by using the design model in Equations (5.13) and (5.14). A conventional CUSUM chart is also designed for the best combination of the reference parameter k and upper control limit H so that the chart produces the minimum AND (Equation (5.9)) and has an ATS_0 equal to or larger than τ.

5.4.1 Comparison under a general case

This general case demonstrates the application of the conventional CUSUM chart and Curt_CUSUM chart in transformer manufacturing. A transformer is classified as nonconforming if any of the three defects (wrong orientation, misalignment and spot) is detected. The current in-control p_0 is estimated as 0.01 from the records of pilot runs. Based on some investigation records of the out-of-control cases, the random shift δ is found to approximately follow a Rayleigh distribution with a mean μ_δ of 3. The allowable minimum τ is set as 650 hours. A sample size n of 100 is selected based on the operational capability and managerial conditions. The design specifications are summarized as follows:

$$\tau = 650, p_0 = 0.01, \mu_\delta = 3, n = 100 \quad (5.15)$$

The two charts are designed for this case and the results are shown next:

Conv. CUSUM chart: $k = 1.95$, $H = 0.051$, $AND = 502.2$.

Curt_CUSUM chart: $k = 1.80$, $H = 0.207$, $AND = 371.4$.

As mentioned before, the value of δ_{max} can be calculated by Equation (5.11) based on μ_δ so that the probability of ($\delta > \delta_{max}$) is below 0.0001 and negligible. For this case, the value of δ_{max} is approximately equal to 7. The values of the in-control ATS_0 (where $\delta = 1$) and out-of-control ATS (where $1 < \delta \leq 7$) of the two charts are calculated within the process shift range, and the results are displayed in Table 5.1. The normalized ATS curve (i.e., ATS/ATS_{Curt_CUSUM}) of the

conventional CUSUM chart is illustrated in Figure 5.2. It is interesting to observe the following from Table 5.1 and Figure 5.2:

(1) Firstly, the two charts generate ATS_0 values larger than but close to τ (constraint (5.14)) when the process is in control. This suggests that both charts have nearly identical false alarm rate which provides a common ground for the comparison.

(2) The Curt_CUSUM chart is always more effective (has smaller *ATS* values) than the conventional CUSUM chart over the entire *p* shift range. It is clear that the curtailment feature of the Curt_CUSUM chart makes this scheme very effective from an overall viewpoint.

(3) It can be observed that the superiority of the Curt_CUSUM chart over the conventional CUSUM chart increases with the increase in δ. When δ = 7, the *ATS* value of the Curt_CUSUM chart is larger than that of the conventional CUSUM chart by 153%.

The *AND* values (Equation (5.9)) of the two charts are also calculated. The ratio of (AND_{CUSUM} /AND_{Curt_CUSUM}) = 502.2/371.4 = 1.35. This value indicates that, for this general case, the Curt_CUSUM chart reduces the average number of defectives by 35% compared with the conventional CUSUM chart over the range of *p* shifts.

Table 5.1: *ATS* of the Two Charts

δ	*ATS*	
	Conv. CUSUM chart	Curt_CUSUM chart
1	678.510	669.904
2	250.171	213.405
3	156.393	112.922
4	124.392	76.897
5	111.034	58.478
6	105.123	48.182
7	102.412	40.458

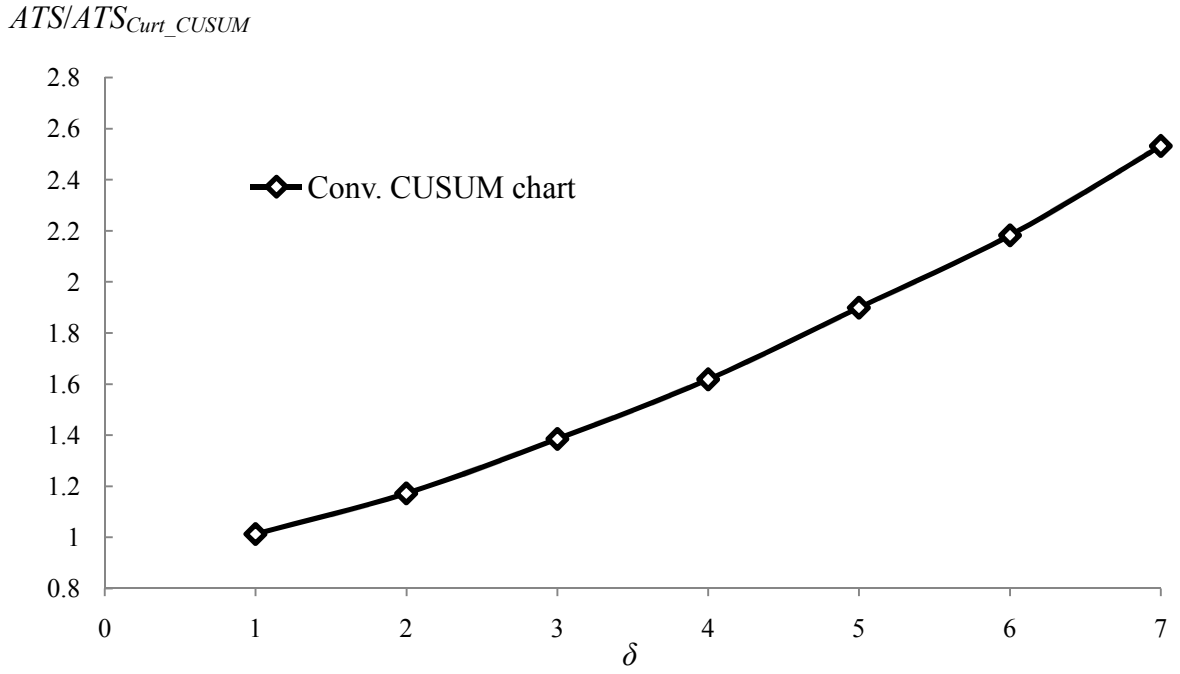

Figure 5.2: Normalized *ATS* of the Conventional CUSUM Chart

If the Curt_CUSUM chart is selected for this application, 100 units in each sample are inspected one by one. If the count g_{ti} of nonconforming units in a sample exceeds the threshold G_t (Equation (5.6)) at any time, the inspection is terminated immediately and the process is considered as out of control. Otherwise, the process is thought to be currently in control.

5.4.2 Comparison under a factorial experiment

Next, the two charts are further studied under different circumstances through a 2^4 factorial experiment in which the four specifications (τ, p_0, μ_{δ_μ} and n) are used as the input factors and each of them is varied at two levels as follows:

τ:	300,	1200.
p_0:	0.005,	0.03.
μ_δ:	2,	4.
n:	$0.6 / p_0$,	$1.2 / p_0$.

This 2^4 experiment results in 16 different cases or combinations of τ, p_0, μ_{δ_μ} and n as shown in Table 5.2 (in cases 1 to 16). Case 0 represents the general case conducted in the last section. For each case, the two control charts are designed and each of them produces an ATS_0 no smaller than τ. In all these 16 cases, the relative detection effectiveness of the charts is similar to that revealed in Table 5.1. Namely, the Curt_CUSUM usually produces smaller out-of-control *ATS* values than the conventional CUSUM chart.

The charting parameters of the two charts and the overall performance, as reflected by *AND*, in this factorial experiment are listed in Table 5.2. The value of $AND_{CUSUM}/AND_{Curt\_CUSUM}$ is always larger than one. This indicates that the Curt_CUSUM chart always outperforms the conventional CUSUM chart from an overall viewpoint. The former significantly excels the latter when n is large. For example, in case 4, when $n = 240$, the ratio of $AND_{CUSUM}/AND_{Curt\_CUSUM}$ has its maximum value of 2.31. The rightmost column in Table 5.2 displays the reduction ratio (*RR*) that can be obtained when the Curt_CUSUM chart is adopted.

Finally, a grand average $\overline{AND_{CUSUM}/AND_{Curt\_CUSUM}}$ is calculated. It indicates the average of the $AND_{CUSUM}/AND_{Curt\_CUSUM}$ values encompassing all the 16 cases in Table 5.2. The result is $\overline{AND_{CUSUM}/AND_{Curt\_CUSUM}} = 1.36$. This reveals that, from the most comprehensive viewpoint (covering all different values of τ, p_0, μ_{δ_μ} and n), the Curt_CUSUM chart is more effective than the conventional CUSUM chart by 36%. This reflects the unique contribution of the curtailment mechanism to the improvement of overall detection effectiveness. The curtailment enables the Curt_CUSUM chart to signal a p shift before all of the n units in a sample are inspected. This feature is most effective when the sample size n is large and/or the p shift is large.

Table 5.2: Comparison of the Two Charts in the 2^4 Factorial Design

Case	τ	p_0	μ_δ	n	Chart	k	H	AND	AND/AND_{Curt_CUSUM}	RR
0	650	0.01	3	100	Conv. CUSUM	1.950	0.051	502.20	1.349	0.260
					Curt_CUSUM	1.800	0.207	371.44	1.000	0.000
1	300	0.005	2	120	Conv. CUSUM	0.950	0.052	234.75	1.214	0.176
					Curt_CUSUM	0.950	0.050	193.41	1.000	0.000
2	300	0.005	2	240	Conv. CUSUM	1.900	0.001	326.14	1.459	0.315
					Curt_CUSUM	1.900	0.001	223.56	1.000	0.000
3	300	0.005	4	120	Conv. CUSUM	0.950	0.056	272.58	1.571	0.363
					Curt_CUSUM	0.950	0.054	173.56	1.000	0.000
4	300	0.005	4	240	Conv. CUSUM	1.900	0.001	451.50	2.305	0.566
					Curt_CUSUM	1.900	0.001	195.87	1.000	0.000
5	300	0.03	2	20	Conv. CUSUM	0.950	1.100	511.51	1.098	0.090
					Curt_CUSUM	0.950	1.117	465.69	1.000	0.000
6	300	0.03	2	40	Conv. CUSUM	1.900	0.200	538.13	1.171	0.146
					Curt_CUSUM	1.900	0.203	459.70	1.000	0.000
7	300	0.03	4	20	Conv. CUSUM	0.950	1.121	419.74	1.284	0.221
					Curt_CUSUM	0.950	1.100	326.91	1.000	0.000
8	300	0.03	4	40	Conv. CUSUM	1.900	0.218	537.26	1.643	0.391
					Curt_CUSUM	1.900	0.203	326.99	1.000	0.000
9	1200	0.005	2	120	Conv. CUSUM	0.950	1.050	427.44	1.101	0.092
					Curt_CUSUM	0.950	1.053	388.19	1.000	0.000
10	1200	0.005	2	240	Conv. CUSUM	1.900	0.125	480.56	1.239	0.193
					Curt_CUSUM	1.900	0.126	388.01	1.000	0.000
11	1200	0.005	4	120	Conv. CUSUM	0.950	1.050	385.87	1.333	0.250
					Curt_CUSUM	0.950	1.051	289.53	1.000	0.000
12	1200	0.005	4	240	Conv. CUSUM	1.900	0.125	520.14	1.743	0.426
					Curt_CUSUM	1.900	0.102	298.36	1.000	0.000
13	1200	0.03	2	20	Conv. CUSUM	0.950	2.285	1074.5	1.041	0.039
					Curt_CUSUM	0.950	2.252	1032.5	1.000	0.000
14	1200	0.03	2	40	Curt_CUSUM	1.900	2.104	1159.2	1.078	0.073
					Conv. CUSUM	1.900	2.101	1075.1	1.000	0.000
15	1200	0.03	4	20	Curt_CUSUM	0.950	2.252	662.76	1.149	0.130
					Conv. CUSUM	0.950	2.250	576.67	1.000	0.000
16	1200	0.03	4	40	Curt_CUSUM	2.150	1.734	763.66	1.283	0.221
					Conv. CUSUM	1.900	2.124	595.13	1.000	0.000

5.5 Concluding Remarks

This research proposes a new binomial CUSUM chart with curtailment (Curt_CUSUM chart). While the basic idea of the curtailment is quite simple, the new Curt_CUSUM chart outperforms the conventional CUSUM chart under different settings. On average, the former is more effective than the latter by 36% in terms of *AND*. In spite of the discrete nature of the attributes, the Curt_CUSUM chart usually generates an ATS_0 value close to the allowable value τ.

The high overall effectiveness of the Curt_CUSUM chart is mainly attributable to the use of curtailment. If a p shift occurs, the curtailment mechanism will come to play and signal the out-of-control condition before all of the n units in a sample are inspected.

The interpretation of the Curt_CUSUM chart is slightly more difficult than the conventional CUSUM chart as a curtailment threshold G_t is needed to be defined for each sample and the count of nonconforming units g_{ti} is required to be updated during the inspection of each sample and compared with G_t.

The whole design of the Curt_CUSUM chart can be easily carried out by a computer program by following a well developed procedure. Once the Curt_CUSUM chart is designed, it can be used continually (until the process settings change) and the enhancement in performance can be reaped on a long-term basis.

Although the Curt_CUSUM chart is developed based on a 100% inspection, it can also be applied to situations in which a random sampling inspection is used, as explained by Bourke (1991). In such cases, only the inspected items are taken into account and any items produced during the non-inspection periods are ignored.

Chapter 6

Optimal SPRT Chart

This chapter proposes a new *optimal SPRT chart* for monitoring the fraction nonconforming p. The Sequential Probability Ratio Test (SPRT) has been proven to be an effective procedure to produce a much lower expected sampling size than any other tests. Many SPC charts have been developed based on SPRT to effectively monitor manufacturing and service processes. The SPRT control chart is one of the most powerful monitoring techniques in SPC. It is highly suitable for the applications where testing is destructive or very expensive, such as the automobile airbags test, ammunition test and uniaxial tensile test. In this research, an algorithm is developed to design the optimal charting parameters of the SPRT chart for monitoring the fraction nonconforming p. By optimizing the charting parameters, the average detection speed of the SPRT chart is almost doubled. It is also found that the optimal SPRT chart significantly outperforms the optimal np and CUSUM charts by 221% and 171%, respectively, in terms of Average Number of Defectives (*AND*), under different circumstances. It is observed that the SPRT chart using a relatively smaller *ASN* and a shorter sampling interval (h) has a higher overall detection effectiveness.

6.1 Introduction

The np chart is the most popular and simple control chart for attributes. More advanced charts including the binomial CUSUM chart and SPRT chart have also been developed to monitor p (Roberts 1959, Gan 1993, Reynolds and Stoumbos 1998, Wu *et al*. 2008*a*). The np and CUSUM charts have been introduced in Chapter (3) and Chapter (4), respectively.

Traditional control charts are operated by taking samples of fixed size (n) from the process using a fixed sampling interval (h). Contrary to these traditional charts, n may be varied based on the data observed in the current sample. This is the idea of sequential analysis (Wald

1947, Ghosh 1970). Wald (1947) first defined the Sequential Probability Ratio Test (SPRT) and showed that it is optimal to produce a lower expected sampling size than any other tests with the same probability of error. Woodall and Reynolds (1983) used tests that can be represented exactly by discrete Markov chains to approximate the properties of the SPRT.

An SPRT control chart for detecting shifts in fraction nonconforming p was proposed by Reynolds and Stoumbos (1998). Inside a sample of an SPRT chart, individual observations are taken sequentially, with the possibility of a decision about the process after each observation. The statistical properties of the SPRT chart are evaluated based on the assumption that the time required to obtain an individual observation is short enough to be neglected relative to the sampling interval h between two samples. The SPRT chart has the administrative advantage of using a fixed sampling interval (FSI). Since the SPRT chart allows the sample size used at each sample to vary, it is similar to a variable sample size (VSS) chart. However, while the sample size of a VSS chart used at the current sample point depends on the data obtained in the last sample, the sampling size of an SPRT chart is determined based on the data observed at the current sample point.

Reynolds and Stoumbos (1998) found that the SPRT chart is substantially more effective than the Fixed Sampling Rate (FSR) charts, such as the p chart, the binomial CUSUM chart, or the Bernoulli CUSUM chart. However, neither the p chart, CUSUM chart, nor the SPRT chart had been optimized in their study. In other words, none of these charts perform at their highest detection effectiveness. Moreover, no systematic procedure was provided to determine the charting parameters of the SPRT chart. If these parameters are determined analytically and optimally, the overall effectiveness of the SPRT chart can be further increased to a significant degree.

An SPRT chart has five charting parameters: Average Sample Number (ASN) (or average sample size), reference value (γ), sampling interval (h), lower limit (g) and upper limit (H). A sample is taken at the end of each fixed sampling interval h. Within a sample, when the tth

observation x_t is taken, it is used to update the test statistic S_t. For an upper one-sided SPRT chart (where $-\infty < g < H < \infty$),

$$\begin{aligned} S_0 &= 0 \\ S_t &= S_{t-1} + x_t - \gamma \end{aligned} \tag{6.1}$$

where x_t is a Bernoulli random variable which is defined as $x_t = 1$ if the tth item is nonconforming and $x_t = 0$ otherwise. The choice of γ ($0 < \gamma < 1$) affects the performance of the chart. A small γ increases the sensitivity of the chart to small p shifts while a large γ makes the chart more effective in detecting large p shifts.

In a sample, if $S_t > H$, the process is deemed out of control and a signal is produced. If $g \le S_t \le H$, sampling is continued sequentially. Finally, if $S_t < g$, the process is considered in control and the current sample is terminated. The next sample is taken at the end of a fixed time interval h. It can be seen that the number n_i of observations (or the sample size) taken during a sample i is a random number. The mean value of n_i is *ASN*. This means that *ASN* is the average of sample sizes (n_i) of all the samples inspected during the monitoring of the process. Obviously, *ASN* is a continuous variable rather than an integer. In this research, only the in-control (or long run) value of *ASN* is of concern, because a stable process usually runs in an in-control condition for a long period and only occasionally falls into an out-of-control status for a short time period (Montgomery 2013). The *ASN* value in the out-of-control period has little influence on the long run *ASN* and is of much less concern (Arnold and Reynolds 2001).

This research proposes a new optimal SPRT chart for monitoring the fraction nonconforming p. The main objective is to identify the optimal charting parameters of an SPRT chart so that the best overall performance can be obtained. The results of performance studies reveal that the SPRT chart using a relatively small *ASN* (together with a short h) has a very high effectiveness. However, the optimal value of *ASN* of each SPRT chart needs to be determined by the optimal design. The sample size n and sampling interval h of the np and binomial CUSUM charts will also be optimized in order to achieve their best overall performance. Actually,

optimizing n and h for these traditional attribute control charts will also significantly improve their detection effectiveness so that they can stand as firm competitors to the SPRT chart.

In addition to the new optimal SPRT chart, a semi-optimal SPRT chart will also be developed in this research. While both γ and *ASN* are optimized in the design of the optimal SPRT chart, only γ is optimized in the design of the semi-optimal SPRT chart. In the design of both the semi-optimal and optimal SPRT charts, the *AND* is used as the objective function to be minimized so that the overall performance of the SPRT chart is improved. The SPRT chart proposed by Reynolds and Stoumbos (1998) is called the basic SPRT chart in this research. In the design of a basic SPRT chart, the *ASN* and reference value γ are given in advance.

The remainder of this chapter is organized as follows. Firstly, the implementation of the optimal SPRT chart is presented in Section (6.2). Secondly, the design procedure of the optimal SPRT chart is detailed in Section (6.3). Then, a comparative study is conducted in Section (6.4). Finally, the concluding remarks are drawn in Section (6.5).

6.2 Implementation of the optimal SPRT Chart

The optimal SPRT chart has five charting parameters: Average Sample Number (*ASN*) or average sample size, reference value (γ), sampling interval (h), lower limit (g) and upper limit (H). An optimal SPRT chart is implemented as follows:

(1) Take a sample at the end of each fixed sampling interval h.

(2) Within each sample, first initialize the statistic S_0 in Equation (6.1) as zero.

(3) Take an observation x_t and update S_t as follows (referring to Equation (6.1))

$$S_t = S_{t-1} + x_t - \gamma \tag{6.2}$$

(4) If $S_t < g$, the process is deemed to be in control and the current sample is terminated, and go back to step (2) for the next sample.

(5) If $S_t > H$, an out-of-control signal is produced and the process is stopped immediately for further investigation.

(6) Otherwise (i.e., if $g \le S_t \le H$), go back to step (3) and continue the sampling sequentially.

6.3 Design of the optimal SPRT Chart

6.3.1 Objective function

As indicated in the previous chapters, the objective function should be able to measure the detection effectiveness against all p shifts within the range of ($1 < \delta \le \delta_{max}$) because the optimal design aims at achieving the best overall performance. Therefore, the Average Number of Defectives (*AND*) is adopted as the objective function in this chapter too.

$$AND = 100 \int_{1}^{\delta_{max}} \delta \times p_0 \times ATS(\delta) \times f_\delta(\delta) \; d\delta \tag{6.3}$$

In this chapter, the shift δ in fraction nonconforming p is assumed to follow a Rayleigh distribution which has been introduced in Section (5.3.1). The density function $f_\delta(\delta)$ and the cumulative distribution function $F_\delta(\delta)$ of the Rayleigh distribution can be determined as follows:

$$f_\delta(\delta) = \frac{\pi(\delta-1)}{2(\mu_\delta-1)^2} \exp\left(-\frac{\pi(\delta-1)^2}{4(\mu_\delta-1)^2}\right) \tag{6.4}$$

$$F_\delta(\delta) = 1 - \exp\left(-\frac{\pi(\delta-1)^2}{4(\mu_\delta-1)^2}\right) \tag{6.5}$$

The value of μ_δ can be estimated from the historical data of the out-of-control cases (Wu *et al*. 2002) following the same procedure mentioned in Section (5.3.1).

$$\mu_\delta = \frac{\sum_{i=1}^{m} \hat{\delta}_i}{m} \tag{6.6}$$

6.3.2 Specifications

In the optimal design of an SPRT chart, four parameters have to be specified: (1) the allowable minimum value (τ) of the in-control ATS_0, (2) the in-control fraction nonconforming p_0, (3) the allowable inspection rate (r) and (4) the mean value (μ_δ) of the random shift δ.

The values of τ and p_0 are determined according to the same criteria mentioned in the earlier chapters. The inspection rate is the ratio between the average sample size n and the average sampling interval h. The allowable value r of the inspection rate depends on the available resources such as manpower and measurement instruments. Usually, only the in-control (or long run) value of r is considered, as a process often runs in an in-control condition for a long period and only occasionally falls into an out-of-control status for a short time period. The inspection rate in the short out-of-control period has a little influence on the long run value of r and is of much less concern (Arnold and Reynolds 2001). Finally, the value of μ_δ is estimated from the historical data of the out-of-control cases, using Equation (6.6).

6.3.3 Design model

In the optimal design of an SPRT chart, the Average Sample Number ASN and the reference value γ are used as the independent design variables. For a given inspection rate r, the relationship between ASN and the sampling interval h is given by

$$r = \frac{ASN}{h} \tag{6.7}$$

This equation indicates that an SPRT chart may use a larger ASN with less frequent sampling or a smaller ASN with more frequent sampling as long as Equation (6.7) stands. This also implies that there must be an optimal ASN (or an optimal combination of ASN and h) that optimizes the overall performance of an SPRT chart. During the design, the optimal values of ASN and γ are searched in order to minimize the objective function AND.

In the design of the basic SPRT chart (Reynolds and Stoumbos 1998), *ASN* is given. The value of γ can be chosen according to the size of the shift δ. A small γ renders the chart sensitive to small p shifts and a large γ makes the chart sensitive to large p shifts. In particular, if a basic SPRT chart is designed to detect a specified fraction nonconforming p_1, the value of γ can be determined from (Reynolds and Stoumbos 1998):

$$\gamma = \left(-\ln\left(\frac{1-p_1}{1-p_0} \right) \right) \Big/ \left(\ln\left(\frac{p_1(1-p_0)}{p_0(1-p_1)} \right) \right) \tag{6.8}$$

Once the aforementioned design specifications (τ, p_0, r, μ_δ) are made, the optimal values of the independent design variables (*ASN*, γ) and dependent design variables (h, g, H) of the optimal SPRT chart can be determined by using the following model:

Objective:	Minimize *AND*	(6.9)
Constraints:	$ATS_0 \geq \tau$	(6.10)
	$r = ASN / h$	(6.11)
Independent design variables:	*ASN*, γ	
Dependent design variables:	h, g, H	

The optimal design searches for the optimal values of the independent design variables *ASN* and γ in order to minimize the objective function *AND*. The index *AND* is a function of the *ATS* and random shift δ (Equation (6.3)) which has a probability density function of $f_\delta(\delta)$ (Equation (6.4)). Meanwhile, the *ATS* itself is also a function of δ. The minimization of *AND* will in turn shorten the *ATS* values for different values of δ over the p shift range, or reduce the average number of nonconforming units incurred in the out-of-control cases. The calculation of *ATS* and *ASN* can be found in Reynolds and Stoumbos (1998).

The dependent design variables (the sampling interval h, the lower limit g and upper limit H) are adjusted simultaneously so that both the constraints (6.10) and (6.11) are met at the same time. The two limits (g and H) have an effect on both *ASN* and ATS_0. However, the lower limit g mainly affects the value of *ASN* and the satisfaction of constraint (6.11), while the upper limit H only influences the value of ATS_0, or constraint (6.10).

6.3.4 Optimal search

The optimal design is implemented by a two-level search as outlined below:

(1) Specify the design parameters τ, p_0, r and μ_δ.

(2) Initialize variable AND_{min} as a very large number.

(3) At the first level, search optimal ASN (where $ASN \geq 1$). For each trial ASN value, the corresponding h is determined so that constraint (6.11) is satisfied:

$$h = ASN / r \tag{6.12}$$

(4) At the second level, with the values of ASN and h determined at the first level, search γ with a step size of 0.001 within the range of ($0 < \gamma < 1$). For a given set of values of (ASN, h, γ),

(4.1) Adjust the lower limit g to make the resultant or actual value $\bar{n}$ of the average sample number equal to ASN.

(4.2) Adjust the upper limit H to make the resultant or actual ATS_0 larger than but closest to τ (constraint (6.10)).

(4.3) Check if both the constraints (6.10) and (6.11) are met within the predetermined tolerances (note, step (4.2) may make the resultant $\bar{n}$ different from ASN by more than an allowed tolerance. If this occurs, repeat steps (4.1) and (4.2). Namely, if

$$\left|\frac{ATS_0 - \tau}{\tau}\right| < 0.05 \text{ and } \left|\frac{\bar{n} - ASN}{ASN}\right| < 0.10 \tag{6.13}$$

then advance to step (4.4); otherwise go back to step (4.1) to adjust g and H recursively. Here, the allowed tolerance for ATS_0 is set to 0.05, and that for ASN is set to 0.10.

(4.4) When the values of all the five charting parameters ASN, h, γ, g and H, are determined, the objective function AND is calculated by Equation (6.3).

(4.5) If the calculated *AND* is smaller than the current AND_{min}, replace the latter by the former and the current values of *ASN*, *h*, *γ*, *g* and *H* are stored as a temporary optimal solution.

(5) At the end of the two-level search, the optimal SPRT chart that produces the minimum *AND* and satisfies both constraints (6.10) and (6.11) is identified. The corresponding optimal values of *ASN*, *h*, *γ*, *g* and *H* are also finalized.

6.4 Comparative Studies

Reynolds and Stoumbos (1998) compared the performance of the basic SPRT chart, *p* chart and binomial CUSUM chart. They showed the superiority of the basic SPRT chart over the other two charts. In this section, the detection effectiveness of five control charts (the optimal np chart, the optimal CUSUM chart, the basic SPRT chart, the semi-optimal SPRT chart and the optimal SPRT chart) is studied and compared under six cases which are the most representative cases in Reynolds and Stoumbos (1998). The charts are studied only for detecting increases in the fraction nonconforming *p*.

The design of an optimal np chart finds the optimal combination of the sample size *n*, sampling interval *h* and the upper control limit *UCL* so that the chart produces the minimum *AND* (Equation (6.3)) and satisfies the constraints (6.10) and (6.11). For all the control charts, while a larger *n* (together with a long *h*) improves the effectiveness of the chart in detecting smaller shifts, a smaller *n* (together with a short *h*) enhances the chart's capability for signaling larger shifts for the same inspection rate. An optimal *n* can be identified that minimizes *AND*.

Similarly, the design of an optimal CUSUM chart finds the optimal combination of *n*, *h*, reference parameter *k* and control limit *U* so that the chart produces the minimum *AND* and satisfies constraints (6.10) and (6.11). The *ATS* of the CUSUM chart is determined by a Markov chain approach in Wu *et al.* (2008*a*).

The *ASN* of a basic SPRT chart is specified and the reference value γ is determined by Equation (6.8). The design of a semi-optimal SPRT chart can be carried out using the same design model in section (6.3.3) except that γ is the only independent design variable while *ASN* is known as in the basic SPRT chart. In fact, the basic SPRT chart and semi-optimal SPRT chart are just a special case of the optimal SPRT chart.

Reynolds and Stoumbos (1998) did not specify a value for μ_δ in their case studies as they did not consider the probability distribution of the p shift. However, a δ_{max} was specified for each of the cases they studied. In this research, μ_δ is determined so that the probability of ($\delta > \delta_{max}$) is equal to 0.0001.

6.4.1 Comparison under a general case

The five charts are first studied under a general case. This general case concerns the quality of the thrust washers manufactured in an automotive company. A control chart is to be designed to detect the increase in the fraction nonconforming p of the product. Based on the records when the process is in control, the quality engineer estimated the in-control p_0 as 0.01.

It was also found, after some investigation of the out-of-control cases, that the random shift δ can be fitted approximately to a Rayleigh distribution with a mean μ_δ of 7.41. The value of δ_{max} can be determined from Equation (6.5) based on μ_δ so that the probability of ($\delta > \delta_{max}$) is as negligible at 0.0001. When $\mu_\delta = 7.41$, the value of δ_{max} is approximately equal to 20.

The allowable minimum τ is set as 931 hours. Based on the available manpower, the company presently uses an SPRT chart with an *ASN* of 200 and an inspection rate r of 50 units / hr. The design fraction nonconforming p_1 is set as $3 \times p_0$. The design specifications are summarized as follows:

$$\tau = 931,\ p_0 = 0.01,\ r = 50,\ \delta_{max} = 20,\ p_1 = 0.03,\ \mu_\delta = 7.41 \qquad (6.14)$$

The company is interested in testing more alternative charts in an attempt to identify the most suitable one for monitoring the process. Five control charts are considered for this test, including an optimal np chart, an optimal CUSUM chart, a basic SPRT chart, a semi-optimal SPRT chart, and an optimal SPRT chart. The five charts are designed for this case and the results are shown in Table 6.1.

Table 6.1: Comparison of the Five Charts

Chart	Charting parameters				
	n or ASN	h	k or γ	g	UCL or U or H
Optimal np	140	2.80	-	-	5
Optimal CUSUM	44	0.88	0.870	-	3.955
Basic SPRT	200	4.00	0.018	-1.662	4.420
Semi-optimal SPRT	200	4.00	0.015	-1.122	5.852
Optimal SPRT	10	0.20	0.018	-0.074	5.192

The values of the in-control ATS_0 (when $\delta = 1$) and out-of-control ATS (when $1 < \delta \leq 20$) of the five charts are calculated within the process shift range, and the results are displayed in Table 6.2. The normalized ATS curves (i.e., $ATS/ATS_{optimal\ SPRT}$) of the optimal np, optimal CUSUM, basic SPRT and semi-optimal SPRT charts are illustrated in Figure 6.1. It is interesting to observe the following from Table 6.2 and Figure 6.1:

(1) Firstly, the five charts generate ATS_0 values larger than but close to τ when the process is in control. This ensures that constraint (6.10) on the false alarm rate is satisfied.

(2) As expected, the optimal CUSUM chart outperforms the np chart for small p shifts (when $\delta \leq 4$). But surprisingly the former is still more sensitive than the latter to larger p shifts (when $\delta \geq 8$). The reason is that the np chart uses a large sample size which helps reduce *AND* but weakens its effectiveness in detecting large shifts.

(3) The *ATS* curve of the basic SPRT chart almost coincides with that of the semi-optimal SPRT chart. This shows that optimizing γ only marginally improves the detection effectiveness of the basic SPRT chart in this general case.

(4) The optimal np and CUSUM charts outperform the basic SPRT and semi-optimal SPRT charts for large p shifts (when $\delta \geq 7$) while they are less effective than the basic and semi-optimal SPRT charts for smaller p shifts (when $\delta \leq 5$). The optimal np and optimal CUSUM charts can optimize their sample size n for better overall performance while the *ASN* of both basic SPRT and semi-SPRT charts is fixed.

(5) The optimal SPRT chart is always more effective than all other charts over the whole p shift range, except for $\delta = 2$ where the semi-optimal SPRT chart slightly outperforms it. The superiority of the optimal SPRT chart over the optimal np, basic SPRT and semi-optimal SPRT charts increases with the increase in δ. When $\delta = 20$, the optimal SPRT chart produces an *ATS* smaller than that of the optimal np, basic SPRT and semi-optimal SPRT charts by 608%, 912% and 912%, respectively. On the other hand, the optimal SPRT chart becomes more superior to the optimal CUSUM chart for small p shifts. When $\delta = 3$, the *ATS* of the optimal SPRT chart is smaller than that of the optimal CUSUM chart by 276%.

The *AND* values (Equation (6.3)), as well as the ratios of ($AND/AND_{optimal\ SPRT}$), of the five charts are enumerated in case 1 in Table 6.4. The values of ($AND/AND_{optimal\ SPRT}$) indicate that, for this general case, the optimal SPRT chart reduces the average number of defectives by 242%, 167%, 190% and 182% compared with the optimal np chart, optimal CUSUM chart, basic SPRT chart and semi-optimal SPRT chart, respectively, over the range of p shifts.

It is worth noting that the lower limit g of the optimal SPRT chart is quite tight (i.e., has a high value) compared with that of the basic SPRT and semi-optimal SPRT charts. Thus, when

the process is in control, the optimal SPRT chart can reach an in-control conclusion quickly and terminate SPRT sampling after taking just a few observations. It is reflected by the small *ASN* (= 10) of the optimal SPRT chart. A small *ASN* in turn results in a small sampling interval *h* for a given inspection rate. A small *h* means a more frequent sampling and helps increase the detection effectiveness. It can be seen that the values of *ASN* and *h* of the optimal SPRT chart are smaller than those of the optimal np, basic SPRT and semi-optimal SPRT charts. Also, it can be observed that the optimal SPRT chart has a relatively smaller *ASN* and *h* compared with the CUSUM chart that usually adopts a small sample size and frequent sampling in order to achieve a high overall performance.

Table 6.2: *ATS* of the Five Charts

δ	*ATS*				
	Optimal np chart	Optimal CUSUM chart	Basic SPRT chart	Semi-optimal SPRT chart	Optimal SPRT chart
1	931.906	939.387	945.090	941.159	933.413
2	42.924	24.506	8.313	6.175	7.544
3	10.036	7.371	2.718	2.789	1.963
4	4.312	4.095	2.171	2.267	1.154
5	2.567	2.781	2.049	2.104	0.844
6	1.891	2.079	2.017	2.044	0.682
7	1.604	1.647	2.005	2.019	0.570
8	1.482	1.357	2.002	2.008	0.491
11	1.404	0.875	2.000	2.001	0.352
14	1.400	0.646	2.000	2.000	0.278
17	1.400	0.530	2.000	2.000	0.230
20	1.400	0.475	2.000	2.000	0.198

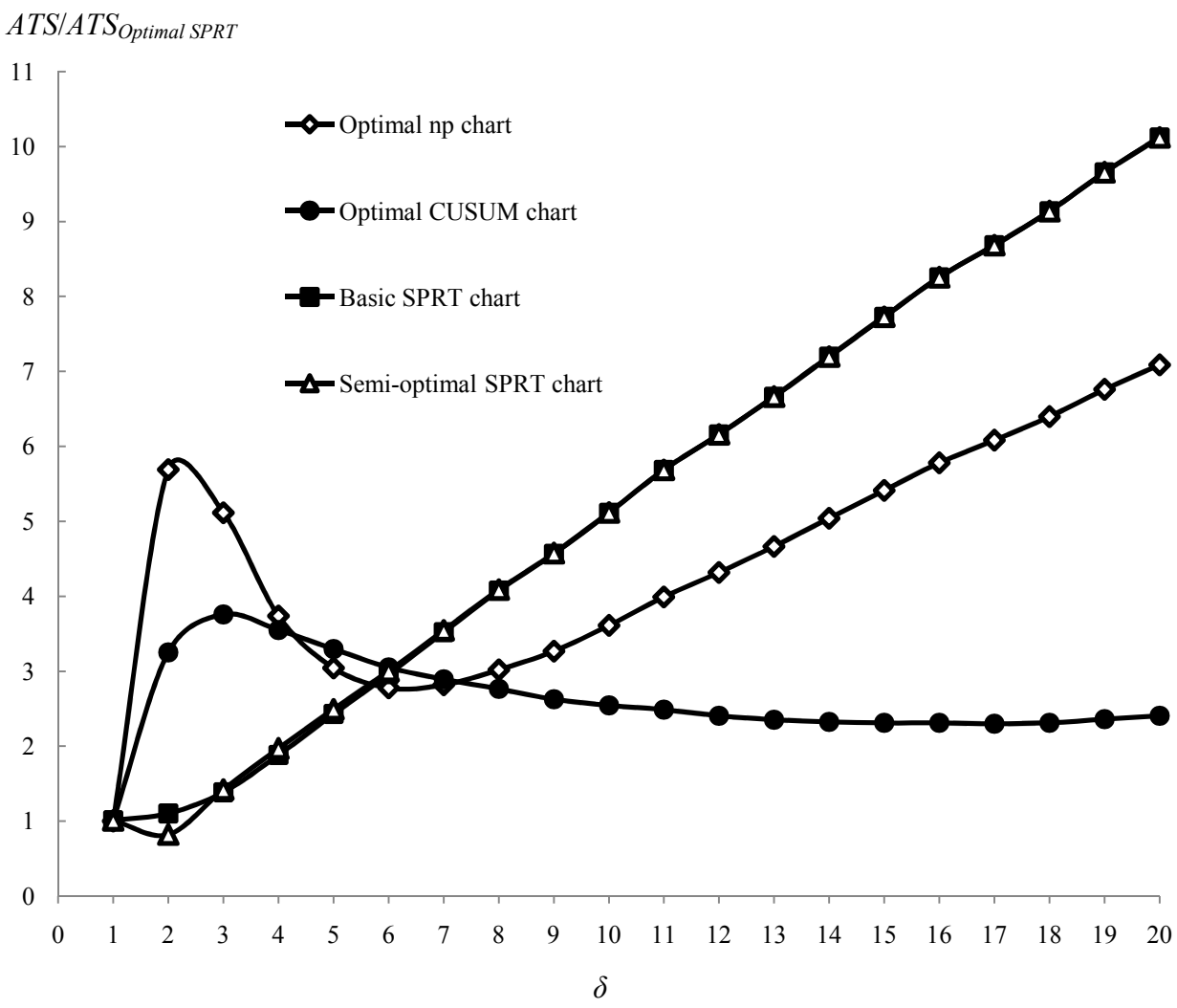

Figure 6.1: Normalized *ATS* of the Optimal np, Optimal CUSUM, Basic SPRT and Semi-optimal SPRT Charts

If the optimal SPRT chart is selected for this general case, the following statistic S_t can be used to detect the increasing p shifts in the produced thrust washers.

$$S_0 = 0$$
$$S_t = S_{t-1} + x_t - \gamma \qquad (6.15)$$

The statistic S_t is updated and plotted for each inspected washer in the current sample. Table 6.3 shows the values of the updated statistic S_t and Figure 6.2 illustrates a sample run of this SPRT chart. As shown, one sample is inspected every 0.2 hr. The sequential inspection inside the first sample is terminated after the fourth washer is inspected and the process is concluded to be in control as S_4 becomes smaller than g. Then, an increasing p shift occurs.

Therefore, when inspecting the second sample, S_6 goes above H, and the SPRT chart signals an out-of-control status. As a result, the inspection is terminated and the process is stopped immediately for further investigation.

Table 6.3: Values of S_i for the Sample Run of the Optimal SPRT Chart

1st Sample	S_0	S_1	S_2	S_3	S_4		
	0	-0.018	-0.037	-0.056	-0.075		
2nd Sample	S_0	S_1	S_2	S_3	S_4	S_5	S_6
	0	0.982	1.964	2.946	3.928	4.910	5.892

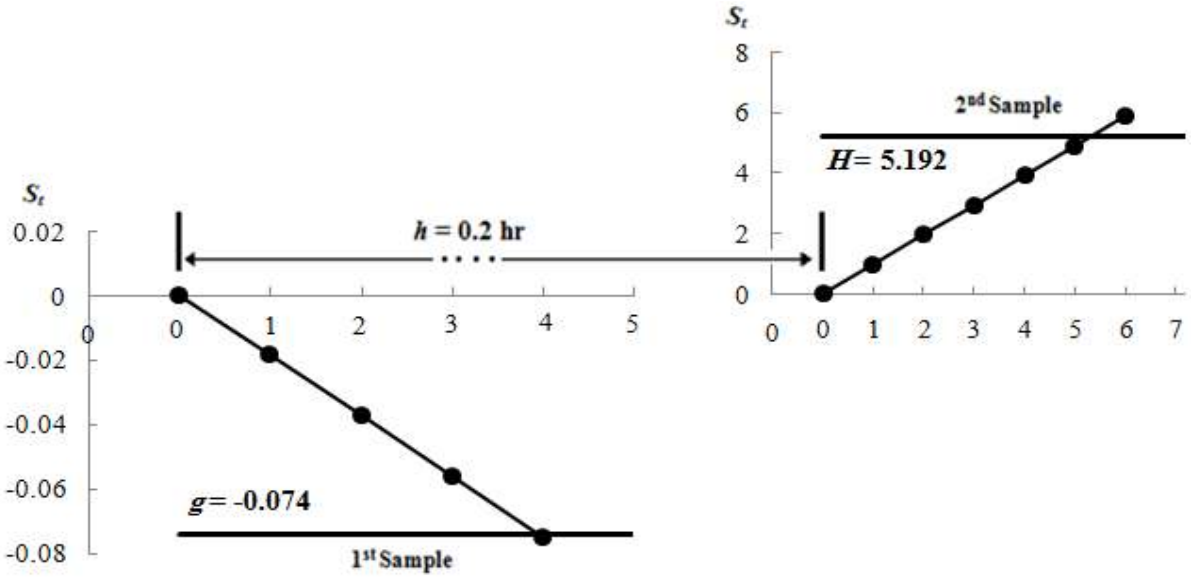

Figure 6.2: A Sample Run of the Optimal SPRT Chart

6.4.2 Comparison under additional cases

Next, the five charts are compared under five other cases. As mentioned before, these five cases together with the general case above are selected by Reynolds and Stoumbos (1998) to illustrate the relative performance of the charts under different combinations of the design specifications. In all of these five cases, the same specifications (τ, p_0, r, δ_{max}, p_1) determined by Reynolds and Stoumbos (1998) are used in this comparison, and μ_δ is acquired based on δ_{max} as explained before. For the basic SPRT chart, the reference value γ is set with reference to p_1 (Equation (6.8)).

For each case, the five control charts are designed and each of them produces an ATS_0 larger than but close to τ. Table 6.4 displays the charting parameters, values of *AND* and ($AND/AND_{optimal\ SPRT}$) of each chart under the five additional cases (cases 2 to 6), as well as the general case (case 1). In all these 5 cases, the relative operating characteristics of the charts are similar to that in Table 6.2 and Figure 6.1. The optimal SPRT chart is more effective than the other four charts for detecting *p* shifts of almost all sizes.

The overall performance, as reflected by *AND*, is summarized in Table 6.4 for the six cases. In all of the six cases, the values of ($AND/AND_{optimal\ SPRT}$) are larger than one. This indicates that the optimal SPRT chart always has a better overall performance than the other charts. The optimal SPRT chart always outperforms the optimal np and optimal CUSUM charts to a significant degree. The ratios of $AND_{optimal\ np}/AND_{optimal\ SPRT}$ and $AND_{optimal\ CUSUM}/AND_{optimal\ SPRT}$ have their maximum values of 3.66 and 3.15, respectively, in case 5. Moreover, the optimal SPRT chart is always considerably more effective than the basic SPRT and semi-optimal SPRT charts. The rightmost column in Table 6.4 shows the reduction ratio (*RR*) that can be obtained when the optimal SPRT chart is adopted.

It can be observed that in some cases (cases 1 and 2), the optimal CUSUM chart outperforms the basic SPRT and semi-optimal SPRT charts in terms of *AND,* especially when the *ASN* values of these two SPRT charts are large. This indicates the key role of the optimization in the design of the control charts and reflects the fact that if the SPRT chart is not optimized, it may not be necessarily better than the traditional charts such as the CUSUM chart from an overall viewpoint. Also, it is noted that the semi-optimal SPRT chart always outperforms, or at least performs as well as, the basic SPRT chart in terms of *AND*. In cases 2 and 3, these two SPRT charts are almost equally effective. The reason is that, in these two cases, the charting parameters of the basic SPRT chart are close to the optimal values. In all other cases, the semi-optimal SPRT chart outperforms the basic SPRT chart. It is noteworthy that neither the basic SPRT chart nor the semi-optimal SPRT chart can have higher overall effectiveness than the optimal SPRT chart under any circumstances, because each of them is just a special case of the optimal SPRT chart, as explained before.

Table 6.4: Comparison of the Five Charts under Different Six Cases

Case	τ	R	p_0	p_1	δ_{max}	μ_δ	Chart	n or ASN	h	g	UCL or U	k or γ	AND	$AND/AND_{Optimal\ SPRT}$	RR
1	931	50	0.01	0.030	20	7.41	Optimal np	140	2.80	-	5	-	19.68	3.418	0.707
							Optimal CUSUM	44	0.88	-	3.955	0.870	15.40	2.674	0.626
							Basic SPRT	200	4.00	-1.662	4.420	0.018	16.73	2.905	0.656
							Semi-optimal SPRT	200	4.00	-1.122	5.852	0.015	16.26	2.823	0.646
							Optimal SPRT	10.0	0.20	-0.074	5.192	0.018	5.76	1.000	0.000
2	931	50	0.01	0.020	20	7.41	Optimal np	140	2.80	-	5	-	19.68	3.418	0.707
							Optimal CUSUM	44	0.88	-	3.955	0.870	15.40	2.674	0.626
							Basic SPRT	200	4.00	-0.940	6.408	0.014	16.28	2.827	0.646
							Semi-optimal SPRT	200	4.00	-1.122	5.852	0.015	16.26	2.823	0.646
							Optimal SPRT	10.0	0.20	-0.074	5.192	0.018	5.76	1.000	0.000
3	931	25	0.01	0.025	20	7.41	Optimal np	107	4.28	-	4	-	31.40	2.985	0.665
							Optimal CUSUM	36	1.44	-	3.161	0.810	26.20	2.491	0.598
							Basic SPRT	100	4.00	-0.645	4.692	0.016	19.03	1.810	0.447
							Semi-optimal SPRT	100	4.00	-0.745	4.328	0.017	18.95	1.802	0.445
							Optimal SPRT	10.0	0.40	-0.090	4.501	0.018	10.52	1.000	0.000
4	931	12.5	0.01	0.025	20	7.41	Optimal np	72	5.76	-	3	-	50.84	2.652	0.623
							Optimal CUSUM	46	3.68	-	3.044	0.900	42.88	2.237	0.553
							Basic SPRT	5	0.40	-0.028	4.297	0.016	22.96	1.198	0.165
							Semi-optimal SPRT	5	0.40	-0.028	4.661	0.015	22.28	1.162	0.140
							Optimal SPRT	7.5	0.60	-0.068	3.755	0.019	19.17	1.000	0.000
5	1000	25	0.05	0.100	4	2.01	Optimal np	159	6.36	-	15	-	233.24	3.660	0.727
							Optimal CUSUM	13	0.52	-	6.145	0.990	200.52	3.147	0.682
							Basic SPRT	100	4.00	-2.135	6.995	0.072	106.46	1.671	0.401
							Semi-optimal SPRT	100	4.00	-0.895	12.971	0.058	70.80	1.111	0.100
							Optimal SPRT	5.0	0.20	0.086	12.795	0.059	63.72	1.000	0.000
6	1000	12.5	0.05	0.100	4	2.01	Optimal np	156	12.48	-	14	-	317.15	3.181	0.686
							Optimal CUSUM	9	0.72	-	5.705	0.690	305.94	3.069	0.674
							Basic SPRT	50	4.00	-1.095	6.471	0.072	146.80	1.472	0.321
							Semi-optimal SPRT	50	4.00	-0.795	8.375	0.064	111.64	1.120	0.107
							Optimal SPRT	5.0	0.40	0.036	11.633	0.058	99.70	1.000	0.000

Finally, a grand average $\overline{AND / AND_{optimal\ SPRT}}$ is calculated for each chart. It indicates the average of the $AND/AND_{optimal\ SPRT}$ values encompassing all the six cases in Table 6.4. The results are $\overline{AND_{optimal\ np} / AND_{optimal\ SPRT}}$ = 3.21, $\overline{AND_{optimal\ CUSUM} / AND_{optimal\ SPRT}}$ = 2.71, $\overline{AND_{basic\ SPRT} / AND_{optimal\ SPRT}}$ = 1.98 and $\overline{AND_{semi-optimal\ SPRT} / AND_{optimal\ SPRT}}$ = 1.80. This indicates that, from the most comprehensive viewpoint (covering all different values of τ, p_0, r, δ_{max}, p_1 and μ_δ), the optimal SPRT chart is more effective than the optimal np chart by 221%, the optimal CUSUM chart by 171%, the basic SPRT chart by 98% and the semi-optimal SPRT chart by 80%.

In summary, the optimal SPRT chart outperforms the other charts under different settings, thanks to the optimization of the Average Sampling Number (*ASN*) and the reference value γ. Moreover, since the optimal design only changes the values of the charting parameters, the implementation of the optimal SPRT chart is the same as that of the basic SPRT chart. In particular, the optimal SPRT chart still uses a fixed sampling interval.

6.5 Concluding Remarks

This research proposes an optimal SPRT chart for monitoring the fraction nonconforming p. A design algorithm is developed for determining the optimal charting parameters. The performance of the optimal SPRT chart is compared with those of the optimal np chart, optimal CUSUM chart and basic SPRT chart. The basic SPRT chart itself is very effective for detecting p shifts. However, by optimizing the Average Sample Number (*ASN*) and the reference value (γ), the optimal SPRT chart doubles the overall detection effectiveness compared with the basic SPRT chart in terms of *AND*. This reflects the importance of the optimal design of the SPRT chart. This also indicates that more significant gain in the detection effectiveness of some control charts may be obtained by improving the design algorithm of an existing chart rather than proposing a completely new chart.

The optimal SPRT chart also demonstrates a substantial superiority over the optimal np chart and optimal CUSUM chart. The semi-optimal SPRT chart in which only γ is optimized also enhances the detection effectiveness under certain conditions. The results of the comparative studies reveal that the SPRT chart using a relatively small *ASN* and short *h* has a very high detection effectiveness. It may happen that the optimal SPRT chart is inferior to the other charts for detecting one or a few shift points in terms of *ATS*, but the former will definitely outperform other charts in terms of *AND* over the entire shift range.

In alignment with numerous studies in the literature that investigate the optimal sample size of variable control charts (such as the $\bar{X}$ and CUSUM charts) (Reynolds and Stoumbos 2004*a*, Wu *et al*. 2011, Yang *et al*. 2012), this research also explores the optimal sample size *n* of some traditional control charts such as the np and binomial CUSUM charts in an attempt to enhance their overall performance. It is found that optimizing *n* and *h* for the traditional charts such as np and CUSUM charts significantly improves their detection performance. The np chart usually requires a larger *n* for a better overall performance. On the contrary, the CUSUM chart prefers a smaller *n* and the SPRT chart in general uses a smaller *ASN* in order to achieve a higher overall detection effectiveness. These findings are certainly useful to all potential users of the attribute control charts.

The optimal design of an SPRT chart only changes the values of the charting parameters. The implementation of an optimal SPRT chart is identical to that of a basic SPRT chart. In particular, the optimal SPRT chart still benefits from using a fixed sampling interval during the implementation. The whole optimal design can be implemented with a computer program.

The implementation of the SPRT chart is usually more difficult than the Fixed Sampling Rate (FSR charts). The in-control sample number (SN_0) of the SPRT chart may be extremely long occasionally in a particular sample. This may cause some operational problems. In practice, a threshold for the SN_0 can be adopted. If SN_0 in a sample exceeds this threshold, the sampling inspection is truncated and the process in concluded to be in control.

Chapter 7

Attribute Chart for Monitoring a Variable (AFV Chart)

This chapter proposes an attribute chart for variables (*AFV chart*). It employs an attribute inspection (checking whether a unit is conforming or nonconforming) to monitor not only the mean but also the variance of a variable. The salient feature of the AFV chart is its ability to determine the process status (i.e., in control or out of control) by applying the very simple attribute inspection to a single unit. By selecting its inspection limits appropriately, the AFV chart usually outperforms the $\bar{X}$&R and $\bar{X}$&S charts from an overall viewpoint under different circumstances. The AFV chart has the advantage of being extremely simple in design and implementation, and having a very low cost for operation. In particular, the AFV chart uses a single attribute inspection for each sample and therefore, eliminates the need for the computation of any statistic and the expensive measurements for variable inspection. In addition, the AFV chart works as a leading indicator of trouble and allows operators to take the proper corrective action before many defectives are actually produced. Since the AFV chart is simpler, more effective and less costly than the $\bar{X}$&R and $\bar{X}$&S charts, it may be highly preferred for many SPC applications, in which both the mean and variance of a variable need to be monitored.

7.1 Introduction

In SPC for variables, the foremost task of a control chart is to effectively detect process shifts in mean and variance (Montgomery 2013). The combination of a Shewhart $\bar{X}$ chart and an R chart (or an S chart) has been employed widely for this purpose. Many models for the optimal designs of the $\bar{X}$&R and $\bar{X}$&S charts have been proposed (Saniga 1989, Wu and Wang 1997, Costa 1999). A sample size *n* between 4 and 6 is usually recommended for the $\bar{X}$&R and $\bar{X}$&S

charts (Montgomery 2013, Reynolds and Stoumbos 2004*a*). A single X chart (a special $\bar{X}$ chart with a sample size $n = 1$) is also able to detect two-sided mean shifts δ_μ and/or an increasing variance shift δ_σ (Reynolds and Stoumbos 2004*a*, Yang *et al*. 2012). In fact, many researchers point out that there is essentially no advantage to using the X and moving range (X&MR) combination for detecting δ_μ and/or δ_σ when $n = 1$ (Reynolds and Stoumbos 2001, Stoumbos *et al*. 2003). It is only slightly more effective than the X chart (Reynolds and Stoumbos 2004*b*).

More sophisticated cumulative sum (CUSUM), exponentially weighted moving average (EWMA) and sequential probability ratio test (SPRT) schemes have also been developed to detect mean shift δ_μ and standard deviation shift δ_σ. However, the design of these advanced charts is challenging and requires a substantial computational effort compared with Shewhart control charts. Moreover, these charts may be difficult to understand and implement by operators. As a result, up to now, the Shewhart $\bar{X}$&R and $\bar{X}$&S charts are still the most widely used techniques for monitoring the mean and variance of a variable and are explained in detail in any SPC textbook.

The control charts for attributes are mainly used to monitor manufacturing processes in which quality characteristics cannot be measured on a continuous numerical scale. However, an attribute chart can also be employed to monitor a variable x, based on whether x falls within the specification limits (conforming), or beyond (nonconforming). Here, a simple attribute inspection is used to determine if a unit is conforming or nonconforming. The attribute inspection (e.g., using a gauge to check if the diameter x of a shaft exceeds the specification limits) is widely used owing to its simplicity in implementation and low operational cost, compared with the variable inspection (e.g., using a micrometer to measure the actual value of x). By using attribute charts, "expensive and time-consuming measurements may be avoided by attributes inspection" (Montgomery 2013). The sample sizes of the attribute charts are usually much larger than those of the variable charts. This also implies that the attribute inspection is much simpler and less time-consuming than the variable inspection.

In spite of the common belief that the attribute charts are inefficient to deal with a quality characteristic that is of a variable type, some research work has been recently developed in an attempt to monitor the mean of a variable x, by using an attribute chart based on an attribute inspection. Montgomery (2013) gave an example in which a variable chart ($\bar{X}$ chart) and an attribute chart (np chart) are compared for detecting the mean shift of a quality characteristic x with a normal distribution ~ $N(50, 2^2)$. When using the np chart to monitor the mean of x, the upper and lower specification limits *USL* and *LSL* are used to decide if a unit is conforming or nonconforming. Then, the number of nonconforming units is compared against the control limits of the np chart. The $\bar{X}$ chart uses the 3-sigma control limits and a sample size $n_{\bar{x}}$ of nine. The power of the $\bar{X}$ chart for detecting a mean shift of 1σ is equal to 0.50. In contrast, to detect the same mean shift, the sample size n_{np} of the np chart must be at least equal to 60, in order to achieve the same detection power.

Wu and Jiao (2008) proposed an attribute chart, the MON chart, for monitoring the mean of a variable. This chart checks the run length between two consecutive nonconforming samples. Wu *et al*. (2009*b*) also proposed an np chart, called np_x chart, to monitor the mean of a variable. This chart uses the statistical warning limits to replace the specification limits for the classification of conforming or nonconforming units. Ho and Costa (2011) employed the np_x chart to monitor the wandering behavior of the process mean. However, all these charts only monitor the mean of a variable. When dealing with a variable, it is usually necessary to monitor both its mean and variance. In addition, these charts always use a sample size ($n \geq 1$). These attribute charts may outperform the $\bar{X}$ chart for detecting mean shifts under some circumstances, but are less effective than the latter in other cases.

This research proposes a new control chart, the AFV chart, to monitor both the mean and variance of a variable x. The AFV chart employs an attribute inspection (checking whether a unit is conforming or nonconforming) and uses a sample size of one ($n = 1$). The choice of $n = 1$ for

the AFV chart is made based on the results of some earlier studies (Yang *et al*. 2012). These studies found that using a sample size of one (n = 1) generally increases the overall effectiveness of a control chart for detecting both δ_μ and δ_σ. The reason is that the small sample size allows the use of short sampling interval, or high sampling frequency, for a given inspection rate. The short sampling interval in turn makes the control chart particularly effective for detecting moderate and large process shifts. Moreover, using n = 1 greatly simplifies the implementation and design of the chart, especially for coping with the attribute inspection.

The new AFV chart is systematically compared with the $\bar{X}$&R, $\bar{X}$&S and X&MR charts to monitor a variable quantitatively under different specifications. It is found that even though the AFV chart is extremely simple, it competes well with the $\bar{X}$&R, $\bar{X}$&S and X&MR charts for detecting the mean shift δ_μ and standard deviation shift δ_σ. The AFV chart is more effective than the $\bar{X}$&R and $\bar{X}$&S charts by 7% and 6%, respectively, on average, under different circumstances. This contradicts the conventional belief that the attribute charts require a higher sampling rate, in order to achieve the same level of the detection effectiveness as the variable charts, such as the $\bar{X}$&R and $\bar{X}$&S charts. Moreover, since it is well known that variable-type inspection used by the $\bar{X}$&R and $\bar{X}$&S charts is usually much more expensive and time consuming on a per unit basis than the attribute inspection (Montgomery 2013) used by the AFV chart, the AFV chart is highly recommended to replace the $\bar{X}$&R and $\bar{X}$&S charts in many SPC applications for variables.

The remainder of this chapter is organized as follows: firstly, the implementation and design of the AFV chart are presented in Sections (7.2) and (7.3), respectively. Then, a comparative study is conducted under different scenarios in Section (7.4). The concluding remarks are drawn in Section (7.5).

7.2 Implementation of the AFV Chart

While the variable charts, such as the $\bar{X}$&R, $\bar{X}$&S and X&MR charts, adopt variable inspections, the AFV chart employs a simple attribute inspection to decide if the process is in control or out of control. The AFV chart has four parameters: the sample size n which is fixed at one, sampling interval h, upper inspection limit I_U and lower inspection limit I_L. The inspection limits I_U and I_L are continuous parameters and symmetrical about the in-control mean μ_0. The AFV chart detects the two-sided mean shift and increasing variance shift of a variable x, based on whether the x value of the inspected unit falls within or beyond I_U and I_L. An AFV chart is implemented as follows:

(1) A single unit is checked by means of an attribute inspection at the end of each sampling interval h.

(2) If the quality characteristic x falls within I_L and I_U, the inspected unit is classified as fitting and the process is thought to be in control; otherwise (i.e., x falls beyond I_L or I_U), the inspected unit is classified as unfitting and the process is signalled as out of control.

It is obvious that the implementation of the AFV chart as explained above is very easy and fast, owing to the simplicity of attribute inspection, as well as the elimination of the need of recording the data of n units and calculating a statistic. A typical example of an attribute inspection is using a 'Go/No Go' ring gauge to check whether the diameter x of a shaft exceeds a limit (Kennedy *et al*. 1987).

Suppose the major and minor diameters of a double-end ring gauge are calibrated to be equal to the upper and lower inspection limits I_U and I_L, respectively (Figure 7.1). A shaft is deemed to be fitting, if it can pass through the major diameter I_U and cannot pass through the minor diameter I_L of the gauge. Otherwise, it is classified as unfitting. In this way, both oversizing and undersizing can be checked in one run. One more example is using a fixed load to

check if the Ultimate Tensile Strength (UTS) of a bar element exceeds a limit (Wu *et al*. 2009*b*). During this attribute test, a fixed load equal to the lower inspection limit I_L is directly exerted on the specimen. If necking occurs under this load, the specimen is classified as unfitting.

Conversely, the variable inspection is intrinsically more difficult for an operator. In addition, a variable chart usually requires the calculation of the statistics, such as $\bar{X}$, R and S. For example, when an $\bar{\text{X}}$&R chart is used to monitor the mean and variance of a variable, a sample of n units is inspected (e.g., using a micrometer to measure the x value of each unit). Then, the sample mean $\bar{X}$ and range R are calculated. Finally, each of the two statistics $\bar{X}$ and R are plotted against their corresponding control limits to determine if the process is in control or out of control.

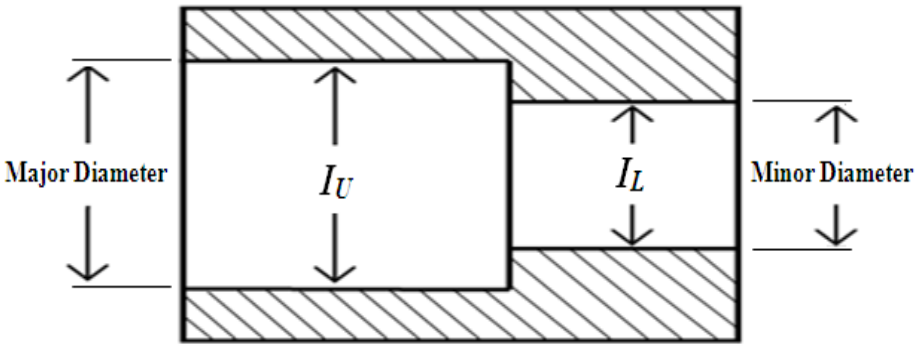

Figure 7.1: Double-end Ring Gauge

A distinctive feature of the AFV chart is using the statistical inspection limits (I_U and I_L), rather than the specification limits (*USL* and *LSL*), to determine if a unit is fitting, or if the process is in control. The specification limits are determined by design engineers and used to classify the item as conforming or nonconforming. The purpose is to ensure the proper function of the unit rather than the efficiency of SPC. On the other hand, the inspection limits I_U and I_L can be set as tight as possible by the quality engineer, so that the requirement on false alarm rate can be satisfied and the detection effectiveness of the AFV chart can be maintained at the highest possible level. Moreover, since the inspection limits are usually much closer to the target value than the specification limits, an unfitting unit that falls beyond an inspection limit of an AFV

chart may still lie within the specifications. It means that the AFV chart is able to provide an indication of impending trouble and allows operators to take corrective action, before the nonconforming unit is actually produced. It is an advantage that only the variable charts have had in the past (Montgomery 2013). It is noted that an unfitting unit classified by the AFV chart may be conforming. In fact, SPC and control charts are mainly used to determine if the process is in control or out of control rather than classifying the individual inspected unit as conforming or nonconforming.

7.3 Design of the AFV Chart

7.3.1 Objective function

Since the goal of this research is to develop a new attribute chart (AFV chart) for monitoring the mean and variance of a variable, an overall performance measure should be used to evaluate the detection effectiveness of the charts over the whole shift domain of ($0 < \delta_\mu \leq \delta_{\mu,max}$, $1 < \delta_\sigma \leq \delta_{\sigma,max}$). Therefore, the *Average Extra Quadratic Loss* (*AEQL*) (Serel and Moskowitz 2008, Yang and Rahim 2009) and *Average Ratio of ATS* (*ARATS*) (Wu *et al*. 2009*c*) are adopted as the objective functions to be minimized in this research.

$$AEQL = \int_0^{\delta_{\mu,max}} \int_1^{\delta_{\sigma,max}} (\delta_\mu^2 + \delta_\sigma^2 - 1) \cdot ATS(\delta_\mu, \delta_\sigma) \cdot f(\delta_\mu) \cdot f(\delta_\sigma) d\delta_\sigma d\delta_\mu \quad (7.1)$$

$$ARATS = \int_0^{\delta_{\mu,max}} \int_1^{\delta_{\sigma,max}} \frac{ATS(\delta_\mu, \delta_\sigma)}{ATS(\delta_\mu, \delta_\sigma)_{benchmark}} \cdot f(\delta_\mu) \cdot f(\delta_\sigma) d\delta_\sigma d\delta_\mu \quad (7.2)$$

where $f(\delta_\mu)$ and $f(\delta_\sigma)$ are the probability density functions of δ_μ and δ_σ, respectively.

The index *AEQL* is quite similar to the objective function *AND* used in the earlier chapters. While *AND* is used to evaluate the overall performance of the charts in detecting shifts in fraction nonconforming, *AEQL* is used to evaluate the overall performance for detecting shifts in mean and variance. *AEQL* is also a weighted average of *ATS* using the extra loss $(\delta_\mu^2 + \delta_\sigma^2 - 1)$ as the weight (Reynolds and Stoumbos 2004*b*). The smaller the *AEQL*, the better the overall

performance of the chart is. The rationale and derivation of *AEQL* and *ARATS* have been detailed in Sections (2.7.4) and (2.7.5), respectively in Chapter (2).

In this chapter, the random shifts δ_μ and δ_σ are assumed to follow a Rayleigh distribution. This distribution is a reasonable representative of the distributions of many process shifts. The Rayleigh distribution has been introduced in Section (5.3.1). When the Rayleigh distribution is used to represent δ_μ and δ_σ, the probability density functions $f(\delta_\mu)$ and $f(\delta_\sigma)$ in Equations (7.1) and (7.2) can be represented as follows:

$$f(\delta_\mu) = \frac{\pi\delta_\mu}{2\left(\mu_{\delta_\mu}\right)^2}\exp\left(-\frac{\pi\left(\delta_\mu\right)^2}{4\left(\mu_{\delta_\mu}\right)^2}\right) \tag{7.3}$$

$$f(\delta_\sigma) = \frac{\pi(\delta_\sigma - 1)}{2(\mu_{\delta_\sigma} - 1)^2}\exp\left(-\frac{\pi(\delta_\sigma - 1)^2}{4(\mu_{\delta_\sigma} - 1)^2}\right) \tag{7.4}$$

Also, the cumulative distribution functions $F(\delta_\mu)$ and $F(\delta_\sigma)$ of the Rayleigh distribution can be calculated as follows:

$$F(\delta_\mu) = 1 - \exp\left(-\frac{\pi\left(\delta_\mu\right)^2}{4\left(\mu_{\delta_\mu}\right)^2}\right) \tag{7.5}$$

$$F(\delta_\sigma) = 1 - \exp\left(-\frac{\pi(\delta_\sigma - 1)^2}{4(\mu_{\delta_\sigma} - 1)^2}\right) \tag{7.6}$$

Both density functions in Equations (7.3) and (7.4) are characterized by a single parameter, which is μ_{δ_μ} (the mean of δ_μ), or μ_{δ_σ} (the mean of δ_σ). Figure 7.2 displays the probability density functions of different Rayleigh distributions with different μ_{δ_μ} and μ_{δ_σ} values while Figure 7.3 shows a joint probability distribution of δ_μ and δ_σ. The values of the $\delta_{\mu,max}$ or $\delta_{\sigma,max}$ in Equations (7.1) and (7.2) can be determined from Equations (7.5) and (7.6), respectively, so that the probability of ($\delta_\mu > \delta_{\mu,max}$) or ($\delta_\sigma > \delta_{\sigma,max}$) is negligible (say < 0.0001).

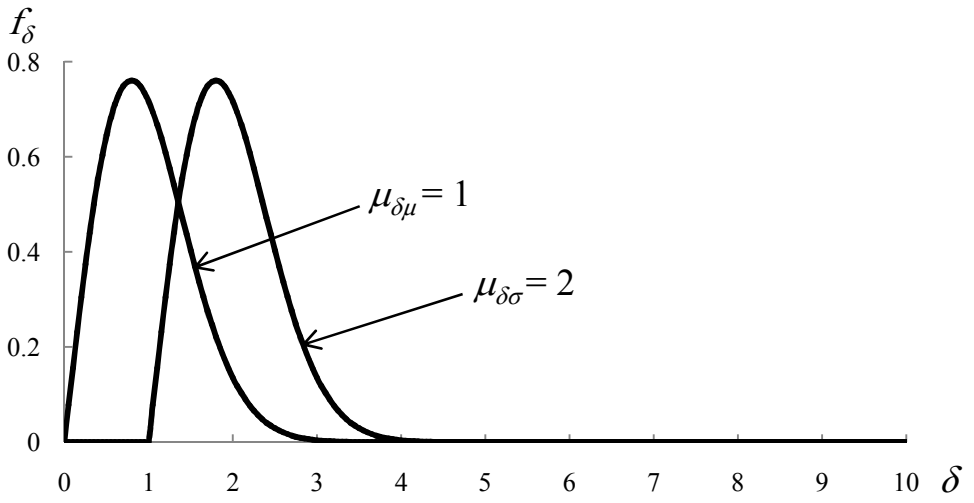

(*a*)

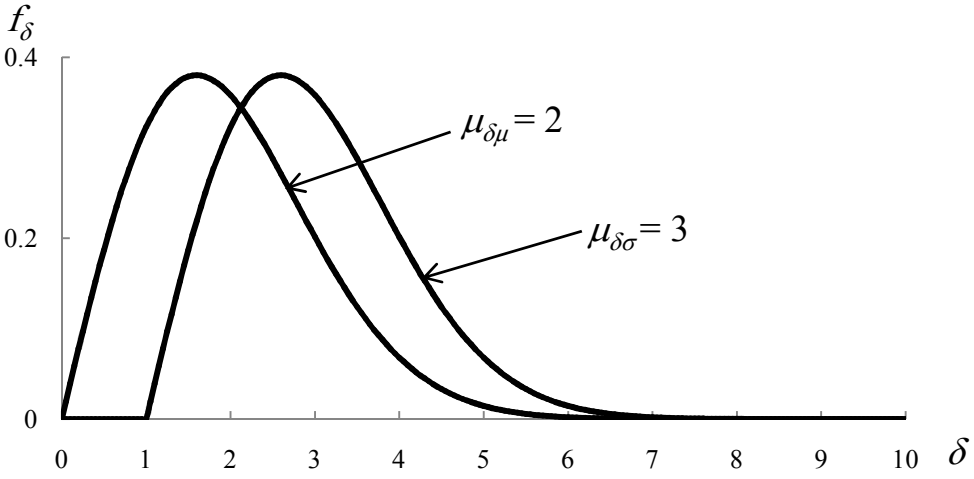

(*b*)

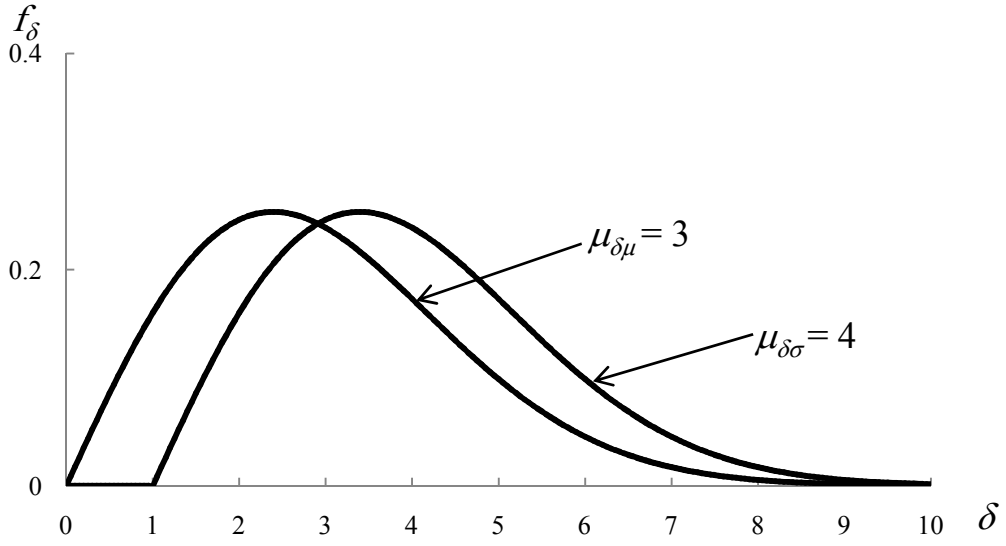

(*c*)

Figure 7.2: Three Sets of Rayleigh Probability Density Functions of Different μ_{δ_μ} and μ_{δ_σ}

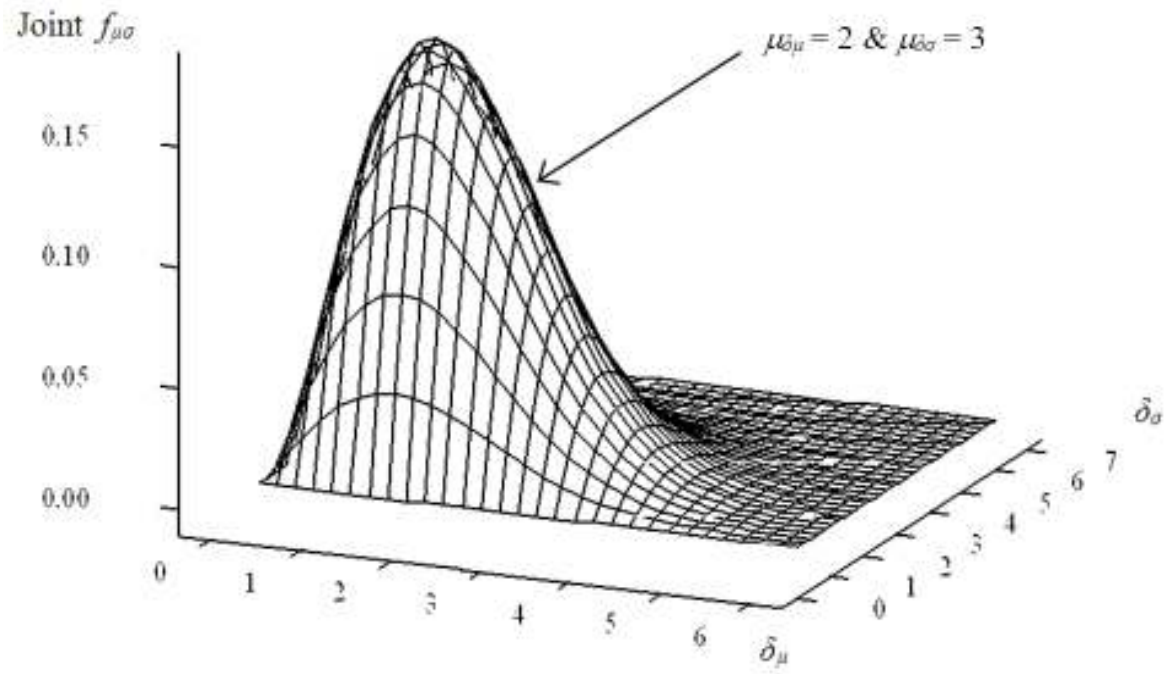

Figure 7.3: Joint Rayleigh Probability Density Function of δ_μ and δ_σ

7.3.2 Specifications

To design an AFV chart, the following three parameters have to be specified: (1) The minimum allowable value (τ) of the in-control Average Time to Signal ATS_0, (2) the allowable inspection rate (r) and (3) the mean values $\mu_{\delta\mu}$ and $\mu_{\delta\sigma}$ of the random shifts δ_μ and δ_σ, respectively. The values of these three parameters can be determined based on the same criteria mentioned in Section (6.3.2) for the SPRT chart.

Since the sample size of the AFV chart is always fixed as one, the sampling interval h of this chart is equal to ($1/r$). However, for some other charts (e.g., $\bar{X}$&R chart), the designers may try different combinations of n and h under the constraint ($r = n/h$) in order to find the best design (Reynolds and Stoumbos 2004*a*).

In this research, without loss of generality, the time unit is made equal to the time period in which one unit (or one product) can be inspected. It is called the calibrated time unit. For example, if the available resource allows five units to be inspected per hour (i.e., $r = 5$ hr^{-1}), the calibrated time unit is 12 (= 60 / 5) minutes. This setting has a benefit of making the sampling

interval h of the AFV chart is always equal to one. It only influences the scaling of the sampling interval h, but has no effect on the results of the performance comparison.

7.3.3 Design model

Since the AFV chart always uses a sample size of $n = 1$, its design becomes very simple, in which only the inspection limit I_U is adjusted ($I_L = 2\mu_0 - I_U$), so that $ATS_0 = \tau$. That is,

$$I_U = \sigma_0 \cdot \Phi^{-1}\left(1 - \frac{0.5}{\tau}\right) + \mu_0 \tag{7.7}$$

The in-control ATS_0 and out-of-control ATS of the AFV chart can be calculated as follows:

$$ATS_0 = \frac{1}{1 + \Phi\left(\frac{I_L - \mu_0}{\sigma_0}\right) - \Phi\left(\frac{I_U - \mu_0}{\sigma_0}\right)} \tag{7.8}$$

$$ATS = \frac{1}{1 + \Phi\left(\frac{I_L - (\mu_0 + \delta_\mu \sigma_0)}{\delta_\sigma \sigma_0}\right) - \Phi\left(\frac{I_U - (\mu_0 + \delta_\mu \sigma_0)}{\delta_\sigma \sigma_0}\right)} - 0.5 \tag{7.9}$$

where $\Phi(\ )$ is the cumulative probability function of the standard normal distribution. Once the AFV chart is designed, its overall detection effectiveness can be determined in terms of $AEQL$ by Equation (7.1).

7.4 Comparative Studies

This section carries out a comparison of the detection effectiveness and ease of use among the AFV, $\bar{X}$&R, $\bar{X}$&S and X&MR charts. The description and implementation of each of the $\bar{X}$&R, $\bar{X}$&S and X&MR charts are as follows:

(1) The $\bar{X}$&R chart: This chart has five parameters which are the sample size n, sampling interval h, upper control limit UCL and lower control limit LCL for the $\bar{X}$ chart element, and the upper control limit H for the R chart element. When running an $\bar{X}$&R chart, a

sample of n units is taken and the sample mean $\bar{X}$ and range R are calculated. If $LCL \leq \bar{X} \leq UCL$ and the sample range $R \leq H$, the process is deemed to be in control. Otherwise, it is considered to be out of control.

(2) The $\bar{X}$&S chart: This chart has the same parameters and operational rules as the $\bar{X}$&R chart except that H stands for the upper control limit of the S chart element for monitoring the sample standard deviation S.

(3) The X&MR chart: This chart has the same parameters and operational rules as the $\bar{X}$&R chart except that the sample size n is always equal to one. Moreover, H is the upper control limit of the moving range (MR) chart element for monitoring the moving range MR.

The optimal design of the $\bar{X}$&R, $\bar{X}$&S and X&MR charts can be carried out by the following model:

Objective function: Minimize $AEQL$ (7.10)

Subject to:

Constraint for ATS_0: $ATS_0 = \tau$ (7.11)

Constraint for inspection rate: $r = n / h$ (7.12)

Independent design variable: n, H

Dependent design variables: h, UCL, LCL

The optimal values of the independent design variables n and H are searched so that the objective function $AEQL$ is minimized. The sampling interval h is made equal to n / r so that constraint (7.12) is satisfied. Finally, the control limits UCL and LCL are determined to make ATS_0 equal to τ (constraint (7.11)). In design practice, the two constraints (7.11) and (7.12) are treated as equality constraints rather than inequality ones. This helps to fully utilize the available resources and chart capacity. It is worth emphasizing that the sample size of the $\bar{X}$&R and $\bar{X}$&S charts must be no smaller than two ($n \geq 2$), otherwise the sample range R, or standard deviation S, cannot be calculated.

7.4.1 Comparison of detection effectiveness

In this section, the four charts (i.e., the AFV chart, $\bar{X}$&Rchart, $\bar{X}$&S chart and X&MR chart) are studied and compared for detecting two-sided mean shifts and an increasing variance shift. Furthermore, without loss of generality, μ_0 and σ_0 are set as zero and one, respectively. The AFV chart is always used as the benchmark.

7.4.1.1 *Comparison under a general case*

The four charts are first studied under a general case in which the diameter x of a shaft is required to be continuously monitored. The $\bar{X}$&R chart, $\bar{X}$&S chart, X&MR chart and AFV chart are studied in order to identify the best one for monitoring the mean and variance of x. The probability distribution of x can be very well approximated by a normal distribution.

The quality engineer desires an ATS_0 close to 370 hours. The random shifts δ_μ and δ_σ are assumed to follow a Rayleigh distribution. Based on some historical records of the out-of-control cases, the mean values μ_{δ_μ} and μ_{δ_σ} of the random shifts δ_μ and δ_σ are estimated as 2 and 3, respectively, using the approach suggested by Wu *et al*. (2002). Based on the available manpower, only one unit can be inspected per minute. This means that the calibrated time unit is one minute. Two types of inspections are considered for this general case based on the type of the control chart:

(1) An attribute inspection used by the AFV chart: the operator uses a simple ring gauge (Figure 7.1) to check whether the diameter x of each unit is oversized or undersized. The minor and major diameters of this ring gauge are designed to be equal to I_L and I_U, respectively.

(2) A variable inspection and computer-aided calculation employed by the $\bar{X}$&R, $\bar{X}$&S and X&MR charts: the operator uses a more delicate digital micrometer to measure the diameters x of n units in a sample and key in the n readings one by one from a keyboard

of a computer. Then the calculation of $\bar{X}$, R, MR and S for each sample is handled by a computer program.

Obviously, the attribute inspection is much less costly and time consuming than the variable inspection on a per unit basis. The initial investment on equipment (i.e., a ring gauge for the AFV chart and a digital micrometer plus a computer for the $\bar{X}$&R chart, $\bar{X}$&S chart or X&MR chart) is neglected. The design specifications are summarized as follows:

$$\tau = 370,\ r = 1,\ \mu_{\delta_\mu} = 2,\ \mu_{\delta_\sigma} = 3. \tag{7.13}$$

The four charts are designed for this case and the resultant charting parameters and performance measures are all listed in Table 7.1. The *ATS* values of the four charts are displayed in Table 7.2. It is interesting to observe the following from Tables 7.1 and 7.2:

(1) As shown in Table 7.2, there are a total of 35 out-of-control cells (combinations of the discrete values of δ_μ and δ_σ) and one in-control cell ($\delta_\mu = 0$ and $\delta_\sigma = 1$). It is noted that all the four charts produce ATS_0 values equal to τ (= 370).

(2) The smallest out-of-control *ATS* in each cell has been bolded. It is always the AFV chart or the X&MR chart that produces the smallest *ATS* values over the process shift domain ($0 \le \delta_\mu \le 6$ and $1 \le \delta_\sigma \le 7$), except for very small pure mean shifts (($\delta_\mu = 1.2$ and $\delta_\sigma = 1$) and ($\delta_\mu = 2.4$ and $\delta_\sigma = 1$)) where the $\bar{X}$&S chart has the smallest *ATS* values.

(3) It is also noteworthy that the differences between the *ATS* values of the AFV chart and X&MR chart are generally negligible.

(4) It can be seen from Table 7.2 that the superiority of the AFV chart over the $\bar{X}$&R and $\bar{X}$&S charts increases with increasing δ_μ.

(5) As a rule of thumb in SPC, a sample size n between 4 and 6 is commonly recommended as the best choice for the $\bar{X}$&R and $\bar{X}$&S charts. Surprisingly, the optimal n of these two

charts for the highest overall detection effectiveness against both δ_μ and δ_σ is found to be two.

Table 7.1: Comparison of the Four Charts

Chart	Charting parameters							*AEQL*	$AEQL/AEQL_{AFV}$	*ARATS*
	n	*h*	I_U	I_L	*UCL*	*LCL*	*H*			
$\bar{X}$&R	2	2	-	-	2.0702	-2.0702	4.3785	25.8984	1.0873	1.0752
$\bar{X}$&S	2	2	-	-	2.0702	-2.0702	3.0911	25.8786	1.0865	1.0744
X&MR	1	1	-	-	3.0190	-3.0190	4.9727	23.6531	0.9930	0.9933
AFV	1	1	2.9997	-2.9997	-	-	-	23.8178	1.0000	1.0000

The values of the two overall performance indices *AEQL* (Equation (7.1)) and *ARATS* (Equation (7.2)), as well as the ratios of ($AEQL/AEQL_{AFV}$), are shown in Table 7.1. These three indices provide fairly comprehensive information regarding the comparison of the overall performance of the charts. The values of $AEQL/AEQL_{AFV}$ indicate that, for this general case (where $\tau = 370$, $\mu_{\delta_\mu} = 2$, $\mu_{\delta_\sigma} = 3$), the AFV chart reduces the average loss in quality by 8.73% and 8.65% compared with the $\bar{X}$&R and $\bar{X}$&S charts, respectively, over the whole range of δ_μ and δ_σ. The relative difference in $AEQL/AEQL_{AFV}$ values between the AFV and X&MR charts is negligible (less than 1%).

It is interesting to note that the performance rankings of the charts based on $AEQL/AEQL_{AFV}$ and *ARATS* are the same. The AFV and X&MR charts are the most effective ones, followed by the $\bar{X}$&S chart and the $\bar{X}$&R chart ranks last. In view of this, only *AEQL* is pursued in the following discussions.

Table 7.2: *ATS* of the Four Charts

δ_σ	Chart	δ_μ					
		0	1.2	2.4	3.6	4.8	6.0
1.0	$\bar{X}$&R	370	17.020	1.940	1.031	1.000	1.000
	$\bar{X}$&S	370	**17.019**	**1.938**	1.031	1.000	1.000
	X&MR	370	28.440	3.221	0.887	0.538	**0.501**
	AFV	370	27.300	3.145	**0.878**	**0.537**	**0.501**
2.2	$\bar{X}$&R	5.382	3.804	2.068	1.317	1.069	1.010
	$\bar{X}$&S	5.371	3.798	2.066	1.316	1.069	1.010
	X&MR	**5.105**	**3.698**	2.005	1.148	0.763	0.596
	AFV	5.289	3.759	**2.002**	**1.142**	**0.760**	**0.594**
3.4	$\bar{X}$&R	2.275	2.093	1.717	1.385	1.175	1.067
	$\bar{X}$&S	2.273	2.091	1.716	1.384	1.174	1.067
	X&MR	**2.110**	**1.931**	**1.546**	**1.175**	0.904	0.728
	AFV	2.148	1.959	1.557	1.177	**0.903**	**0.727**
4.6	$\bar{X}$&R	1.622	1.576	1.460	1.323	1.201	1.113
	$\bar{X}$&S	1.621	1.575	1.460	1.322	1.201	1.113
	X&MR	**1.430**	**1.380**	**1.251**	**1.089**	**0.933**	**0.802**
	AFV	1.444	1.392	1.259	1.093	0.934	**0.802**
5.8	$\bar{X}$&R	1.373	1.356	1.310	1.248	1.183	1.125
	$\bar{X}$&S	1.372	1.355	1.309	1.247	1.182	1.125
	X&MR	**1.146**	**1.126**	**1.071**	**0.992**	**0.904**	**0.819**
	AFV	1.153	1.132	1.075	0.995	0.906	**0.819**
7.0	$\bar{X}$&R	1.249	1.242	1.220	1.189	1.153	1.117
	$\bar{X}$&S	1.249	1.241	1.220	1.189	1.153	1.117
	X&MR	**0.993**	**0.983**	**0.955**	**0.912**	**0.861**	**0.806**
	AFV	0.996	0.986	0.958	0.914	0.862	0.807

7.4.1.2 *Comparison under a factorial experiment*

Next, the four charts are further studied under different conditions through a 3^2 factorial experiment, in which τ and μ_{δ_μ} are used as the input factors. The mean μ_{δ_σ} of the standard deviation shift δ_σ is set as (μ_{δ_μ} + 1) (Reynolds and Stoumbos 2004*a*). The inspection rate *r* is fixed at one as the calibrated time unit is still used. Each of τ and μ_{δ_μ} is varied at three levels as shown in Table 7.3.

This results in nine different combinations of the two factors. The general case discussed in the last section is at the center of this experimental space. The charting parameters of the four charts in this factorial experiment are listed in Table 7.4 and the $AEQL/AEQL_{AFV}$ values are displayed in Table 7.5.

It is worth noting that the optimal sample sizes *n* of the $\bar{X}$&R and $\bar{X}$&S charts are usually smaller than four (Table 7.4). More specifically, *n* is equal to two when $\delta_{\mu,max}$ and $\delta_{\sigma,max}$ are moderate or large. This contradicts the traditional wisdom that a sample size *n* between 4 and 6 should be adopted for the $\bar{X}$&R (or $\bar{X}$&S) combination.

It can be seen from Table 7.5 that the AFV chart usually outdoes the $\bar{X}$&R and $\bar{X}$&S charts in terms of $AEQL/AEQL_{AFV}$ while it is slightly inferior to the X&MR chart. The $\bar{X}$&R and $\bar{X}$&S charts are superior to the AFV chart only in a few cases (1, 4 and 7) when μ_{δ_μ} and μ_{δ_σ} are small. The reason is that, the process shifts are generally small in these three cases, hence the $\bar{X}$&R and $\bar{X}$&S charts with a larger sample size are more effective. In all other cases, where the shift is moderate or large, the AFV chart with *n* = 1 outperforms the $\bar{X}$&R and $\bar{X}$&S charts. For example, in case 6, where μ_{δ_μ} = 3 and μ_{δ_σ} = 4, the AFV chart produces an *AEQL* smaller than that of the $\bar{X}$&R and $\bar{X}$&S charts by 21.96% and 21.91%, respectively.

Table 7.3: Levels of the Input Factors in the 3^2 Factorial Design

Factor		Level 1	Level 2	Level 3
1	τ	200	370	1200
2	μ_{δ_μ}	1	2	3

Table 7.4: Charting Parameters of the Four Charts in the 3^2 Factorial Design

Case	τ	μ_{δ_μ}	μ_{δ_σ}	Chart	n	h	I_U	I_L	UCL	LCL	H
1	200	1	2	$\bar{X}$&R	3	3	-	-	1.5187	-1.5187	4.3084
				$\bar{X}$&S	3	3	-	-	1.5222	-1.5222	2.2379
				X&MR	1	1	-	-	2.8309	-2.8309	4.6415
				AFV	1	1	2.8070	-2.8070	-	-	-
2	200	2	3	$\bar{X}$&R	2	2	-	-	1.9310	-1.9310	4.1079
				$\bar{X}$&S	2	2	-	-	1.9310	-1.9310	2.9026
				X&MR	1	1	-	-	2.8269	-2.8269	4.6919
				AFV	1	1	2.8070	-2.8070	-	-	-
3	200	3	4	$\bar{X}$&R	2	2	-	-	1.9430	-1.9430	4.0696
				$\bar{X}$&S	2	2	-	-	1.9430	-1.9430	2.8765
				X&MR	1	1	-	-	2.8269	-2.8269	4.6919
				AFV	1	1	2.8070	-2.8070	-	-	-
4	370	1	2	$\bar{X}$&R	4	4	-	-	1.3872	-1.3872	4.6724
				$\bar{X}$&S	4	4	-	-	1.3909	-1.3909	2.0541
				X&MR	1	1	-	-	3.0255	-3.0255	4.8940
				AFV	1	1	2.9997	-2.9997	-	-	-
5	370	2	3	$\bar{X}$&R	2	2	-	-	2.0702	-2.0702	4.3785
				$\bar{X}$&S	2	2	-	-	2.0702	-2.0702	3.0911
				X&MR	1	1	-	-	3.0190	-3.0190	4.9727
				AFV	1	1	2.9997	-2.9997	-	-	-

Table 7.4: Charting Parameters of the Four Charts in the 3^2 Factorial Design (cont.)

Case	τ	μ_{δ_μ}	μ_{δ_σ}	Chart	n	h	I_U	I_L	UCL	LCL	H
6	370	3	4	$\bar{X}$&R	2	2	-	-	2.0815	-2.0815	4.3426
				$\bar{X}$&S	2	2	-	-	2.0815	-2.0815	3.0664
				X&MR	1	1	-	-	3.0185	-3.0185	4.9749
				AFV	1	1	2.9997	-2.9997	-	-	-
7	1200	1	2	$\bar{X}$&R	5	5	-	-	1.3766	-1.3766	5.2329
				$\bar{X}$&S	6	6	-	-	1.2368	-1.2368	1.9148
				X&MR	1	1	-	-	3.3650	-3.3650	5.4108
				AFV	1	1	3.3415	-3.3415	-	-	-
8	1200	2	3	$\bar{X}$&R	2	2	-	-	2.3067	-2.3067	4.9114
				$\bar{X}$&S	2	2	-	-	2.3052	-2.3052	3.4536
				X&MR	1	1	-	-	3.3650	-3.3650	5.4108
				AFV	1	1	3.3415	-3.3415	-	-	-
9	1200	3	4	$\bar{X}$&R	2	2	-	-	2.3268	-2.3268	4.8394
				$\bar{X}$&S	2	2	-	-	2.3268	-2.3268	3.4032
				X&MR	1	1	-	-	3.3650	-3.3650	5.4108
				AFV	1	1	3.3415	-3.3415	-	-	-

Table 7.5: $AEQL/AEQL_{AFV}$ Values of the Four Charts in the 3^2 Factorial Design

Case	1	2	3	4	5	6	7	8	9	
Chart	$\tau = 200$			$\tau = 370$			$\tau = 1200$			$\overline{AEQL / AEQL_{AFV}}$
	$\mu_{\delta_\mu} = 1$, $\mu_{\delta_\sigma} = 2$	$\mu_{\delta_\mu} = 2$, $\mu_{\delta_\sigma} = 3$	$\mu_{\delta_\mu} = 3$, $\mu_{\delta_\sigma} = 4$	$\mu_{\delta_\mu} = 1$, $\mu_{\delta_\sigma} = 2$	$\mu_{\delta_\mu} = 2$, $\mu_{\delta_\sigma} = 3$	$\mu_{\delta_\mu} = 3$, $\mu_{\delta_\sigma} = 4$	$\mu_{\delta_\mu} = 1$, $\mu_{\delta_\sigma} = 2$	$\mu_{\delta_\mu} = 2$, $\mu_{\delta_\sigma} = 3$	$\mu_{\delta_\mu} = 3$, $\mu_{\delta_\sigma} = 4$	
$\bar{X}$&R	0.9827	1.0831	1.1806	0.9502	1.0873	1.2196	0.8616	1.0518	1.1762	1.0659
$\bar{X}$&S	0.9764	1.0827	1.1805	0.9309	1.0865	1.2191	0.8169	1.0477	1.1741	1.0572
X&MR	0.9896	0.9943	0.9964	0.9872	0.9930	0.9964	0.9829	0.9896	0.9939	0.9915
AFV	1.0000	1.0000	1.0000	1.0000	1.0000	1.0000	1.0000	1.0000	1.0000	1.0000

The rightmost column in Table 7.5 displays the average $\overline{AEQL/AEQL_{AFV}}$ of the $AEQL/AEQL_{AFV}$ values of each chart over the nine cases. The average $\overline{AEQL/AEQL_{AFV}}$ is the most holistic measure of the effectiveness of a chart, considering different combinations of the design specifications τ and μ_{δ_μ}. Considering $\overline{AEQL/AEQL_{AFV}}$, the AFV chart and X&MR chart have the highest overall detection effectiveness followed by the $\bar{X}$&S chart, and the $\bar{X}$&R chart ranks last. Specifically, the $\overline{AEQL/AEQL_{AFV}}$ values indicate that, from the overall viewpoint, the AFV chart is more effective than the $\bar{X}$&R chart and $\bar{X}$&S chart by 6.59% and 5.72%, respectively.

It is worth noting that the difference in $\overline{AEQL/AEQL_{AFV}}$ values between the AFV chart and X&MR chart is less than 1%. As shown in Table 7.4, while the *UCL* and *LCL* of the X&MR chart in all cases are slightly wider than the I_U and I_L of the AFV chart, the control limit *H* of the X&MR chart is very wide and almost ineffective. This manifests the fact that that if I_U and I_L of the AFV chart are determined appropriately, they will be efficient at detecting the mean and variance of a variable. This also closely matches the results of some earlier studies (Reynolds and Stoumbos 2001, Stoumbos *et al.* 2003) that adding an MR chart to the X chart will only increase the difficulty in design and implementation without any significant increase in detection effectiveness.

7.4.1.3 *Comparison under different inspection rate*

In the general case and factorial design, the AFV chart has the same inspection rate as the $\bar{X}$&R, $\bar{X}$&S and X&MR charts. Since the attribute inspection is usually much less expensive on a per unit basis than the variable inspection (Montgomery 2013), it thereby may not be adequate to compare the charts under condition of the same inspection rate. It may be more appropriate to

allow the inspection rate r_{AFV} of the AFV chart to be higher than the inspection rate r of the $\bar{X}$&R, $\bar{X}$&S and X&MR charts.

The reasonable value of the ratio (r_{AFV} / r) in a particular application depends on the extent of simplicity of the attribute inspection compared with that of the variable inspection. For example, if the charts are implemented manually, the operator of an $\bar{X}$&R chart has to carry out the time consuming variable inspection and also calculate the sample mean $\bar{X}$ and range R. Under such circumstances, the inspection rate r_{AFV} should be much higher than r. As a result, the AFV chart may use a much smaller sampling interval.

On the other hand, if a computer-aided system is available for the SPC implementation, the operators are released from calculating the sample statistics, such as $\bar{X}$ and R. They only have to measure the sample values of x and enter the readings into a computer through the keyboard. However, the variable inspection used by the $\bar{X}$&R chart is still intrinsically more difficult than the attribute inspection. In fact, in many applications, just keying in a reading (for example, the measured diameters 74.030, 74.002, 74.019, 73.992, 74.008, …. of the forged piston rings (Montgomery 2013)) through a keyboard may take longer time than carrying out an attribute inspection using a gauge.

Wu *et al*. (2009*b*) conducted a field experiment to find the average times $t_{attribute}$ for an attribute inspection and $t_{variable}$ for a variable inspection. Both inspections were applied to the same product. The attribute inspection test checks whether a specimen is oversized or undersized, by using a simple Mitutoyo ring gauge, while the variable inspection test measures the diameter x of each specimen, by using a more delicate digital micrometer and keying in the reading to a computer. It was reported that the ratio ($t_{attribute}$ / $t_{variable}$) = 0.2231. Since $t_{attribute}$ is much shorter, the inspection rate for the attribute inspection can be much higher, that is

$$r_{attribute} / r_{variable} = 4.482 \qquad (7.14)$$

This means that if an operator can complete *m* variable inspections in a certain time period, he should be able to complete (4.482×*m*) attribute inspections in the same time period. Hence, it may also be interesting to compare the detection effectiveness of the AFV chart with that of the $\bar{X}$&R, $\bar{X}$&S and X&MR charts, if the above ratio (Equation (7.14)) is used, that is

$$r_{AFV} / r = 4.482 \tag{7.15}$$

The four charts are compared under the same specifications as in the general case (i.e., τ = 370, μ_{δ_μ} = 2 and μ_{δ_σ} = 3). The inspection rate r_{AFV} of the AFV chart is set as one. In order to satisfy Equation (7.15), the $\bar{X}$&R, $\bar{X}$&S and X&MR charts will use an inspection rate *r* of (1/4.482). The four charts are then designed and their charting parameters, *AEQL* and $AEQL/AEQL_{AFV}$ values are listed in Table 7.6. It is noted that, since the inspection rate *r* of the $\bar{X}$&R, $\bar{X}$&S and X&MR charts has been reduced, their sampling intervals *h* are increased by a factor of 4.482 compared with those in Table 7.1.

The *ATS* values of the four charts are displayed in Table 7.7. The smallest *ATS* in each out-of-control cell is bold. As shown, the out-of-control *ATS* values of the AFV chart are always much smaller than those of the $\bar{X}$&R, $\bar{X}$&S and X&MR charts over the entire process shift range.

The values of $AEQL/AEQL_{AFV}$ in Table 7.6 indicate that the AFV chart significantly outperforms the $\bar{X}$&R , $\bar{X}$&S and X&MR charts by 303.52%, 303.49% and 249.96%, respectively. This study reveals that the AFV chart outperforms the $\bar{X}$&R, $\bar{X}$&S and X&MR charts in detecting δ_μ and δ_σ, if the lower cost of attribute inspection is taken into consideration.

Table 7.6: Comparison under Different Inspection Rate

Chart	Charting parameters							*AEQL*	$AEQL/AEQL_{AFV}$
	n	*h*	I_U	I_L	*UCL*	*LCL*	*H*		
$\bar{X}$&R	2	8.964	-	-	1.7280	-1.7280	3.6519	96.1097	4.0352
$\bar{X}$&S	2	8.964	-	-	1.7280	-1.7280	2.5818	96.1030	4.0349
X&MR	1	4.482	-	-	2.5232	-2.5232	4.3229	83.3543	3.4996
AFV	1	1	2.9997	-2.9997	-	-	-	23.8178	1.0000

7.4.2 Simplicity in implementation and design comparison

In addition to detection effectiveness, other considerations, such as the ease of implementation, design and diagnosis are also important when selecting a control chart. The AFV chart is seen to be the most preferable chart from these perspectives due to the following:

(1) The number of charting parameters to be determined is four for the $\bar{X}$&R, $\bar{X}$&S and X&MR charts (i.e., *n*, *h*, *UCL* and *H*, where *LCL* is symmetrical to *UCL*) and only two for an AFV chart (i.e., *h* and I_U, where I_L is symmetrical to I_U). This suggests that the AFV chart is simpler to design and easier to operate.

(2) While the AFV chart uses a simple attribute inspection, the $\bar{X}$&R, $\bar{X}$&S and X&MR charts rely on the variable inspection. In addition, the latter three charts require the calculations of some statistics, such as the sample mean $\bar{X}$, range R, moving range *MR* or standard deviation *S*. The calculation of *S* is particularly difficult.

(3) Using the AFV chart, operators can directly figure out if the process is in control or out of control from one chart. On the other hand, the user of an $\bar{X}$&R, $\bar{X}$&S or X&MR chart has to synthesize the sample points on the $\bar{X}$ chart and R (or S or MR) chart, in order to reach a conclusion on the process status. Cheng and Thaga (2006) concluded that the single charts are more applicable and appealing than simultaneous charts because they

are easy to interpret and clearly show the direction of the shift when an out-of-control signal occurs.

(4) One may believe that the control schemes consisting of several charts (e.g., the $\bar{X}$&R or $\bar{X}$&S chart) will help to identify the type of shifts (mean shift, or variance shift, or both) based on the chart signal. However, Reynolds and Stoumbos (2004*b*) found that no combination of charts can actually diagnose the type of shifts reliably in all situations. Cheng and Thaga (2006) also emphasized that it is impossible to identify whether the change in the process has actually occurred due to a mean shift or variance shift. In fact, when using an AFV chart, if identifying the type of the shift is really helpful, it can be determined by some post-signal procedures (Reynolds and Stoumbos 2006) using a variable chart such as X&MR chart.

(5) The design of an AFV chart is simple, as only the inspection limits I_U and I_L have to be determined by Equation (7.7), based on the specified τ. The inspection limits I_U and I_L can be even determined manually with the help of a calculator and a table of the standard normal cumulative distribution function. The calculations of the in-control ATS_0 and out-of-control *ATS* of the AFV chart are also easy as shown in Equations (7.8) and (7.9). In contrast, the design and *ATS* evaluation of the $\bar{X}$&R, $\bar{X}$&S and X&MR charts that produce the minimum *AEQL* and satisfy ($ATS_0 = \tau$) are quite difficult, due to the interactions among the $\bar{X}$ chart and R (or S or MR) chart. The design of the $\bar{X}$&R and X&MR charts is particularly challenging.

(6) It is quite straightforward to integrate an AFV chart with other enhancing features (e.g., variable sampling interval (VSI) scheme), in order to further improve the overall performance. Such a combination is difficult for the $\bar{X}$&R, $\bar{X}$&S and X&MR charts.

Table 7.7: *ATS* of the Four Charts under Different Inspection Rate

δ_σ	Chart	δ_μ					
		0	1.2	2.4	3.6	4.8	6.0
1.0	$\bar{X}$&R	370	33.620	6.309	4.518	4.482	4.482
	$\bar{X}$&S	370	33.619	6.307	4.518	4.482	4.482
	X&MR	370	45.820	7.665	2.968	2.292	2.242
	AFV	370	**27.300**	**3.145**	**0.878**	**0.537**	**0.501**
2.2	$\bar{X}$&R	15.750	12.060	7.467	5.333	4.650	4.503
	$\bar{X}$&S	15.750	12.050	7.467	5.333	4.650	4.503
	X&MR	15.170	11.600	6.854	4.239	3.027	2.510
	AFV	**5.289**	**3.759**	**2.002**	**1.142**	**0.760**	**0.594**
3.4	$\bar{X}$&R	8.171	7.674	6.608	5.626	4.992	4.670
	$\bar{X}$&S	8.170	7.673	6.607	5.625	4.992	4.670
	X&MR	7.436	6.907	5.723	4.526	3.615	3.010
	AFV	**2.148**	**1.959**	**1.557**	**1.177**	**0.903**	**0.727**
4.6	$\bar{X}$&R	6.347	6.214	5.874	5.463	5.094	4.822
	$\bar{X}$&S	6.347	6.213	5.874	5.463	5.094	4.822
	X&MR	5.394	5.236	4.822	4.289	3.759	3.305
	AFV	**1.444**	**1.392**	**1.259**	**1.093**	**0.934**	**0.802**
5.8	$\bar{X}$&R	5.616	5.566	5.429	5.242	5.043	4.865
	$\bar{X}$&S	5.616	5.565	5.429	5.241	5.043	4.865
	X&MR	4.486	4.420	4.237	3.973	3.675	3.378
	AFV	**1.153**	**1.132**	**1.075**	**0.995**	**0.906**	**0.819**
7.0	$\bar{X}$&R	5.247	5.224	5.159	5.064	4.954	4.844
	$\bar{X}$&S	5.246	5.223	5.159	5.064	4.954	4.844
	X&MR	3.979	3.945	3.850	3.706	3.529	3.339
	AFV	**0.996**	**0.986**	**0.958**	**0.914**	**0.862**	**0.807**

7.5 Concluding Remarks

This research proposes a new attribute control chart, named the AFV chart, to monitor the mean and variance of a variable. This chart employs a simple attribute inspection and eliminates the need for the computation of any statistic. The foremost important feature of the AFV chart is its simplicity of design and implementation compared with all variable charts. Moreover, the instruments used for attribute inspections are often relatively simpler and need less adjustment, and are therefore less expensive and more reliable than the instruments used for variable inspections.

The AFV chart also outperforms the variable $\bar{X}$&R and $\bar{X}$&S charts by 7% and 6%, respectively, on average, in terms of *AEQL* under different circumstances. The high effectiveness of the AFV chart is attributable to the use of inspection limits (I_U and I_L) and a single sample size ($n = 1$).

The average time required for an attribute inspection used by an AFV chart is substantially less than the time required by a variable inspection used by a variable chart. If that is taken into consideration, the AFV chart may use a larger inspection rate than a variable chart, and may overwhelm the latter in detection effectiveness.

It has also been found that the AFV chart can work as a leading indicator of trouble, by producing a timely out-of-control signal before many nonconforming units are actually produced, as the inspection limits are tighter than the specification limits. It is an advantage that only the variable charts have had in the past.

A drawback of the AFV chart is its inapplicability to monitor the processes whose parameters (e.g., μ and σ) change frequently. The reason is that if a change occurs, some attribute inspection instruments (e.g., the "Go/No Go" gauge) also have to be changed to reflect the new inspection limits of the AFV chart. This replacement may incur some extra cost. However, since the production processes often run in an in-control condition for most of the time (Montgomery 2013) unless a fundamental improvement effort is made on the process, this extra

cost may be marginal over a long run. Furthermore, this drawback of the AFV chart can be overcome by using an adjustable inspection instrument that can be adjusted by the user whenever necessary.

A limitation of the AFV chart is its inability to detect decreasing variance shifts because it doesn't have a variance chart element (such as the S chart element of the $\bar{X}$&S combination). The reduction in variability is usually due to a process improvement. Therefore, a decreasing variance shift doesn't jeopardize the process quality directly and is often much less critical than increasing variance shifts.

Currently, almost all SPC text books discuss the variable $\bar{X}$&R and $\bar{X}$&S charts in detail and advocate them for monitoring process mean and variance. Now, the results of this research stand out as evidence that a very simple attribute chart, the AFV chart, is often able to outperform the $\bar{X}$&R and $\bar{X}$&S charts for monitoring the process mean and variance. As a result, the replacement of these charts by the AFV chart should be considered for SPC applications in which the mean and variance need to be monitored.

Chapter 8

Conclusions

The main objective of this Ph.D. thesis is to develop and investigate new attribute SPC control charts having high detection effectiveness and/or simplicity in design and implementation. Five new attribute control charts are proposed in this thesis. The original contribution is reflected by the improved performance of these charts compared with the existing charts. The results of this thesis make significant contributions to both academia and industry, provide attribute SPC practitioners with some useful guidelines to select the most suitable chart, and pave the way for a new cutting-edge research in attribute SPC. The results of this research also lay a foundation for the design methodology and evaluation of attribute control charts, and ultimately promote the use of the attribute control charts in a wide variety of applications. This chapter summarizes the main contributions of this thesis and also sketches some schemes for future research.

8.1 Summary and Contributions

SPC is a systematic method in quality control used to monitor and control a process. The majority of the research effort in SPC is focused on the development of new control charts with high detection effectiveness so that the average loss and damage incurred in an abnormal out-of-control status can be minimized over the whole range of process shifts. This Ph.D. thesis focuses on the development of effective attribute control charts. A summary of the main contributions is given below:

8.1.1 Developing new attribute charts

As highlighted before, the primary objective of this Ph.D. thesis is to develop new attribute control charts to achieve the highest detection effectiveness. Five new charts are successfully developed. A brief description of each of these charts is given below:

(1) Synthetic & np (Syn-np) chart

This new Syn-np chart has both the strength of the synthetic chart in quickly detecting small *p* shifts and the advantage of the np chart in being sensitive to large *p* shifts. As a result, it has a better and more uniform overall performance. The Syn-np chart is more effective than the np chart and synthetic chart by 100% and 29%, respectively, in terms of *AND* over a wide range of *p* shifts, under different conditions.

(2) Optimal np & CUSUM (np-CUSUM) chart

This new np-CUSUM chart is an optimal version of the np & CUSUM chart. The new np-CUSUM chart integrates the salient features of the np chart for detecting large shifts and the power of the CUSUM chart for detecting small and moderate shifts. While the design algorithm effectively improves the overall performance of the np & CUSUM scheme over the entire process shift range, it does not increase the difficulty for understanding and implementing this scheme. On average, the np-CUSUM chart outperforms the np chart, EWMA chart and CUSUM chart by 213%, 15% and 5%, respectively, under different conditions.

(3) CUSUM chart with curtailment (Curt_CUSUM)

This new Curt_CUSUM chart applies the curtailment technique to improving the overall detection effectiveness of the conventional CUSUM chart. The results of the comparative studies show that the Curt_CUSUM chart excels the CUSUM chart without curtailment by 36% in terms of *AND* under different circumstances. The high effectiveness of the Curt_CUSUM chart is mainly attributable to the curtailment technique. The Curt_CUSUM chart can be applied to a 100% inspection as well as a random sampling inspection.

(4) Optimal SPRT chart

This new optimal SPRT chart is an optimal version of the basic SPRT chart. By optimizing the charting parameters, the optimal SPRT chart is able to increase the overall detection effectiveness by more than 100% compared with the basic SPRT chart and outperform the np and CUSUM charts by 221% and 171%, respectively, in terms of *AND* under different

circumstances. It is noted that the SPRT chart using a relatively smaller *ASN* and a shorter sampling interval (*h*) has a higher overall detection effectiveness. While the optimal design algorithm significantly enhances the overall performance of the SPRT chart, it does not increase the difficulty of implementing this chart.

(5) Attribute chart for monitoring a variable (AFV chart)

This new AFV chart employs an attribute inspection to monitor both the mean and variance of a variable. The distinctive feature of the AFV chart is its ability to determine the process status by applying the very simple attribute inspection to a single unit. By selecting its inspection limits appropriately, the AFV chart outperforms the $\bar{X}\&R$ and $\bar{X}\&S$ charts by 7% and 6%, respectively, from an overall viewpoint under different circumstances. If the AFV chart is allowed to use a larger inspection rate than a variable chart due to the lower cost of the attribute inspection, it will overwhelmingly outperform the latter in detection effectiveness. The AFV chart has the advantage of being extremely simple in design and implementation, and having a very low cost for operation. As a result, it lends itself to be a pragmatic replacement of the $\bar{X}\&R$ and $\bar{X}\&S$ charts for monitoring both the mean and variance of a variable.

In summary, it is worth emphasizing that each control chart can find its application in SPC practice and there is always a trade-off between the detection effectiveness of a chart and the complexity of its design and implementation. Usually, the better the performance is, the more complicated the design and the implementation of the chart. The user can always choose between extremely high effectiveness, and simple design and implementation based on his priority. Table 8.1 indicates the performance and complexity ranking of the attribute charts developed in this research, with (1) for the most effective and complex chart and (7) for the least effective and complex one. Table 8.1 also recommends the shift range to be handled by each chart.

Table 8.1: Performance and Complexity Ranking of the Charts

Chart	Performance and Complexity Ranking	Shift size
Optimal SPRT	1	Small, moderate and large
np-CUSUM	2	Small, moderate and large
Syn-np	3	Small, moderate and large
Curt_CUSUM	4	Moderate and large
CUSUM EWMA	5	Small and moderate
Synthetic	6	Small and moderate
np	7	Large

Since distributed computing systems become a norm in today's SPC practice (Woodall and Montgomery 1999, Chan *et al*. 2009), advanced charts such as EWMA, CUSUM, SPRT and np-CUSUM charts can be easily implemented with the help of an on-site computer. However, if a computer is unavailable, simple charts such as np and synthetic charts may be considered.

8.1.2 Evaluating the overall performance of charts

Another objective of this thesis is to evaluate and compare the overall performance of the major attribute control charts. To achieve this objective, a broad literature survey on the attribute control charts is carried out and the characteristics of different control charts are studied. A systematic performance comparison among different control charts is conducted in each chapter. The comparison has considered two criteria: one is the effectiveness in detecting shifts and another is the simplicity in understanding, design and implementation. The advantages and disadvantages of all main attribute control charts are highlighted. The results of this evaluation and comparison can provide SPC users with useful guidelines for the selection of the suitable attribute chart.

8.1.3 Proposing a general model for the design of charts

The final objective of this thesis is to propose a general model for the optimal design of the attribute control charts. This objective is inspired by the importance of the optimization in the design of control charts and the fact that more significant gain in the detection effectiveness may be obtained by improving the design algorithm of an existing chart rather than proposing a completely new chart. For example in Chapter (6), it is found that if the SPRT chart is not optimized, it may not necessarily be better than the traditional charts such as the CUSUM chart.

In this thesis, a general optimal design model is formulated. This model aims at increasing the speed of detecting the out-of-control status and controlling the false alarm rate. In SPC terminology, the goal of the optimal design model is to minimize the Average Number of Defectives (*AND*) and satisfy the requirement of false alarm rate which is indicated by the in-control Average Time to Signal (ATS_0). The optimal values of the independent and dependent charting parameters are identified for the design of each individual chart. This general model greatly facilitates the optimal design of the attribute control charts under different specifications and requirements in order to achieve the highest possible detection effectiveness.

8.2 Future Research

The development of advanced attribute control charts with high detection effectiveness is the target of the future work. It will eventually promote the applications of the attribute SPC techniques in many areas such as the finance, biology, medicine and service sectors, in addition to the traditional applications in manufacturing industry.

Based on the results of this thesis, further research can be conducted to investigate and develop more effective attribute SPC schemes in order to provide a wide variety of monitoring techniques and useful aids for attributes that enable SPC users to select the most suitable control chart for their applications. The following nine research directions can be explored and carried out in the future. It is believed that most of them will bring out fruitful results.

(1) Adaptive control charts

One promising avenue for the future work is to develop adaptive charts in which the charting parameters such as the sample size n, sampling interval h and control limits are varied adaptively based on the status of the process. For example, the sampling interval h until the next sample can be made short if a sample shows some indication of a change in the process or long if there is no indication of a change. The adaptive charts are becoming more and more popular due to their high detection effectiveness compared with the traditional control charts and their capability in tracking time-varying patterns.

For the Syn-np and np-CUSUM charts developed in Chapters (3) and (4), respectively, of this thesis, both the sample size n and sampling interval h are specified or fixed for each application, where n depends on available inspection resource and h corresponds to the rational subgroup concept. Therefore, it is also worthwhile to investigate the adaptive Syn-np and np-CUSUM charts in which n and h are varied based on the online observed data from the process. The adaptive charts are expected to detect process changes even faster than its static counterparts with fixed n and h.

(2) Control charts with estimated parameters

The studies in this thesis are conducted assuming that the number d of nonconforming units in a sample follows a binomial distribution with known in-control fraction nonconforming p_0 and the random shift δ follows a predetermined probability distribution, such as the Rayleigh distribution. It is also interesting to carry out further studies on the developed charts when d and δ are assumed to follow other distributions, and p_0 is estimated from the historical data.

(3) Control charts with curtailment

The curtailment technique has been widely employed in acceptance sampling plans to significantly reduce the Average Sample Number (*ASN*). In Chapter (5) of this thesis, a new CUSUM chart with curtailment (Curt_CUSUM chart) is proposed under 100% inspection and is found to considerably outperform the conventional CUSUM chart. The idea of the curtailment can be extended to develop a series of new charts with high detection effectiveness such as the

Exponentially Weighted Moving Average (EWMA) and synthetic charts and to cover a broader scope of designing more powerful control charts.

(4) Multi-attribute control charts

There are many situations where the quality of a product depends on more than one quality attribute such as the number of different defect types in a product. In these cases, the common practice is to monitor each attribute with a separate chart. It is more practical and more economical to use a single multi-attribute control scheme to replace several uni-attribute ones for multi-attribute monitoring. As one of the future researches, new effective multi-attribute charts may be developed to cope with the need for monitoring the simultaneous attributes of a product in many SPC applications.

(5) Renewal synthetic chart

One drawback of the synthetic chart is that it is slow in detecting out-of-control status under steady-state mode. When the process is in steady-state, the first *CRL* after the *p* shift is usually very long and the first ensuing nonconforming sample is unlikely to detect the *p* shift. This makes the synthetic chart slow under the steady-state mode. A renewal synthetic chart may be explored to reset *CRL* to zero whenever appropriate so that the first *CRL* tends to be smaller than before, and the out-of-control status is more likely to be signalled by the first ensuing nonconforming sample. It is expected that the renewal synthetic chart will be more effective than the basic synthetic chart. This renewal feature can be further applied to all other charts based on CRL and TBE (Time Between Events).

(6) Syn-CUSUM chart

Based on the idea of the Syn-np chart, more advanced charts can be developed subsequently. These charts aim to achieve even substantial reduction in *AND*. One example is an integration of a CUSUM chart with a synthetic chart (Syn-CUSUM chart). Since the CUSUM-type charts are generally more effective than the Shewhart-type charts, the new combined scheme (Syn-CUSUM chart) is expected to be highly efficient and to have better overall performance than the Syn-np chart.

(7) Syn-np-CUSUM chart

Syn-np-CUSUM chart can be a further extension to the Syn-np chart developed in Chapter (3) and the Syn-CUSUM chart proposed above. This new chart is the combination of three different charts (np chart, synthetic chart and CUSUM chart). It is expected that the addition of CUSUM chart element to the Syn-np chart will improve its detection effectiveness and make it more sensitive to p shifts of different sizes, especially small and moderate shifts so that the overall performance can be enhanced.

(8) Syn-SPRT chart

A new chart named as Syn-SPRT chart can also be developed. The new Syn-SPRT chart could be able to use both the information about the time interval between the last two nonconforming samples and the information about the cumulative sum of sample data. While the synthetic chart is sensitive to detect small p shifts, the SPRT chart is effective in detecting large p shifts. It is expected that the proposed Syn-SPRT chart may result in the least *AND* or the best overall performance compared with any control chart that can be found in the current literature.

(9) Effect of sampling cost on the performance of charts

The sampling cost consists of two components: b and c. b represents the fixed cost per sample and c is the variable cost per unit. While the sample size directly influences c, it does not have an effect on b (Duncan 1956, Montgomery 2013). The fixed component b includes interrupting a process, walking a distance, cleaning hands and platform, switching the computer, and so on. While the variable sampling inspection cost c is usually considered in most research work, the impact of the fixed sampling inspection cost b is often neglected. Therefore, it is worthwhile to study the statistical design of the charts when the sampling cost (including both the fixed and variable components) is taken into consideration. This study will reflect the effect of the sampling cost on the performance of the charts and show how neglecting the fixed sampling cost b can negatively affect the design of the charts.

References

Abdurrahman C., Serteser M., Fraterman A., Unsal I. (2008) A new internal quality control chart based on biological variation. *Accreditation and Quality Assurance*, 13, pp. 69-75.

Abel V. (1990) On one-sided combined Shewhart-CUSUM quality control schemes for Poisson counts. *Computational Statistics Quarterly,* 6, pp. 31–39.

Acosta-Mejia C. A. (1999) Improved p charts to monitor process quality. *IIE Transactions*, 31, pp. 509-516.

Albers W. (2011) Control charts for health care monitoring under overdispersion. *Metrika*, 74, pp. 67-83.

Anderson M. J., Thompson A. A. (2004) Multivariate control charts for ecological and environmental monitoring. *Ecological Applications*, 14, pp. 1921-1935.

Aparisi F., De Luna M. A. (2009) The design and performance of the multivariate synthetic-T^2 control chart. *Communications in Statistics– Theory and Methods*, 38, pp. 173–192.

APICS: American Production and Inventory Control Society (1995). *APICS dictionary*. Falls Church, VA: APICS.

Arnold J. C., Reynolds M. R. (2001) CUSUM control charts with variable sample sizes and sampling intervals. *Journal of Quality Technology*, 33, pp. 66-81.

Aroian L. A., Levene H. (1950) The effectiveness of quality control charts. *American Statistical Association*, 45, pp. 520-529.

Arthur B., Richard N., Mark A., Qi S. (2008) EWMA control charts for monitoring high-yield processes based on non-transformed observations. *International Journal of Production Research*, 46, pp. 5679-5699.

AT&T Technologies (1985) *Statistical quality control handbook*. Delmar printing Company, Charlotte, North Carolina.

Bagchi T. P. (1992) Sequential tests to monitor lot attribute quality in the presence of inspection errors. *Opsearch*, 29, pp. 165-183.

Bakir S. T. (2004) A distribution-free Shewhart quality control chart based on signed-ranks. *Quality Engineering*, 16 , pp. 613-623.

Bicking C. A., Gryna F. M. (1979) *Process control by statistical methods* in Juran J. M., Gryna F. M., Bingham R. S. *Quality control handbook*. McGraw-Hill, New York.

Borror C. M., Champ C. W., Rigdon S. E. (1998) Poisson EWMA control charts. *Journal of Quality Technology*, 30, pp. 352–361.

Bourke P. D. (1991) Detecting a shift in fraction nonconforming using run-length control charts with 100% inspection. *Journal of Quality Technology*, 23, pp. 225-238.

Bourke P. D. (2001*a*) Sample size and the binomial CUSUM control chart: the case of 100% inspection. *Metrika*, 53, pp. 51-70.

Bourke P. D. (2001*b*) The geometric CUSUM chart with sampling inspection for monitoring fraction defective. *Journal of Applied Statistics*, 28, pp. 951–972.

Bourke P. D. (2008) Performance comparisons for the synthetic control chart for detecting increases in fraction nonconforming. *Journal of Quality Technology*, 40, pp. 461-475.

Box G. E., Jenkins G. M., Reinsel G. C. (1994) *Time series analysis, forecasting and control*. Prentice-Hall, Englewood Cliffs, NJ.

Box G. E., Luceno A. (1994) Selection of sampling interval and action limit for discrete feedback adjustment. *Technometrics*, 36, pp. 369-378.

Brassard M., Ritter D. (1994) *The memory jogger II*. Methuen, MA:GOAL/QPC.

British Standard Institution (1985) *Quality management systems BSI handbook 24*. Quality Control, London.

Brook D., Evans D. (1972) An approach to the probability distribution of CUSUM run length. *Biometrika*, 59, pp. 539-549.

Cannon J., Krokhmal P. A., Chen Y., Murphey R. (2012) Detection of temporal changes in psychophysiological data using statistical process control methods. *Computer Methods and Programs in Biomedicine*, 107, pp. 367-381.

Carot V., Jabaloyes J. M., Carot T. (2002) Combined double sampling and variable sampling interval X chart. *International Journal of Production Research*, 40, pp. 2175-2186.

Castagliola P., Celano G., Psarakis S. (2011) Monitoring the coefficient of variation using EWMA charts. *Journal of Quality Technology*, 43, pp. 249-265.

Castagliola P., Celano G., Fichera S. B., Nenes G. (2012) The variable sample size t control chart for monitoring short production runs. *International Journal of Advanced Manufacturing Technology*, 66, pp. 1353-1366.

Castagliola P., Khoo M. B. C. (2009) A Synthetic scaled weighted variance control chart for monitoring the process mean of skewed populations. *Communications in Statistics-Simulation and Computation*, 38, pp. 1659-1674.

Celano G., Castagliola P., Trovato E., Fichera S. (2012) The economic performance of the Shewhart t chart. *Quality and Reliability Engineering International*, 28, pp. 159–180.

Chakraborti S., Human S. W. (2006) Parameter estimation and performance of the p-chart for attributes data. *IEEE Transactions on Reliability*, 55, pp. 559-566.

Chan K. Y., Chan K. W., Pong G. T., Aydin M. E., Fogarty T. C., Ling S. H. (2009) A statistics-based genetic algorithm for quality improvements of power supplies. *European Journal of Industrial Engineering*, 3, pp. 468-492.

Chang T. C, Gan F. F. (2001) Cumulative sum charts for high yield processes. *Statistica Sinica*, 11, pp. 791-805.

Chase R. B., Stewart D. M. (1995) *Mistake-proofing: designing errors out*. Productivity Press, Portland.

Chen A., Chen Y. K. (2007) Design of EWMA and CUSUM control charts subject to random shift sizes and quality impacts. *IIE Transactions*, 39, pp. 1127 – 1141.

Chen F. L., Huang H. J. (2006) Variable sampling interval synthetic charts for jointly monitoring process mean and standard deviation. *International Journal of Industrial Engineering*, 13, pp. 136-146.

Chen G., Cheng S. W. (1998) Max chart: combining x-bar chart and s chart. *Statistica Sinica*, 8, pp. 263-271.

Chen G., Cheng S. W., Xie H. (2001) Monitoring process mean and variability with one EWMA chart. *Journal of Quality Technology*, 33, pp. 223–233.

Cheng P. C., Dawson C. D. (1998) A study of statistical process control: practice, problems, and training needs. *Total Quality Management*, 9, pp. 3-20.

Cheng S. W., Thaga K. (2006) Single variables control charts: an overview. *Quality and Reliability Engineering International*, 22, pp. 811-820.

Chou C. Y., Chen C. H., Liu H. R. (2000) Economic-statistical design of X charts for non-normal data by considering quality loss. *Journal of Applied Statistics*, 27, pp. 939-951.

Coory M., Duckett S. Sketcher-Baker K. (2008) Using control charts to monitor quality of hospital care with administrative data. *International Journal for Quality in Health Care*, 20, pp. 31-39.

Costa A. F. (1997) X chart with variable sample size and sampling intervals. *Journal of Quality Technology*, 29, pp. 197-204.

Costa A. F. (1999) Joint $\overline{X}$ and R charts with variable sample size and sampling intervals. *Journal of Quality Technology*, 31, pp. 387-397.

Costa A. F., De Magalhães M. S. (2007) An adaptive chart for monitoring the process mean and variance. *Quality and Reliability Engineering International*, 23, pp. 821–831.

Costa A. F., De Magalhães M. S., Epprecht E. K. (2009) Monitoring the process mean and variance using a synthetic control chart with two-stage testing. *International Journal of Production Research*. 47, pp. 5067-5086.

Costa A. F., Rahim M. A. (2006) A synthetic chart for monitoring the process mean and variance. *Journal of Quality in Maintenance Engineering*, 12, pp. 81-88.

Crosby P. (1979) *Quality is free*. McGraw-Hill, New York.

Crowder S. V., Hawkins D. M., Reynolds M. R., Yashchin E. (1997) Process control and

statistical inference. *Journal of Quality Technology*, 29, pp. 134-139.

Dasgupta T. (2003) Maximizing the effectiveness of control charts: a framework for reacting to out-of-control signals. *ASQC'S Annual Quality Congress Proceedings*, 57, pp. 327-337.

Daudin J. J. (1992) Double sampling X charts. *Journal of Quality Technology*, 24, pp. 78-87.

Davis R. B., Woodall W. H. (2002) Evaluating and improving the synthetic chart. *Journal of Quality Technology*, 34, pp. 200-208.

De Vries A., Reneau J. K. (2010) Application of statistical process control charts to monitor changes in animal production systems. *Journal of Animal Science*, 88, pp. E11-E24.

Delmar D., Sheldon G. (1998) *Introduction to quality control*. West Publishing Company, New York.

Deming W. E. (1986) *Out of the crisis*. Massachusetts Institute of Technology Center for Advanced Engineering Study, Cambridge: MA.

Devor R. E., Chang T., Sutherland L. W. (1992) *Statistical design and control*. Macmillan Publishing Company, New York.

Dhafr N., Ahmad M., Burgess B., Canagassababady S. (2006) Improvement of quality performance in manufacturing organizations by minimization of production defects. *Robotics and Computer-Integrated Manufacturing*, 22, pp. 536-542.

Dokouhaki P., Noorossana R. (2012) Surveillance of diabetes prevalence rate through the development of a Markov-based control chart. *Journal of Mechanics in Medicine and Biology*, 12.

Domangue R., Patch S. C. (1991) Some omnibus exponentially weighted moving average statistical process monitoring schemes. *Technometrics*, 33, pp. 299-313.

Donnell A. J., Singhal S. C. (1996) SPC implementation for improving product quality. *Nineteenth IEEE/CPMT International Electronics Manufacturing Technology Symposium*, pp. 416-421.

Du S., Xi L. (2011) Fault diagnosis in assembly processes based on engineering-driven rules and PSOSAEN algorithm. *Computers and Industrial Engineering*, 60, pp. 77-88.

Duclos A., Voirin N. (2010) The p-control chart: a tool for care improvement. *International Journal for Quality in Health Care*, 22, pp. 402-407.

Dudewicz E. J., Mishra S. N. (1988) *Modern mathematical statistics*. Wiley, New York.

Duncan A. J. (1956) The economic design of $\overline{X}$ chart to maintain current control of a process. *Journal of the American Statistical Association*, 51, pp. 228-241.

Duncan A.J. (1986) *Quality Control and Industrial Statistics*. Richard, D. Irwin, Illinois.

Elsayed E. A., Chen A. (1994) An economic design of control chart using quadratic loss

function. *International Journal of Production Research*, 32, pp. 873-887.

Epprecht E. K., Simões B. F. T., Mendes F. C. T. (2010) A variable sampling interval EWMA chart for attributes. *International Journal of Advanced Manufacturing Technology*, 49, pp. 281-292.

Evans J. R., Lindsay W. M. (2002) *The management and control of quality*. South-Western College Publishing, Cincinnati: OH.

Friedman D. J., Albin S. (1991) Clustered defects in IC fabrication: impact on process control charts. *IEEE Transactions on Semiconductor Manufacturing*, 4, pp. 36-42.

Gadre M. P., Rattihalli R. N. (2005) Unit and group-runs chart to identify increases in fraction nonconforming. *Journal of Quality Technology*, 37, pp. 199-209.

Gan F. F. (1990) Monitoring observations generated from a binomial distribution using modified exponentially weighted moving average control chart. *Journal of Statistical Computation and Simulation*, 37, pp. 45–60.

Gan F. F. (1993) An optimal design of CUSUM control charts for binomial counts. *Journal of Applied Statistics*, 20, pp. 445-460.

Ghosh B. K. (1970) *Sequential tests of statistical hypotheses*. Addison-Wesley Publishing Company, Boston: MA.

Glushkovsky E. A. (1994) On-line G-control chart for attribute data. *Quality and Reliability Engineering International*, 10, pp. 217–227.

Grant E. L., Leavenworth R. S. (1996) *Statistical Quality Control*. McGraw-Hill, Inc., New York.

Grenier R. W., Heldt J. J., Kimber R. J. (1997) *Quality management handbook*. Marcel Dekker, New York.

Grygoryev K., Karapetrovic S. (2005) Tracking classroom teaching and learning: an SPC application. *Quality Engineering*, 17, pp. 405-418.

Haridy S., Gouda S. A. and Wu Z. (2011) An integrated framework of statistical process control and design of experiments for optimizing wire electrochemical turning process. *International Journal of Advanced Manufacturing Technology*, 53, pp. 191-207.

Haridy S., Wu Z. (2009) Univariate and multivariate control charts for monitoring dynamic-behavior processes: a case study. *Journal of Industrial Engineering and Management*, 2, pp. 464-498.

Haridy S., Wu Z., Khoo M. B. C., Yu F. J. (2012*a*) A combined synthetic & np scheme for detecting increases in fraction nonconforming. *Computers & Industrial Engineering*, 62, pp. 979-988.

Haridy S., Wu Z., Flaig J. (2012*b*) Chi-squared control chart for multiple attributes. *International*

Journal of Industrial and Systems Engineering, 12, pp. 316-330.

Hart M. K., Lee K. Y, Hart R. F., Robertson J. W. (2003) Application of attribute control charts to risk-adjusted data for monitoring and improving health care performance. *Quality Management in Healthcare*, 12, pp. 5-19.

Hawkins D. M. (1992) Evaluation of average run lengths of cumulative sum charts for an arbitrary data distribution. *Communications in Statistics-Simulation and Computation*, 21, pp. 1001-1020.

Hawkins D. M., Olwell D. H. (1998) *Cumulative sum charts and charting for quality improvement*. Springer – Verlag. New York, NY.

He D., Grigoryan A. (2006) Joint statistical design of double sampling X and S charts. *European Journal of Operational Research*, 168, pp. 122-142.

Herbert D., Curry A., Angel L. (2003) Use of quality tools and techniques in service. *Service Industries Journal*, 23, pp. 61-80.

Ho L. L., Costa A. F. (2011) Monitoring a wandering mean with an np chart. *Produção*, 21, 254-258.

Hsieh K., Tong L. (2007) The application of control chart for defects and defect clustering in IC manufacturing based on fuzzy theory. *Expert Systems with Applications*, 32, pp. 765-776.

Huang C., Chen F. (2010) Economic design of max charts. *Communications in Statistics-Theory and Methods*, 39, pp. 2961-2976.

Hung C., Hong J. (2010) Simulated Shewhart control charts for monitoring the variance components of two-factor mixed effect model. *ICIC Express Letters*, 4, pp. 2281-2286.

Hunter J. S. (1986) The exponentially weighted moving average. *Quality Technology*, 18, pp. 203-210.

Jafari J. M., Mirkamali S. J. (2011) Control charts for attributes with maxima nominated samples. *Journal of Statistical Planning and Inference*, 141, pp. 2386-2398.

Jones P., Dent M. (1994) Lessons in consistency: SPC in Forte plc. *The TQM Magazine*, 6, pp. 18-23.

Jumah J. A., Burt R. B., Buttram B. (2012) An exploration of quality control in banking and finance. *International Journal of Business and Social Science*, 3, p. 273.

Kaminsky F. C., Benneyan J. C., Davis R. D. (1992) Statistical control charts based on a geometric distribution. *Journal of Quality Technology*, 24, pp. 63–69.

Kaya I., Engin O. (2007) A new approach to define sample size at attributes control chart in multistage processes: An application in engine piston manufacturing process. *Journal of Materials Processing Technology*, 183, pp. 38-48.

Kemp K. W. (1962) The use of cumulative sums for sampling inspections schemes. *Journal of*

the Royal Statistical Society. Series C (Applied Statistics), 11, pp. 16–31.

Kennedy C. W., Hoffman E. G., Bond S. D. (1987) *Inspection and Gaging*. Industrial Press Inc., New York.

Khilare S. K., Shirke D. T. (2010) A nonparametric synthetic control chart using sign statistic. *Communications in Statistics - Theory and Methods*, 39, pp. 3282-3293.

Khilare S. K., Shirke D. T. (2012) Nonparametric synthetic control charts for process variation. *Quality and Reliability Engineering International*, 28, pp. 193-202.

Khoo M. B. C. (2003) Increasing the sensitivity of control chart for fraction nonconforming. *Quality Engineering*, 16, pp. 307-319.

Khoo M. B. C. (2004) A moving average control chart for monitoring the fraction nonconforming. *Quality and Reliability Engineering International*, 20, pp. 617-635.

Khoo M. B. C., Lee H. C., Wu Z., Chen C. H., Castagliola, P. (2011) A synthetic double sampling control chart for the process mean. *IIE Transactions*, 43, pp. 23–38.

Khoo M. B. C., Teh S. Y., Wu, Z. (2010) Monitoring process mean and variability with one double EWMA chart. *Communications in Statistics - Theory and Methods*, 39, pp. 3678-3694.

Khoo M. B. C., Wu Z., Abdu M. A. (2008) A synthetic control chart for monitoring the process mean of skewed populations based on the weighted variance method. *International Journal of Reliability, Quality and Safety Engineering*, 15, pp. 217-245.

Klyatis L. M., Klyatis E. L. (2006) *Accelerated quality and reliability solutions*. Elsevier Science.

Kolesar P. J. (1993) The relevance of research on statistical process control to the total quality movement. *Engineering and Technology Management*, 10, pp. 317-338.

Kooli I., Limam M. (2011) Economic design of an attribute np control chart using a variable sample size. *Sequential Analysis*, 30, pp. 145-159.

Koshy G., Koshy A. (2004) Project management using statistical control chart. *Annual Quality Congress Proceedings*, 58, pp. 517-528.

Krumwiede D., Chwen S. (1996) Implementing SPC in a small organization: a TQM approach. *Integrated Manufacturing Systems*, 7, pp. 45-51.

Kwon D., Azarian M. H., Pecht M. G. (2008) Early detection of interconnect degradation using RF impedance and SPRT. *International Conference on Prognostics and Health Management*, pp. 1-8.

Lee J., Hur Y., Kim S. H., Wilson J. R. (2012) Monitoring nonlinear profiles using a wavelet-based distribution-free CUSUM chart. *International Journal of Production Research*, 42, pp. 6574-659.

Lee M. H. (2010) Multivariate EWMA control chart with adaptive sample sizes. *Communications in Statistics: Simulation and Computation*. 39, pp. 1548-1561.

Lee P. H., Chang Y. C., Torng C. C. (2012) A design of s control charts with a combined double sampling and variable sampling interval scheme. *Communications in Statistics - Theory and Methods*, 41, pp. 153-165.

Leitnaker M. G., Cooper A. (2005) Using statistical thinking and designed experiments to understand process operation. *Quality Engineering*, 17, pp. 279–289.

Li Y., Pu X. L., Tsung F. G. (2009) Adaptive charting schemes based on double sequential probability ratio tests. *Quality and Reliability Engineering International*, 25, pp. 21-39.

Li Z., Luo Y., Wang Z. (2010) Cusum of Q chart with variable sampling intervals for monitoring the process mean. *International Journal of Production Research*, 48, pp. 4861-4876.

Lim T. O., Soraya A., Ding L. M., Morad Z. (2002) Assessing doctors' competence: application of CUSUM technique in monitoring doctors' performance, *International Journal for Quality in Health Care*, 14, pp. 251-258.

Lu C. W., Reynolds M. R. (2001) CUSUM charts for monitoring an auto-correlated process. *Journal of Quality Technology*, 33, pp. 316-334.

Lucas J. M. (1982) Combined Shewhart-CUSUM quality control schemes. *Journal of Quality Technology*, 14, pp. 51-59.

Lucas J. M. (1985*a*) Counted data CUSUM's. *Technometrics*, 27, pp. 129-144.

Lucas J. M. (1985*b*) Cumulative sum (CUSUM) control schemes. *Communications in Statistics-Theory and Methods*, 14, pp. 2689-2704.

Lucas J. M. (1989) Control schemes for low count levels. *Journal of Quality Technology*, 21, pp. 199-201.

Lucas J. M., Saccucci M. S. (1990) Exponentially weighted moving average control schemes: Properties and enhancements. *Technometrics*, 32, pp. 1-29.

Luo P., DeVol T. A., Sharp J. L. (2010) Sequential probability ratio test using scaled time-intervals for environmental radiation monitoring. *IEEE Transactions on Nuclear Science*, 57, pp. 1556-1562.

MacCarthy B. L., Wasusri T. (2002) A review of no-standard applications of statistical process control (SPC) charts. *Quality & Reliability Management*, 19, pp. 295-320.

Machado M. A., Costa A. F., Rahim M. A. (2009) The synthetic control chart based on two sample variances for monitoring the covariance matrix. *Quality and Reliability Engineering International*, 25, pp. 595-606.

Mataragas M., Drosinos E. H., Tsola E. B., Zoiopoulos P. E. (2012) Integrating statistical process control to monitor and improve carcasses quality in a poultry slaughterhouse implementing

a HACCP system. *Food Control*, 28, pp. 205-211.

Mitra A. (1998) *Quality control and improvement*. Prentice-Hall, New Jersey.

Montgomery D. C. (2013) *Introduction to statistical quality control*. John Wiley & Sons, Hoboken, New Jersey.

Montgomery D. C., Keats J. B., Rajavelu G. (1996) Statistical monitoring techniques for contamination data. *Institute of Environmental Sciences-Proceedings, Annual Technical Meeting*, pp. 304-310.

Morais M., Pacheco A. (2006) Combined CUSUM–Shewhart schemes for binomial data. *Economic Quality Control*, 1, pp. 43-57.

Morrison L. W. (2008) The use of control charts to interpret environmental monitoring data. *Natural Areas Journal*, 28, pp. 66-73.

Nelson L. S. (1988) Control charts: rational subgroups and effective applications. *Quality Technology*, 20, pp. 73-75.

Nenes G., Tagaras G. (2008) An economic comparison of CUSUM and Shewhart charts. *IIE Transactions*, 40, pp. 133–146.

Nezhad M. S., Niaki S. T. (2010) A new monitoring design for uni-variate statistical quality control charts. *Information Sciences*, 180, pp. 1051-1059.

Ngo P. (1995) Control charts for assembly operations. *Circuits Assembly*, 6, pp. 40-42.

Noorossana R., Fatahi A. A., Dokouhaki P., Babakhani M. (2011) ZIB-EWMA control chart for monitoring rare health events. J*ournal of Mechanics in Medicine and Biology*, 11, pp. 881-895.

Ou Y., Wen D., Wu Z., Khoo M. B. C. (2012*a*) A comparison study on effectiveness and robustness of control charts for monitoring process mean and variance. *Quality and Reliability Engineering International*, 28, pp. 3-17.

Ou Y., Wu Z., Chen S., Lee K. (2010) An improved SPRT control chart for monitoring process mean. *The International Journal of Advanced Manufacturing Technology*, 51, pp.1045-1054.

Ou Y., Wu Z., Goh T. N. (2011) A new SPRT chart for monitoring process mean and variance. *International Journal of Production Economics*, 132, pp. 303-314.

Ou Y., Wu Z., Lee K. M., Chen S. (2012*b*) An optimal design algorithm of the SPRT chart for minimizing weighted ATS. *International Journal of Production Economics*, 139, pp. 564-574.

Ozkul B., Karaoglan A. D. (2011) Regression control chart for determination of young's modulus: A case study. *Scientific Research and Essays*, 6, pp. 6393-6403.

Page E. S. (1954) Continuous inspection schemes. *Biometrika*, 41, pp. 100-115.

Pastella M., Madsenb H. (2008) Application of CUSUM charts to detect lameness in a milking robot. *Expert Systems with Applications*, 35, pp. 2032–2040.

Pawar V. Y., Shirke D. T. (2010) A nonparametric shewhart-type synthetic control chart. *Communications in Statistics: Simulation and Computation*, 39, pp. 1493-1505.

Perry M. B., Pignatiello J. J. (2011) Estimating the time of step change with Poisson CUSUM and EWMA control charts. *International Journal of Production Research*, 49, pp. 2857-2871.

Pettersson M. (2004) SPC with applications to churn management. *Quality and Reliability Engineering International*, 20, pp. 397-406.

Prabhu S. S., Montgomery D. C., Runger G. C. (1994) A combined adaptive sample size and sampling interval X control scheme. *Journal of Quality Technology*, 26, pp. 164-176.

Quesenberry C. P. (1997) *SPC methods for quality improvement*. John Wiley and Sons, New York.

Radaelli G. (1994) Poisson and negative binomial dynamics for counted data under CUSUM-type charts. *Journal of Applied Statistics*, 21, pp. 347-356.

Rendtel U. (1990) CUSUM schemes with variable sampling intervals and sample sizes. *Statistical Papers*, 31, pp. 103-118.

Reynolds M. R., Amin R. W., Arnold J. C. (1990) CUSUM charts with variable sampling intervals. *Technometrics*, 32, pp. 371-384.

Reynolds M. R., Arnold J.C. (2001) EWMA control charts with variable sample sizes and variable sampling intervals. *IIE Transactions*, 33, pp. 511-530.

Reynolds M. R., Glosh, B. (1981) Designing control charts for means and variances. *ASQ Quality Congress Transaction*. American Society for Quality Control, San Francisco, 400-407.

Reynolds M. R., Stoumbos Z. G. (1998) The SPRT chart for monitoring a proportion. *IIE Transactions*, 30, pp. 545-561.

Reynolds M. R., Stoumbos Z. G. (1999) A CUSUM chart for monitoring a proportion when inspecting continuously. *Journal of Quality Technology*. 31, pp. 87-108.

Reynolds M. R., Stoumbos Z. G. (2001) Monitoring the process mean and variance using individual observations and variable sampling intervals. *Journal of Quality Technology*, 33, pp. 181-205.

Reynolds M. R., Stoumbos Z. G. (2004*a*) Should observations be grouped for effective process monitoring. *Journal of Quality Technology*, 36, pp. 343-366.

Reynolds M. R., Stoumbos Z. G. (2004*b*) Control charts and the efficient allocation of sampling resources. *Technometrics*, 46, pp. 200-214.

Reynolds M. R., Stoumbos Z. G. (2006) Comparisons of some exponentially weighted moving average control charts for monitoring the process mean and variance. *Technometrics*, 48, pp. 550-567.

Reynolds M. R., Stoumbos, Z. G. (2000) A general approach to modeling CUSUM charts for a proportion. *IIE Transaction*, 32, pp. 515-535.

Reynolds M. R., Stoumbos, Z. G. (2005) Should exponentially weighted moving average and cumulative sum charts be used with Shewhart limits. *Technometrics*, 47, pp. 409-424.

Roberts S. W. (1959) Control chart tests based on geometric moving average. *Technometrics*, 1, pp. 239-250.

Rocke D. M. (1990) The adjusted p chart and u chart for varying sample sizes. *Journal of Quality Technology*, 22, pp. 206-209.

Saccucci M. S., Amin R. W., Lucas J. M. (1992) Exponentially weighted moving average control schemes with variable sampling intervals. *Communications in Statistics–Simulation and Computation*, 21, pp. 627–657.

Saniga E. M. (1989) Economic statistical control chart designs with an application to $\bar{X}$ and R chart. *Technometrics*, 31, pp. 313-320.

Saniga E. M., Davis, D. J., Mcwilliams, T. P. (1995) Economic, statistical, and economic-statistical design of attribute charts, *Journal of Quality Technology*, 27, pp. 56-73.

Saniga E., Shirland L. (1977) Quality control in practice - a survey. *Quality Progress*, 10, pp. 30-33.

Scariano S. M., Calzada M. E. (2003) A note on the lower-sided synthetic chart for exponentials. *Quality Engineering*, 15, pp. 677-680.

Schafer W. D., Coverdale B. J., Luxenberg H., Jin Y. (2011) Quality control charts in large-scale assessment programs. *Practical Assessment, Research and Evaluation*, 16, pp. 1-7.

Schneider H., Hui Y., Pruett J. M. (1992) Control charts for environmental data. *Frontiers in Statistical Quality Control*, 4, pp. 216-226.

Schwertman N. C., Ryan T. P. (1999) Using dual np-charts to detect changes. *Quality and Reliability Engineering International*, 15, pp. 317 – 320.

Sefik M. (1998) Importance of the rational subgroups in designing control charts. *Computers and Industrial Engineering*, 35, pp. 205-208.

Sellers K. F. (2012) A generalized statistical control chart for over- or under-dispersed data. *Quality and Reliability Engineering International*, 28, pp. 59-65.

Serel D. A., Moskowitz H. (2008) Joint economic design of EWMA control charts for mean and variance. *European Journal of Operational Research*, 184, pp. 157-168.

Shamsuzzaman M., Wu Z. (2006) Control chart design for minimizing the proportion of defective units. *Journal of Manufacturing Systems*, 25, pp. 269–278.

Shewhart W. A. (1931) *Economic control of quality of manufactured product*. D. Van Nostrand Company, New York: NY.

Shin H. W., Sohn S. Y. (2007) Application of a EWMA combining technique to the prediction of currency exchange rates. *IIE Transactions*, 39, pp. 639-644.

Shu L., Jiang W., Tsui K. L. (2008) A weighted CUSUM chart for detecting patterned means Shifts. *Journal of Quality Technology*, 40, pp. 194-213.

Shu L., Jiang W., Wu S. (2007) A one-sided EWMA control chart for monitoring process means. *Communications in Statistics - Simulation and Computation*, 36, pp. 901-920.

Siddall J. N. (1983) *Probabilistic engineering design: principles and applications*. Marcel Dekker Inc, New York.

Sim C. H. (2003) Combined X-bar and CRL charts for the gamma process. *Computational Statistics*, 18, pp. 547-563.

Singh P., Ranganath M. S., Mishra R. S. (2012) Improving total quality management on technical staff in the technical institutions using SPC techniques. *International Journal of Applied Engineering Research*, 7, pp. 433-447.

Sparks R. S. (2000) CUSUM charts for signaling varying location shifts. *Journal of Quality Technology*, 32, pp. 157-171.

Spliid H. (2010) An exponentially weighted moving average control chart for Bernoulli data. *Quality and Reliability Engineering International*, 26, pp. 97-113.

Stefan A., Ali B., Ingvar C. (1996) Quality monitoring in robotized welding using sequential probability ratio test. *IEEE Region 10 Annual International Conference*, 2, pp. 635-640.

Stoumbos Z. G., Reynolds M. R, Ryan T. P., Woodall W. H. (2000) The state of statistical process control as we proceed into the 21st century. *Journal of the American Statistical Association*, 95, pp. 992-998.

Stoumbos Z. G., Reynolds M. R. (1996) Control charts applying a general sequential test at each sampling point. *Sequential Analysis*, 15, pp. 159-183.

Stoumbos Z. G., Reynolds M. R. (1997*a*) Control charts applying a sequential test at fixed sampling intervals. *Journal of Quality Technology*, 29, pp. 21-40.

Stoumbos Z. G., Reynolds M. R. (1997*b*) Corrected diffusion theory approximations in evaluating properties of SPRT charts for monitoring a process mean. *Nonlinear Analysis*, 30, pp. 3987–399.

Stoumbos Z. G., Reynolds M. R. (2001) The SPRT control chart for the process mean with samples starting at fixed times. *Nonlinear Analysis*, 2, pp. 1-34.

Stoumbos Z. G., Reynolds M. R., Woodall W. H. (2003) Control chart schemes for monitoring the mean and variance of processes subject to sustained shifts and drifts. *Handbook of Statistics*: Statistics in Industry 22, eds. C. R. Rao and R. Khattree, Amsterdam: Elsevier Science, pp. 553-571.

Su C. T., Tong L. I. (1997) A Neural network-based procedure for the process monitoring of clustered defects in integrated circuit fabrication. *Computers in Industry*, 34, pp. 285 – 294.

Subramani J., Balamurali S. (2012) Control charts for variables with specified process capability indices. *International Journal of Probability and Statistics*, 1, pp. 101-110.

Szarka J. L., Woodall W.H. (2012) On the equivalence of the Bernoulli and geometric CUSUM charts. *Journal of Quality Technology*, 44, pp. 54-62.

Taguchi G., Wu Y. (1980) *Introduction to off-line quality control*. Central Japan Quality Control Association, Nagoya, Japan.

Tao Z., Liu F., Shen F., Suh M., Booth D. (2012) A new control chart based on the loess smooth applied to information system quality performance. *International Journal of Operational Research*, 15, pp. 74-93.

Teh S. Y., Khoo M. B. C., Wu Z. (2012) Monitoring process mean and variance with a single generally weighted moving average chart. *Communications in Statistics - Theory and Methods*, 41, pp. 2221-2241.

Teh S. Y., Khoo, M. B. C., Wu Z. (2011) A sum of squares double exponentially weighted moving average chart. *Computers and Industrial Engineering*, 61, pp. 1173-1188.

Testik M. C., McCullough B. D., Borror C. M. (2006) The effect of estimated parameters on Poisson EWMA control charts. *Quality Technology & Quantitative Management*, 3, pp. 513-527.

Thor J., Lundberg J., Ask J., Olsson J., Carli C., Härenstam K., Brommels M. (2007) Application of statistical process control in healthcare improvement: systematic review. *Quality and Safety in Health Care*, 16, pp. 387-399.

Vargas V., Lopes L., Souza, A. (2004) Comparative study of the performance of the CUSUM and EWMA control charts. *Computers and Industrial Engineering*, 46, pp. 707-724.

Wald A. (1947) *Sequential analysis*. Dover Publications Inc., New York.

Wheeler D. J. (2004) *Advanced topics in statistical control - the power of Shewhart's charts*. SPC Press, Knoxville, TN.

Wheeler D. J., Chambers D. S. (1992) *Understanding Statistical Process Control*. SPC Press, Knoxville, TN.

White C. L., Keats J. B. (1996) ARLs and higher-order run-length moments for the Poisson CUSUM. *Journal of Quality Technology*. 28, pp. 363-369.

White C. L., Keats J. B., Stanley J. (1997) Poisson CUSUM versus c chart for defect data. *Quality Engineering*, 9, pp. 673-679.

White E. M., Schroeder R. (1987) A simultaneous control chart. *Journal of Quality Technology*, 19, pp. 1-10.

Wood M. (1994) Statistical methods for monitoring service processes. *International Journal of Service Industry Management*, 5, pp. 53-68.

Woodall W. H. (1984) On the Markov chain approach to the two-sided CUSUM procedures. *Technometrics*, 26, pp. 41-46.

Woodall W. H. (1997) Control charts based on attribute data: bibliography and review. *Journal of Quality Technology*, 29, pp. 172-183.

Woodall W. H. (2006) The use of control charts in health-care and public-health surveillance. *Journal of Quality Technology*, 38, pp. 89-104.

Woodall W. H., Montgomery D. C. (1999) Research issues and ideas in statistical process control. *Journal of Quality Technology*, 31, pp. 376-386.

Woodall W. H., Reynolds, M. R. (1983) A discrete Markov chain representation of SPRT's. *Communications in Statistics - Sequential Analysis*. 2, pp. 27-44.

Woodall, W. H. (1985) The statistical design of quality charts. *Statistician*, 34, pp. 155–160.

Wu Z., Jiao J., He Z. (2009*a*) A control scheme for monitoring the frequency and magnitude of an event. *International Journal of Production Research*, 47, pp. 2887-2902.

Wu Z., Jiao J. (2007) Evaluating and improving the unit and group-runs chart. *Journal of Quality Technology*, 39, pp. 355-363.

Wu Z., Jiao J. (2008) A control chart for monitoring process mean based on attribute inspection. *International Journal of Production Research*, 46, pp. 4331–4347.

Wu Z., Jiao J. X., Yang M., Liu Y., Wang Z. J. (2009*c*) An enhanced adaptive CUSUM control chart. *IIE Transactions*, 41, pp. 642-653.

Wu Z., Jiao J., Liu Y. (2008*a*) A binomial CUSUM chart for detecting large shifts in fraction nonconforming. *Journal of Applied Statistics*, 35, pp. 1267-1276.

Wu Z., Khoo M. B. C., Shu L., Jiang W. (2009*b*) An np control chart for monitoring the mean of a variable based on an attribute inspection. *International Journal of Production Economics*, 121, pp. 141–147.

Wu Z., Luo H. (2003) Three-Triplet np Control Chart. *European Journal of Operational Research*. 149, pp. 614-624.

Wu Z., Luo H. (2004) Optimal design of the adaptive sample size and sample interval np control chart. *Quality and Reliability Engineering International*, 20, pp. 553-570.

Wu Z., Luo H., Zhang X. (2006*a*) Optimal np control chart with curtailment. *European Journal*

of Operational Research, 174, pp. 1723-1741.

Wu Z., Ou Y., Castagliola P., Khoo M. B. C. (2010*a*) A combined synthetic & X chart for monitoring the process mean. *International Journal of Production Research*, 48, pp. 7423-7436.

Wu Z., Spedding T. A. (1999) Evaluation of ATS for CRL control chart. *Process Control & Quality*. 11, pp. 183-191.

Wu Z., Spedding T. A. (2000) A synthetic control chart for detecting small shifts in the process mean. *Journal of Quality Technology*, 32, pp. 32-38.

Wu Z., Tian Y. (2005) Weighted-loss-function CUSUM chart for monitoring mean and variance of a production process. *International Journal of Production Research*, 43, pp. 3027-3044.

Wu Z., Tian Y., Zhang S. (2005) Adjusted-loss-function charts with variable sample sizes and sampling intervals. *Journal of Applied Statistics*, 32, pp. 221-242.

Wu Z., Wang Q. N. (1997) Optimization of joint $\bar{X}$ and *S* control charts with asymmetric control limits. *Process Control and Quality*, 10, pp. 269-281.

Wu Z., Wang Q. N. (2007) A single CUSUM chart using a single observation to monitor a variable. *International Journal of Production Research*, 45, pp. 719-741.

Wu Z., Wang Z., Jiang W. (2010*b*) A generalized conforming run length control chart for monitoring the mean of a variable. *Computers and Industrial Engineering*, 59, pp. 185-192.

Wu Z., Xie M., Liu Q., Zhang Y. (2006*b*) SXC control chart. *International Journal of Advanced Manufacturing Technology*, 30, pp. 444-451.

Wu Z., Xie M., Tian Y. (2002) Optimization design of the X&S charts for monitoring process capability. *Journal of Manufacturing Systems*, 21, pp. 83-92.

Wu Z., Yang M., Jiang W., Khoo M. B. C. (2008*b*) Optimization designs of the combined Shewhart-CUSUM control charts. *Computational Statistics and Data Analysis*, 53, pp. 496-506.

Wu Z., Yang M., Khoo M. B. C., Castagliola P. (2011) What are the best sample sizes for the Xbar and CUSUM charts? *International Journal of Production Economics*, 131, pp. 650-662.

Wu Z., Yeo S. H. (2001) Implementing synthetic charts for attributes. *Journal of Quality Technology*, 33, pp. 112-114.

Wu Z., Yeo S. H., Spedding T. A. (2001*a*) A synthetic control chart for detecting fraction nonconforming increases. *Journal of Quality Technology*, 33, pp. 104-111.

Wu Z., Zhang X., Yeo S. H. (2001*b*) Design of the sum-of-conforming-run-length control charts. *European Journal of Operational Research*, 132, pp. 187-196.

Wu Z., Zhang X., Yeo S., Chen Z. (2001*c*) Fractional control limits for np control chart. *Process Control & Quality*, 11, pp. 491-501.

Xie W., Xie M., Goh T. N. (1995) A Shewhart-like charting technique for high yield processes. *Quality and Reliability Engineering International*, 11, pp. 189–196.

Yang M., Wu Z., Li T. I. (2013) The effect of shift distribution on the design and performance of the X and CUSUM charts in monitoring mean and variability. *European Journal of Industrial Engineering*, 7, pp.224 - 247.

Yang M., Wu Z., Lee K. M., Khoo M. B. C. (2012) The X control chart for monitoring process shifts in mean and variance. *International Journal of Production Research*, 50, pp. 893-907.

Yang S. F., Lin J. S., Cheng S. W. (2011) A new nonparametric EWMA sign control chart. *Expert Systems with Applications*, 38, pp. 6239–6243.

Yang S. F., Yeh J. T. (2011) Using cause selecting control charts to monitor dependent process stages with attributes data. *Expert Systems with Applications*, 38, pp. 667-672.

Yang S., Rahim M. A. (2009) Minimum loss design of asymmetric X and S control charts under two independent Weibull shocks. *International Journal of Productivity and Quality Management*, 4, pp. 247-282.

Yashchin E. (1985) On the analysis and design of CUSUM-Shewhart control schemes. *IBM Journal of Research and Development*, 29, pp. 377–391.

Yi T., Guo Q., Li H. (2012) Detection of displacement shifts by control charts in GPS monitoring. *Applied Mechanics and Materials*, 170-173, pp. 2815-2818.

Yu F. J., Low C. Y., Cheng S. S. (2003) Design for an SPRT control scheme based on linguistic data. *International Journal of Production Research*, 41, pp. 1299-1309.

Zhang J., Li Z., Wang Z. (2012) A new adaptive control chart for monitoring process mean and variability. *International Journal of Advanced Manufacturing Technology*, 60, pp. 1031-1038.

Zhang S., Wu Z. (2007) A CUSUM scheme with variable sample sizes for monitoring process shifts. *International Journal of Manufacturing Technology*, 33, pp. 977-987.

Zhao Y., Tsung F., Wang Z. J. (2005) Dual CUSUM control scheme for detecting a range of mean shift. *IIE Transactions*, 37, pp. 1047-1058.

Zhou W., Lian Z. (2011) Optimum design of a new VSS-NP chart with adjusting sampling inspection. *International Journal of Production Economics*, 129, pp. 8-13.